INFORMATION TO USERS

This was produced from a copy of a document sent to us for microfilming. While the most advanced technological means to photograph and reproduce this document have been used, the quality is heavily dependent upon the quality of the material submitted.

The following explanation of techniques is provided to help you understand markings or notations which may appear on this reproduction.

1. The sign or "target" for pages apparently lacking from the document photographed is "Missing Page(s)". If it was possible to obtain the missing page(s) or section, they are spliced into the film along with adjacent pages. This may have necessitated cutting through an image and duplicating adjacent pages to assure you of complete continuity.

2. When an image on the film is obliterated with a round black mark it is an indication that the film inspector noticed either blurred copy because of movement during exposure, or duplicate copy. Unless we meant to delete copyrighted materials that should not have been filmed, you will find a good image of the page in the adjacent frame.

3. When a map, drawing or chart, etc., is part of the material being photographed the photographer has followed a definite method in "sectioning" the material. It is customary to begin filming at the upper left hand corner of a large sheet and to continue from left to right in equal sections with small overlaps. If necessary, sectioning is continued again—beginning below the first row and continuing on until complete.

4. For any illustrations that cannot be reproduced satisfactorily by xerography, photographic prints can be purchased at additional cost and tipped into your xerographic copy. Requests can be made to our Dissertations Customer Services Department.

5. Some pages in any document may have indistinct print. In all cases we have filmed the best available copy.

University
Microfilms
International

300 N. ZEEB ROAD, ANN ARBOR, MI 48106
18 BEDFORD ROW, LONDON WC1R 4EJ, ENGLAND

JOHNSTON, ERIC RICHARD

NMR STUDIES OF PROTON EXCHANGE IN AMIDES

University of California, San Diego PH.D. 1980

UNIVERSITY OF CALIFORNIA

San Diego

NMR Studies of Proton Exchange in Amides

A dissertation submitted in partial satisfaction of the

requirements for the degree Doctor of Philosophy

in Chemistry

by

Eric Richard Johnston

Committee in charge:

Professor Charles L. Perrin, Chairman
Professor Robert L. Vold
Professor George Feher
Professor David R. Kearns
Professor George N. Somero

1980

The dissertation of Eric Richard Johnston is approved, and it is acceptable in quality and form for publication on microfilm:

David R Kearns

Robert L. Wold

George Lehr

Gary Lorimer

Charles G. Perrin

Chairman

University of California, San Diego

1980

TABLE OF CONTENTS

LIST OF FIGURES

LIST OF TABLES

ACKNOWLEDGMENTS

It is a personal pleasure to thank Professor Charles L. Perrin for the knowledge, understanding and guidance he has so ably extended to me during the past four years. I also wish to thank Professor Robert L. Vold for many enlightening and helpful discussions, and Dr. John Wright for invaluable technical assistance. My thanks also go to Mrs. Dorothy Prior and Mrs. Gwen Robbins for personal and technical assistance throughout my tenure at UCSD.

VITA

March 3, 1951 - Born, Santa Monica, California

1973- B.A. in Chemistry, Amherst College, Amherst, Massachusetts

1974- Graduate student in Oceanography, Scripps Institution of Oceanography, UCSD

1975-1979 Department of Chemistry, University of California, San Diego

PUBLICATIONS

"Saturation-Transfer Studies of Three-Site Exchange Kinetics," J. Magn. Reson., 33, 619-626 (1979), Charles L. Perrin and Eric R. Johnston.

"Saturation-Transfer Study of the Mechanism of Proton Exchange in Amides," J. Am. Chem. Soc., 101, 4753 (1979), Charles L. Perrin and Eric R. Johnston.

"Mechanism of Acid-Catalyzed Proton Exchange in Amidinium Ions," submitted to J. Am. Chem. Soc., Charles L. Perrin, Eric R. Johnston, and José L. Ramírez.

FIELDS OF STUDY

Major Field: Chemistry

Studies in Physical Organic Chemistry
Professor Charles L. Perrin

Studies in Heme Chemistry
Professor Teddy G. Traylor

Studies in Marine Natural Products Chemistry
Professor D. John Faulkner

ABSTRACT OF THE DISSERTATION

NMR Studies of Proton Exchange in Amides

by

Eric Richard Johnston

Doctor of Philosophy in Chemistry

University of California, San Diego, 1980

Professor Charles L. Perrin, Chairman

Acid-catalyzed proton exchange in a number of primary and secondary amides has been studied by NMR methods. Exchange may conceivably occur by protonation on nitrogen, or by protonation on oxygen followed by N-deprotonation to the imidic-acid tautomer. These mechanisms may be distinguished experimentally, since the former pathway requires that the rate of acid-catalyzed intramolecular exchange of the diastereotopic E and Z protons be comparable to the rates of solvent exchange, whereas the latter pathway requires that the rate of acid-catalyzed intramolecular exchange be zero.

To measure rate constants in these three-site proton exchange reactions, we have extended the NMR saturation-transfer

technique of Forsen and Hoffman. The method involves the measurement of intensities and spin-lattice relaxation rates in Fourier transform NMR spectra under conditions of selective saturation. Saturation-transfer experiments have been supplemented with line-broadening and lineshape analysis measurements where necessary.

Uncatalyzed rotation about the C-N bond in a number of amides was initially studied with the saturation-transfer method. The rate of rotation is very small for formaide, N-methylformamide, N-t-butylformamide, ethyl oxamate, malonamide, and dichloroacetamide, and slightly larger for acetamide, cyanoacetamide, and chloroacetamide. The rate of rotation is considerably larger in acrylamide, methacrylamide, benzamide, and salicylamide. These variations in rotation rate are rationalized in terms of the effect of substituents on the transition-state for rotation.

To confirm the reliability of the three-site saturation-transfer method, we have examined the base-catalyzed exchange in a number of primary and secondary amides, where there is no mechanistic ambiguity. In all the amides examined, there is no base-catalyzed intramolecular exchange, as expected, and the E and Z protons exchange at different rates. The latter observation is rationalized in terms of electronic effects in the resulting imidate anions. We have additionally studied solvent effects on exchange rates, and have elucidated the role of the o-hydroxy substituent of salicylamide in

providing intramolecular catalysis of proton exchange in this compound.

Water-catalyzed proton exchange in two protonated imidic esters, ethyl acetimidate and 2-iminotetrahydrofuran, has been studied by saturation-transfer, since exchange in these compounds serves as a model for the imidic-acid route. We find that H_Z exchanges faster than H_E in ethyl acetimidate, and slower than H_E in 2-iminotetrahydrofuran. These results are consistent with the expectations that the E_{ap} and Z_{sp} configurations, respectively, are the more stable forms of the imidic esters.

Proton exchange in fuming sulfuric acid has been examined for acetamide, 3, 5-dinitrobenzamide, and trichloroacetamide. In this solvent, where the amides are quantitatively O-protonated, exchange proceeds by proton removal from oxygen, followed by reprotonation on nitrogen, as evidenced by the observation that H_E and H_Z exchange at equal rates with solvent and with each other.

With a combination of saturation-transfer and lineshape analysis methods, we have elucidated the mechanism of the dilute acid-catalyzed exchange in ten primary and two secondary amides. For acetamide, acrylamide, methacrylamide, benzamide, and formamide, where the rate of acid-catalyzed intramolecular exchange of the E and Z protons is comparable to the rates of solvent exchange, it is concluded that exchange proceeds predominantly by protonation on nitrogen. Nevertheless, H_E exchanges faster, and

this is interpreted in terms of competition between rapid deprotonation of $RCONH_3^+$ and rotation about its C-N single bond. In cyanoacetamide, ethyl oxamate, chloroacetamide, malonamide, and dichloroacetamide, intramolecular exchanges is significantly slower than solvent exchange. This result is evidence for exchange proceeding primarily or exclusively via the imidic-acid pathway. For all these amides except the last one, H_E exchanges faster than H_Z, opposite to the behavior observed in the model compound ethyl acetimidate.

In N-methylformamide, exchange occurs largely via the imidic-acid pathway, whereas in N-t-butylformamide, exchange occurs through protonation on nitrogen. In both cases, H_Z exchanges faster than H_E. These conclusions are supported by the observation of general-acid catalysis in N-methylformamide, and the absence of such catalysis in N-t-butylformamide.

Several additional aspects of the exchange pathways have been investigated, including the effects of solvent polarity on the relative stabilities of the isomeric imidic acids and imidate anions, the interaction between the $-NH_3^+$ group and solvent, and the effect of substituents on the barrier to rotation in the N-conjugate acid. Finally, the variability of mechanism in dilute acid is rationalized in terms of a polar effect of substituents, and the dominance of the N-protonation pathway in strong acid is rationalized in terms of the acidity dependence of the two pathways.

A. Introduction

During recent years proton exchange in amides has been a popular field of research[1-17], with interest in the reaction due in part to its applicability to questions of biochemical significance. It has, for example, been utilized as a probe of static and dynamic aspects of polypeptide molecular structure by biochemists,[18-24] who have inferred that slowly exchanging hydrogens are intramolecularly hydrogen-bonded and/or buried within the hydrophobic protein interior. More recently, amide hydrogen exchange has been used to study binding of NADH to various dehydrogenases,[25] and to study cation binding by cyclic peptides.[26]

Interest in acid-catalyzed amide hydrogen exchange is due as well to its obvious relevance to questions pertaining to the major site of protonation in amides[27-29] and to the mechanism of amide hydrolysis.[30-33] These issues, in turn, have a direct bearing on the question of the mechanism of action of the serine proteases, an important class of enzymes responsible for peptide-bond cleavage.[33-36] However, in spite of the fundamental importance of this hydrogen exchange reaction, its mechanism remains unknown.

The reaction was originally studied by Berger, Loewenstein, and Meiboom,[37] who found that it is both acid- and base-catalyzed. They concluded that acid-catalyzed exchange in N-methylacetamide occurs by direct protonation on nitrogen

$$RCONHR' + H_3O^+ \rightleftharpoons RCONH_2R'^+ + H_2O$$

and this mechanism has been generally accepted. However, the evidence for this mechanism is also consistent with an alternative but more circuitous mechanism, proposed by Martin,[39] that proceeds by protonation on oxygen followed by deprotonation to the imidic-acid tautomer.

$$RCONHR' + H_3O^+ \rightleftharpoons RC(OH)NHR'^+ + H_2O \rightleftharpoons RC(OH)NR' + H_3O^+$$

This mechanism is quite reasonable, especially in view of the well-known[40] fact that the amide oxygen is more basic than the nitrogen.

Molday and Kallen have asserted[38] that the lower pH required to produce proton exchange when R- is electron-withdrawing is evidence against the imidic-acid pathway, on the basis of the assumption that for this pathway the decrease in the concentration of O-protonated amide should be balanced by the increased rate of N-H proton removal from it, so that this mechanism should be relatively insensitive to substituents. However, since both mechanisms involve acid catalysis, both must involve partial positive charge due to the proton in the transition state, and both would be expected to show a rate decrease when R- is electron-withdrawing, so this observation does not constitute evidence in favor of either mechanism.

Martin[39] has favored the latter mechanism on the basis of the observation that rates of acid-catalyzed proton exchange in secondary

amides exceed rates of acid-catalyzed isomerization in tertiary amides. Although proton exchange in secondary amides can conceivably occur through either pathway, isomerization in tertiary amides can occur only by protonation on nitrogen. The rate of this process thus provides an estimate for the rate of exchange occurring by protonation on nitrogen. Martin assumed that the pK_a values for N-protonated secondary and tertiary amides parallel the measured pK_a's of the corresponding O-protonated amides, and, subject to this assumption, estimated the amount of exchange in secondary amides occurring via N-protonation. He then attributed the excess exchange rate in secondary amides to incursion of the imidic-acid mechanism. There is no a priori reason to assume, however, that his assumption concerning the transferability of pK_a's is justified, and his conclusion is therefore not firm.

Bovey and Tiers[41] have also favored the imidic-acid pathway on the basis of NMR evidence for aqueous polyacrylamide solutions which suggests that C-N bond rotation does not occur concurrently with exchange. Their experiments, however, were conducted at 40 MHz, where the amide N-H signals appeared on the shoulder of an intense water peak, and it is doubtful that their spectra were sufficiently sensitive to the small lineshape changes which serve to distinguish the two mechanisms.

In the most recent effort to elucidate the mechanism of the acid-catalyzed exchange, Perrin[42] has studied proton exchange in

primary amides (R' = H) by nuclear magnetic resonance. The E and Z protons (respectively trans and cis to oxygen) are magnetically nonequivalent and separately detectable in the NMR spectrum, due to slow rotation about the C-N bond at room temperature.[40] He demonstrated that these hydrogens undergo acid-catalyzed exchange at different rates, and that, for the amides examined, H_E is the faster to exchange. He reasoned that if exchange proceeded via the imidic-acid pathway, the more stable E configuration[43-45] of the imidic acid, 1, should be formed faster, so that H_Z should exchange faster than H_E.

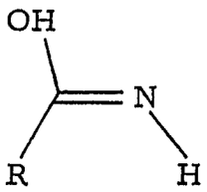

1

Since this is opposite to the observed exchange behavior, he concluded that exchange proceeds entirely by protonation on nitrogen, and that H_E and H_Z, which might have been expected to be equivalent in $RCONH_3^+$, exchange at different rates because hindered rotation about the C-N single bond in the N-protonated species prevents them from becoming equivalent in the very short lifetime of the cation. The N-protonated amide is a strong acid (pK_a ca. -9)[34] which undergoes proton transfer to water at a diffusion-controlled[46] rate, so that rates of rotation and deprotonation might be expected to be comparable. This mechanistic conclusion, however, rests on the assumption that

the relative stabilities of the isomeric imidic acids parallel the known relative stabilities of imidic esters, $RC(OR')NR''$, and it is not clear that imidic esters are adequate models for imidic acids.

The experiments described here were thus initiated to obtain more compelling evidence for the N-protonation mechanism in primary amides, and to further investigate the dynamics of the two very fast processes involved, diffusion-controlled proton transfer and rotation about single bonds. We have additionally sought (and found) examples of exchange proceeding by the imidic-acid mechanism.

Our approach to this problem rests on the mechanistic distinction provided by comparing rate constants for intermolecular and intramolecular exchange in primary amides. Unlike Martin's comparison of rate constants for exchange and isomerization in secondary and tertiary amides,[39] which required an assumption about the transferability of pK_a's, these rate constants can be directly compared in the same primary amide. We define k_{EZ} and k_{ES} to be the pseudo-first-order rate constants for exchange from the E site to the Z site and to the solvent site, respectively; other k_{ij}'s are defined analogously (see Figure 1).

The imidic-acid pathway requires that k_{EZ} and k_{ZE} be zero, since the configurational stability[47] of the resulting imidic acids precludes acid-catalyzed isomerization. In contrast, protonation on nitrogen should result in both proton exchange and isomerization. A

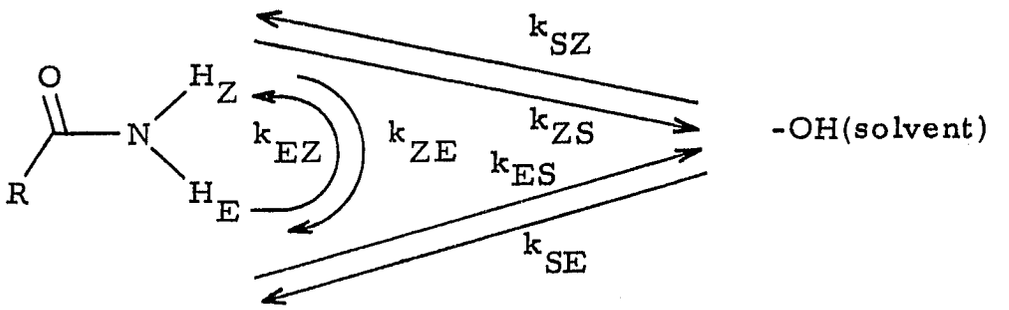

Figure 1. Three-site system in hydrogen exchange in amides.

detailed analysis of these N-protonation exchange kinetics is possible, and (as will be shown later) this mechanism requires that H_Z exchange into the solvent and E sites at equal rates. The distinction between the imidic-acid and N-protonation routes thus depends on whether k_{ZE} is equal to zero or k_{ZS}, respectively. We have followed the same approach in our studies of N-methylformamide and N-t-butylformamide, which exist as equilibrium mixtures of the Z and E forms. For ease of comparison with primary amides, the amide protons of the Z and E stereoisomers are labeled H_E and H_Z, respectively.

Lineshape analysis is too inaccurate for comparing intramolecular exchange with intermolecular exchange. We have therefore extended[48] the NMR saturation-transfer technique of Forsén and Hoffman[49] to the determination of all six rate constants in these three-site systems. The method involves the measurement of intensities and longitudinal relaxation rates in Fourier transform NMR spectra under conditions of selective saturation. When rates of chemical

exchange and longitudinal relaxation are comparable, kinetic transfer of saturation leads to decreases in signal intensities.

From the equations describing the time-dependence of the magnetization of the three-component spin system,[50] expressions for the rate constants in Figure 1 are derived in terms of experimentally measured relaxation rates and magnetization decreases. To check the reliability of the method, we then examine a) the base-catalyzed exchange in a number of primary and secondary amides, where there is no mechanistic ambiguity,[42] and b) water-catalyzed proton exchange in two protonated imidic esters, since these are likewise mechanistically unambiguous and serve as models for the imidic-acid route. We then apply the technique to amide proton exchange in both dilute and strong acid to investigate the dynamics of the proton transfer reactions in these media.

B. Experimental

1. Chemicals and Sample Preparation

Amides were used without further purification. The ratio of solvent protons to amide N-H protons was determined by carefully weighing both amide and solvent. Thorough dissolution of amides in ethylene glycol (Mallinckrodt, Analytical Reagent quality) was effected with a Vortex mixer. Solutions were not degassed. pH measurements were made with a Corning Model 5 pH meter connected to a dual function probe. The electrode was rinsed with distilled water and dried prior to each pH measurement. NMR probe temperature measurements were made with an ethylene glycol sample according to the method of Van Geet.[51]

a. Acetamide

Acetamide was purchased from Eastman Organic Chemicals. Acetamide 99% enriched in ^{15}N was obtained from Stohler Isotope Chemicals. To study proton exchange in strong acid, 364.4 mg acetamide was dissolved, with cooling, in 1.786 g 96% sulfuric acid and 1.920 g 20% fuming sulfuric acid (both purchased from Mallinckrodt). To study the amide in strong acid under nonexchange conditions, 182.3 acetamide was dissolved, with cooling, in 1.984 g 20% fuming sulfuric acid. Acetamide samples in ethylene glycol (Mallinckrodt, Analytical Reagent grade) were about 3 M in amide.

b. Acrylamide

Acrylamide was purchased from Aldrich Chemical Co. and was of Gold Label quality. Ethylene glycol solutions were about 3 M in amide, and a trace of hydroquinone (less than 1 mg/ml) was added to prevent amide polymerization.

c. Methacrylamide

Methacrylamide was purchased from Aldrich Chemical Co. Sample preparation was identical to that for acrylamide.

d. Benzamide

Benzamide was obtained from Matheson, Coleman and Bell. Benzamide 99% enriched in ^{15}N was purchased from Stohler Isotope Chemicals. Proton exchange was studied in both ethylene glycol at ca. 1 M concentration, and in 60% v/v aqueous methanol at ca. 0.5 M concentration.

e. Salicylamide

Salicylamide was purchased from Aldrich and solutions were 0.5 M amide in ethylene glycol.

f. Formamide-d_1

Formamide-d_1, 99% enriched in deuterium at the formyl position, was obtained from Stohler Isotope Chemicals. Samples were about 3 M amide in ethylene glycol.

g. Ethyl Oxamate

This compound was purchased from Aldrich Chemical Co. and was studied at 0.5 M concentration in ethylene glycol.

h. Cyanoacetamide

This compound was obtained from Matheson, Coleman, and Bell, and was studied at 1.5 M amide in ethylene glycol.

i. Malonamide

Malonamide was purchased from Aldrich and was studied at 0.7 M amide in ethylene glycol.

j. Chloroacetamide

Chloroacetamide was obtained from Aldrich Chemical Co. and was studied at 1.5 M amide in ethylene glycol.

k. Dichloroacetamide

This compound was purchased from Aldrich Chemical Co. and was about 3 M amide in ethylene glycol.

l. Trichloroacetamide

Trichloroacetamide was purchased from Tridom Fluka.

m. 3,5-Dinitrobenzamide

This compound was obtained from Aldrich Chemical Co. To study exchange in strong acid, 710.0 mg amide was added, with cooling, to 2.615 g 96% sulfuric acid and 2.660 g 20% fuming sulfuric acid. A second, nonexchanging sample consisted of 299.3 mg amide in 2.351 g 20% fuming sulfuric acid. The amide does not undergo aromatic sulfonation under these conditions.

n. N-Methylformamide

N-Methylformamide was purchased from Aldrich Chemical Co. Amide solutions were 2 M in water. Amide solutions in 10%

and 16% fuming sulfuric acid were prepared, with cooling, to study exchange in strong acid.

o. N-t-Butylformamide

This compound was purchased from Aldrich Chemical Co. Solutions were 2 M amide in ethylene glycol.

p. Ethyl Acetimidate Hydrochloride, $MeC(OEt)NH_2^+Cl^-$

The method of MacKenzie et al.[52] was followed. Equimolar amounts of ethanol (14.5 ml, 0.25 mole) and acetonitrile (13.0 ml, 0.25 mole) were placed in a dry 100 ml 3-necked flask. To this solution was added 25 ml dry ether, and HCl gas was bubbled through the solution for 45 minutes with vigorous stirring. The flask was maintained at room temperature. After 45 minutes the solution was decanted into an Erlenmeyer flask which was stoppered and placed in a freezer to induce crystallization of the imidic ester hydrochloride. Three to seven days were required for crystallization. Crystals were suction filtered, washed twice with cold dry ether, and stored under nitrogen in a freezer. Yield: 6.0 g (20%). In DMSO-d_6, the salt has the following NMR spectrum: δ 1.32 (t, 3 H), 2.45 (s, 3 H), 4.50 (q, 2 H), 11.25 (s, 1 H, broad), 12.20 (s, 1 H, broad). It decomposes slowly at room temperature in this solvent to give acetamide and ethyl chloride, and hydrolyzes slowly in aqueous sulfuric acid to give ethyl acetate and ammonium chloride.[53]

A sample of ethyl acetimidate for saturation-transfer experiments was prepared as follows. To produce water-catalyzed exchange,

a 46% w/w aqueous sulfuric acid solution was first prepared by addition of 2.3774 g 96% H_2SO_4 to 2.5562 g distilled water. To 0.9156 g of this solution was added 712.3 mg of the imidic ester hydrochloride, and dissolution was accomplished with a Vortex mixer. Data acquisition for T_1 and saturation-transfer experiments was complete within two hours from the time of mixing. After this time, less than 5% hydrolysis had occurred, as determined by integration of the NMR spectrum.

To produce nonexchange conditions, a 57% w/w aqueous H_2SO_4 solution consisting of 2.332 g H_2SO_4 and 1.750 g distilled water was prepared. To 0.9181 g of this solution was added 533.6 mg of the imidic ester. No hydrolysis had occurred in the time necessary for data acquisition.

q. 2-Iminotetrahydrofuran hydrochloride.[54]

4-Hydroxybutyronitrile was synthesized according to the method of Asknes and Prue.[55] To 50 ml of 3:1 EtOH/H_2O (v/v) was added 10 g 1-chloro-3-hyroxypropane (purchased from Aldrich Chemical Co.) and 8.5 g KCN. The solution was refluxed with vigorous stirring for 1.5 hr. The solution was then cooled and filtered, and solvent was removed on a rotary evaporator. The brown solution was vacuum distilled, and the fraction boiling at 98-100°C/6 mm was collected (lit bp 107-108°C/11 mm (4), 122°C/15 mm (5)). Yield: 1.8 g (20%). NMR ($CDCl_3$): δ 1.95 (m, 2 H), 2.60 (t, 2 H), 2.80 (s, 1 H, broad), 3.85 (t, 2 H).

Dry hydrogen chloride was passed into a solution of 1.8 g 4-hydroxybutyronitrile in 65 ml dry ether maintained at 10-15°C with external cooling. After 45 minutes, the solution was decanted into a second flask, stoppered, and stored at room temperature for several days. A light yellow oil precipitated out and eventually set to crystals. The NMR spectrum in DMSO-d_6 had the following signals: δ 2.30 (m, 2 H), 3.20 (t, 2 H), 4.80 (t, 2 H), 11.49 (s, 1 H, broad), 11.75 (s, 1 H, broad).

Water-catalyzed exchange of the imine hydrochloride in DMSO-d_6 was produced by addition of several drops of distilled water to the NMR sample tube.

2. pH Adjustment

Acid catalysis was induced by addition of microliter quantities of 0.5 M HCl or concentrated sulfuric acid to 1-ml samples. The 0.5 M HCl solution used in most of the experiments was aqueous, but similar kinetics could be obtained by using a 0.5 M sulfuric acid solution in ethylene glycol. The small amounts of water introduced into ethylene glycol solutions of the amides by use of aq. 0.5 M HCl thus appear to have no significant effecd on the kinetic results (see, e.g., columns 1 and 2 of Table 7. These samples were pH-adjusted with sulfuric acid in ethylene glycol and aqueous HCl, respectively).

In the case of formamide-d_1, addition of sulfuric acid to the sample tube resulted in amide hydrolysis and an unstable pH. To

minimize these effects, acid-catalyzed exchange was produced with trichloroacetate buffers (stock solutions were 0.5 M CCl_3COOH and 0.5 M CCl_3COONa in ethylene glycol), and ST values were constant over the time period required to make the measurements.

Base-catalyzed exchange was induced with phosphate buffers prepared from stock solutions 0.25 M Na_2HPO_4 and 0.25 M NaH_2PO_4 in ethylene glycol. Non-exchanging samples were either unbuffered or were acetate-buffered with stock solutions 0.5 M HOAc and 0.5 M NaOAc in ethylene glycol.

The anions of the E and Z isomers of N-methylformamide in DMSO-d_6 and dixoane were generated by adding a large excess of potassium t-butoxide to a dioxane solution 0.2 M in N-methylformamide and to a DMSO-d_6 solution 1 M in N-methylformamide. The isomeric N-methyl signals appeared as sharp signals, and the anion equilibrium constant was determined by direct integration of the 220 MHz spectrum.

3. Spin Assignment in O-protonated Formamide

The 220 MHz spectrum of a 1 M solution of formamide in 20% fuming sulfuric acid was recorded. In this solvent, amide proton exchange with solvent is slow, and the formyl signals appear upfield of the N-H region. The formyl portion of the spectrum (consisting of four lines) was calculated with the computer program ITRCAL.[56] With assumed trans and cis formyl-NH coupling constants of 15 and 7 Hz, respectively[57] (appropriate to alkenes), spectra were calculated

assuming 1) that the downfield N-H proton was responsible for the (larger) trans coupling, and 2) that the upfield N-H proton was responsible for the trans coupling. The iterative feature of ITRCAL, which requires a nearly complete experimental spectrum in which most transitions are assigned, was not used because the N-H protons were too broad to be delineated.

4. NOE Experiments

Signal assignments were made in 2, 2-dichloroacetamide, salicylamide, N-methylformamide, and N-t-butylformamide with NOE experiments. Dichloroacetamide was examined under non-exchange conditions at 3 M concentration in non-degassed ethylene glycol. H_E and H_Z were separately irradiated, and the intensity change of the α-C-H proton was measured with difference spectra, obtained by subtracting the on-resonance spectrum from the off-resonance spectrum. NOE experiments on salicylamide were conducted under non-exchange conditions at 1 M concentration in non-degassed ethylene glycol. H_E and H_Z were separately irradiated, and the intensity enhancement of the phenyl proton ortho to the amide group was measured with difference spectra.

Signal assignments for the isomeric methyls in N-methylformamide were made with NOE measurements on a non-degassed 2 M solution in D_2O, where N-methyl and formyl signals appear as sharp singlets. N-methyl signals were separately irradiated, and

intensity changes at the corresponding formyl signals were measured.

The isomeric amide protons in N-butylformamide were assigned with NOE experiments on a 2 M solution of the amide in non-degassed ethylene glycol. Amide protons were separately irradiated, and intensity changes at the corresponding formyl sites were measured with difference spectra.

5. Line-shape Measurements

a) Measurements of the line-broadening due to exchange in acrylamide, acetamide, and ^{15}N-benzamide were made on a Varian HR-220 NMR spectrometer in the FT mode. A sweep width of 2000 Hz and memory storage of 16 K were used. Between four and thirty-two acquisitions were obtained, using a 40 microsecond pulse and a delay time between pulses of 3 sec. 3 Hz of artificial line-broadening was employed. Width at half-height was obtained from a 60 Hz expanded plot (50 cm long) of the peak in question. Non-exchange, acid-catalyzed, and base-catalyzed samples were each recorded at several different pH values. t-Butyl alcohol was employed as internal standard. Spectrometer homogeneity was readjusted after each pH adjustment by maximizing the ringing of the t-butanol signal. Finally, the following procedure was used to obtain exchange rates for the N-H protons:

1) Width at half-height of the t-BuOH standard (= $\Delta\nu^{o}_{1/2}$, inhomogeneity) was subtracted from non-exchange N-H half-height

widths ($\equiv \Delta\nu^{o}_{1/2} = \Delta\nu^{o}_{1/2}$, inhomogeneity $+ \Delta\nu^{o}_{1/2}$, quadrupolar).

3) All of the non-exchange widths for a given N-H proton were averaged ($= \Delta\nu^{o}_{1/2}$, quadrupolar).

3) Width at half-height of the t-BuOH standard was subtracted from exchanging N-H half-height widths ($= \Delta\nu_{1/2}$).

4) Total exchange rates were computed from the equation[59] $k = \pi(\Delta\nu_{1/2} - \Delta\nu^{o}_{1/2}$, quadrupolar).

5) The ratio of exchange rates of the N-H protons was then computed at a given pH by taking the quotient of the results in step 4 for H_E and H_Z.

b) The N-H line shape of acrylamide was also recorded for intermediate acid-catalyzed exchange rates on a Varian EM-390 NMR spectrometer. The amide was 3 M in ethylene glycol. The N-H region was expanded to 90 Hz and plotted out 30 cm long. The non-exchange line shape was recorded in unbuffered solution, with successive spectra recorded upon addition of microliter aliquots of 0.5 M HCl, and, finally, concentrated sulfuric acid. Under non-exchange conditions, the N-H signals are 52 Hz apart, and have line-widths of 10.3 Hz.

c) Proton exchange rates in water were measured on a JEOL PFT-100 NMR spectrometer. A concentric tube arrangement was employed in order to use the internal lock system of the spectrometer. An inner 5-mm tube containing the aqueous amide solution was placed

inside a 10-mm tube containing 99% acetone-d_6. The 5-mm tube was held in place by two 10 mm vortex plugs bored with holes large enough to allow the 5 mm tube to be easily inserted and removed, but small enough to keep the arrangement from wobbling during operation. The spectrometer was locked on the deuterium signal and tuned on the free induction decay of the protic solvent.

An ^{14}N-decoupling power of approximately 16 watts at a frequency of 7191148 Hz was used. Spectra had a sweep width of 1000 Hz, and 2 Hz of artificial line-broadening was employed. Spectra were plotted out 33.3 cm long, with a horizontal scale of 50 Hz. Linewidths were measured, and relative exchange rates were computed as in a) above.

d) NMR lineshapes of N-methyl- and N-t-butylformamide under exchange conditions were simulated with a computer program employing Bloch equations modified for chemical exchange effects.[59,60] In the absence of strong coupling, the NMR absorption-mode intensity function $I(\omega)$ is equal to the imaginary part of $iC[\underset{\sim}{1} \cdot (\underset{\sim}{T}_2 + \underset{\sim}{B} + i\underset{\sim}{X})^{-1} \cdot \underset{\sim}{p}]$ where $\underset{\sim}{T}_2$ is a diagonal matrix containing $1/T_2$ values for the various sites, $\underset{\sim}{X}$ is a constant matrix containing the frequency variable ω in radians/sec, and $\underset{\sim}{B} = \underset{\sim}{K} - i\underset{\sim}{\Omega}$, where $\underset{\sim}{\Omega}$ is a diagonal chemical shift matrix with elements ω_{ii} in radians/sec for each site and $\underset{\sim}{K}$ is a rate-constant matrix with off-diagonal elements k_{ij} defined to be the first-order rate constant for exchange from site j to site i and diagonal elements $k_{ii} = -\sum_j k_{ij}$. $\underset{\sim}{1}$ and $\underset{\sim}{p}$ are unit row vectors and

population column vectors, respectively, and C is a scaling constant. To calculate the NMR lineshape from this expression, a matrix inversion must be performed for each frequency value. To avoid this time-consuming process, we have written a computer program which diagonalizes $\underset{\sim}{T}_2 + \underset{\sim}{B}$ by calculating transformation matrices $\underset{\sim}{S}$ and $\underset{\sim}{S}^{-1}$ such $\underset{\sim}{T}_2 + \underset{\sim}{B} = \underset{\sim}{S} \cdot \underset{\sim}{D} \cdot \underset{\sim}{S}^{-1}$. Substituting this expression for $\underset{\sim}{T}_2 + \underset{\sim}{B}$ into the expression above yields $I(\omega) = \text{Im } iC [\underset{\sim}{1} \cdot \underset{\sim}{S} \cdot (\underset{\sim}{D} + i\underset{\sim}{X})^{-1} \cdot \underset{\sim}{S}^{-1} \cdot \underset{\sim}{p}]$. The diagonal matrix sum $\underset{\sim}{D} + i\underset{\sim}{X}$ is then readily inverted and the indicated matrix multiplication performed. Since the diagonalization needs only be performed once, and then inversion of a diagonal matrix is trivial, a considerable savings in computing time is realized. Input parameters are fractional site populations, chemical shifts in Hz, T_2 values in the absence of exchange (related to the width at half-height for each signal by $T_2 = 1/\pi\Delta\nu^{o}_{1/2}$), and first-order rate constants for site interchange. Unequal linewidths resulting from different long-range coupling constants were accounted for with effective T_2 values that duplicated the measured linewidths.[62] For N-methylformamide, the rate constant matrix $\underset{\sim}{K}$ has the form

$$\underset{\sim}{K} = \begin{Vmatrix} & k_{ZS}/2 & k^R_{ZE} & \\ k_{ZS}/2 & & & k^R_{EZ} \\ k^R_{EZ} & & & k_{ES}/2 \\ & k^R_{EZ} & k_{ES}/2 & \end{Vmatrix}$$

where k^R_{EZ} is the rate constant for exchange of the E methyl into the Z site, and site pairs (1, 2) and (3, 4) are doublet components of E and Z methyls, respectively. N-methyl doublet components exchange with each other as a result of proton exchange, and with the corresponding component of the other doublet as a result of isomerization. The rate of doublet collapse is one-half the rate of proton exchange, since only those exchanges which result in replacement of a proton with opposite spin are detectable.

For N-t-butylformamide, the rate constant matrix $\underset{\sim}{K}$ is given by

$$\underset{\sim}{K} = \begin{Vmatrix} & k_{ZS}/2 & & & & & & \\ k_{ZS}/2 & & & & & & & k_{SZ} \\ & & & & & & & k_{SZ} \\ & & & & k_{ES}/2 & & & \\ & & & k_{ES}/2 & & & & \\ & & & & & & & k_{SE} \\ & & & & & & & k_{SE} \\ & k_{ZS} & k_{ZS} & & & k_{ES} & k_{ES} & \end{Vmatrix}$$

where site groups [1, 2 - 3, 4] and [5, 6 - 7.8] are [formyl-amide] doublet components in the E and Z isomers, respectively, and site 9 is solvent. Formyl doublet components exchange with each other as a result of proton exchange, the rate of doublet collapse again being one-half the rate of proton exchange. Amide N-H doublet components exchange directly into the solvent site. For both $\underset{\sim}{K}$ matrices presented above, the diagonal elements have been omitted, but these are added by our computer program. Calculations were performed on a Burroughs B6700 computer, and the best fit between experimental and calculated spectra was based on visible superposition of the spectra.

6. Saturation-transfer Studies

Saturation-transfer studies were performed on a Varian HR-200 NMR spectrometer in the FT mode. Ethylene glycol was used as solvent for exchange studies in dilute acid or base because we have observed that its greater viscosity relative to water decreases scalar relaxation of N-H protons bound to the quadrupolar ^{14}N nucleus.[61] The N-H signals are considerably sharpened, with half-widths of 7-10 Hz. Formamide-d_1, however, has N-H half-widths of 18 Hz. Computer storage size was typically 4 K.

a. Saturation-transfer (ST) Experiments

Saturation-transfer experiments were conducted as follows. Employing a sweep width of 2500 Hz, an offset of zero (OF = 0), and from four to thirty-two acquisitions (depending on sample concentration), an initial spectrum was acquired while irradiating 10^4 Hz downfield of the right-hand edge of the spectrum. Computer-controlled saturation during only the delay part of the acquisition sequence was utilized, and the first acquisition was discarded (DG = 1), since saturation had not been achieved. Sufficient signal attenuation was used to prevent "clipping" of the free induction decay (FID). A pulse time P2 (typically 70 microseconds) approximating a 90° pulse was used to obtain the initial spectrum, which was then phased. With this phasing maintained, 180° pulse times were determined as those which gave pure dispersion spectra for the NH and OH protons. These two 180°

pulses generally differed by 6-8 microseconds, so half their average was taken as the 90° pulse. We have found that a 90° sampling pulse is necessary to reject x-y magnetization created by the saturating irradiation. Using the new P2 value, the off-resonance spectrum was reacquired and rephased. The resultant phasing parameters were used in subsequent ST experiments. A delay between acquisitions (D5) of 3 seconds was adequate, except in the case of N-methylformamide, where a D5 of 15 seconds was employed.

Decoupler power levels slightly more than adequate for saturation were used. Nevertheless, appreciable (about 10%) "spillover" of radiation applied at one N-H site to the other N-H site was sometimes observed, owing to finite frequency synthesizer bandwidth. Therefore, I^o for the upfield site was taken to be the intensity upon irradiating upfield of this site by an amount equal to the chemical shift difference of the two sites, and likewise for the downfield site. These equilibrium intensities were then used to calculate saturation transfer values involving the two sites.

For ^{15}N-substituted acetamide and benzamide, H_E and H_Z appear as sharp 90 Hz doublets due to coupling to ^{15}N. Saturation-transfer measurements involving these protons were performed by simultaneously irradiating both components of H_E or H_Z (vide infra) and measuring intensity changes at the downfield and upfield components of H_E and H_Z, respectively. Direct spillover was not significant with the very low decoupler power levels used.

To measure an N-methyl ST value in N-methylformamide, where the isomeric N-methyls appear as 5 Hz doublets, both components of the E doublet were saturated, a line-broadening parameter of 1 Hz was employed, and the peak height of one component of the Z doublet was used as a measure of signal intensity.

Using computer control of the second irradiating frequency, free induction decays (FID's) were acquired while irradiating downfield of site E, upfield of site Z, and at the solvent site S. This cycle was repeated five times. Another set of FID's was then acquired while irradiating off-resonance (10^4 Hz downfield), at site E, and at site Z. This cycle was also repeated five times. Using the link ZEDGSA at the outset of data acquisition allowed all thirty FID's to be stored on disk. Acquiring raw data as rapidly as possible in this way minimized the effects of amide hydrolysis, instrument instability, and homogeneity changes during the experiments.

After data collection was complete, all FID's were processed and restored with identical line-broadening, phasing, scaling, and baseline-leveling parameters, using the link GAEMFTPSBFAISA. Since heights of Lorentzian lines are proportional to intensity, a line-broadening parameter of 3 Hz was generally used to impart idealized shape to the signals, so that changes in corrected peak heights could be used as a measure of intensity changes. We verified that signal integration gave the same reult as that obtained by use of peak heights, but the latter method was considerably more accurate. The region to

be baseline-fixed was specified by zooming in (using ZO) on a region encompassing the signals of interest. It was not necessary to baseline-fix the solvent signal. Each intensity used in the calculation of saturation-transfer values was thus the average of five separate determinations. Such values typically had a standard deviation of ± 3%, so that the standard error of their mean was typically 1.5%.

b. Measurement of Apparent Spin-Lattice Relaxation Rates (T_1 Experiments)

Two types of transient experiments were performed. Apparent relaxation rates for E and Z sites were determined while saturating the solvent site S, and the apparent relaxation rate of the solvent was measured while simultaneously saturating E and Z sites. The irradiating frequency was fixed and not under computer control. Double irradiation was accomplished by modulation of a saturating side band. This was achieved by using a Wavetek audio generator (Model 131A) connected to a double-balance mixer (Scientific Components Corp., Model ZAD-1H) to add and subtract the proper audio frequency from the carrier frequency, which was positioned midway between the sites to be saturated. In the case of ^{15}N-substituted benzamide and acetamide, both E and Z doublets were simultaneously saturated utilizing a higher decoupler power level and irradiating frequencies centered midway between components of a given doublet. No leakage to the solvent site was detected.

To measure N-methyl relaxation rates in N-methylformamide,

where the isomeric N-methyls appear as 5 Hz doublets, a line-broadening parameter of 1 Hz was employed. Solvent was not decoupled, and the peak height of one component of each doublet was used as a measure of signal intensity.

Relaxation rate data were obtained using a nonselective 180°-τ-90° inversion-recovery pulse sequence. Typically, a total of twenty delay times τ was entered randomly, and included four infinity values (τ = D5). Delay times spanned about four half-lives. From eight to thirty-two acquisitions were used in T_1 E, Z(S) experiments; four acquisitions sufficed for the T_1 S(E, Z) experiment. Transient experiments were performed by applying the saturating frequency or frequencies, waiting long enough to accomplish saturation (= 7 T_1), then executing the 180°-τ-90° pulse sequence. The saturating frequency was maintained continuously except during the actual pulses. The link WTZEGOSA was used to collect and store relaxation data as rapidly as possible, again to minimize the effect of instrumental instabilities on the data. Once collected, stored FID's were processed using the same link and parameters as in ST experiments. Corrected peak heights were used as intensity values, and plots of $\ln(I^{\infty} - I_t)$ vs time were made, where I^{∞} is the average of four infinity values and I_t the NMR intensity at time t. Relaxation data were fitted to straight lines using a weighted linear least-squares program with weighting factors $W_t = (I^{\infty} - I_t)^2$. Weighting minimizes

in importance intensity values at long delay times. These values are inherently less accurate, since the quantity $(I^{\infty} - I_t)$ is the (small) difference between two large numbers. It is especially important to minimize in importance intensity differences at long delay times for E and Z spins, which we expect to be less accurate than intensity differences for delay times near one half-life. Semi-logarithmic plots of relaxation data were always highly linear.

Due to the existence of positive nuclear Overhauser enhancements[58] involving the E and Z protons under nonexchange conditions, it was necessary to perform ST and T_1 experiments on both nonexchanging and exchanging samples. The rate constants measured under nonexchange conditions are equal to $k_{ij}^{o} - \sigma_{ij}$, where k_{ij}^{o} is the uncatalyzed rate of exchange from site i to site j, and σ_{ij} is a term involving transition probabilities linking the mutually relaxing spins. Rate constants measured under exchange conditions are equal to $k_{ij}^{o} - \sigma_{ij} + k_{ij}^{H+}[H+]$ or $k_{ij}^{o} - \sigma_{ij} + k_{ij}^{OH-}[OH^-]$, so k_{ij}(exchange) - k_{ij} (nonexchange) gives the true value of k_{ij}^{H+} or k_{ij}^{OH-}.

C. Results

1. Signal Assignment

It is generally accepted that the E substituent appears downfield of the Z substituent in amides.[40,63,64] We have sought to confirm this assignment, wherever necessary, with lanthanide shift studies, computer simulation of the NMR spectrum, and NOE experiments.

It was particularly important to confirm the signal assignment in ethyl oxamate, where the anisotropy of the second carbonyl group might produce a reversal in chemical shifts, moving H_E upfield of H_Z.[67,68] To make the signal assignment, a shift study was undertaken employing the paramagnetic shift reagent $Eu(fod)_3$ (Aldrich Chemical Company) in a dilute solution of ethyl oxamate in $CDCl_3$. This reagent has been shown to complex at the carbonyl oxygen of tertiary amides,[69] shifting the Z substituent downfield to a greater extent than the E substituent. Moreover, $Eu(fod)_3$ complexes preferentially at amide oxygen relative to ester oxygen by a factor of about five.[70] In the present study, both amide protons moved downfield upon incremental addition of $Eu(fod)_3$, but the upfield proton moved downfield to a greater extent, passing under the downfield proton and re-emerging at lower field, thereby establishing it as H_Z.

In the case of the imidic esters, all NOE experiments were inconclusive. Nevertheless, the lower-field N-H singlet can be

assigned to H_E by analogy to the assignment[66] (based on NOE) in $HC(OMe)N^+Me_2$ of the downfield N-methyl signal to the E methyl. Such a constancy holds in the case of primary and tertiary amides.[40] Further support for this assignment comes from a computer simulation of the 220 MHz spectrum of O-protonated formamide (see Experimental and Figure 2). This spin system is a second order ABC system, and could best be simulated (Fig. 2b) by assuming that the upfield N-H proton is responsible for the larger, presumably trans coupling to the formyl proton (15 Hz). On this basis, the upfield amide proton in O-protonated formamide, and presumably in the structurally analogous imidic esters as well, is H_Z.

Irradiation of the downfield amide proton of 2,2-dichloroacetamide, as shown in Figure 3, results in an intensity enhancement of 8.1% at the α C-H proton, whereas irradiation of the upfield amide signal has no effect. Since the magnitude of the enhancement is proportional to the spatial closeness of the interacting spins,[58] the downfield proton is therefore H_E. Likewise, irradiation of the downfield amide proton in salicylamide resulted in a 12% enhancement of the phenyl proton ortho to the amide group, while irradiation of the upfield amide signal had essentially no effect, thus confirming that the above assignment is applicable to salicylamide.

Signal assignments for the isomeric methyls in N-methylformamide were confirmed with NOE measurements. The less and more abundant N-methyl singlets appear at δ 2.87 and 2.73,

Figure 2. a) 220 MHz spectrum of O-protonated formamide. Plot width is 600 Hz. b) Simulated spectrum (expanded), assuming that the upfield proton is responsible for the larger trans coupling to the formyl proton. c) As b), but with the opposite assignment.

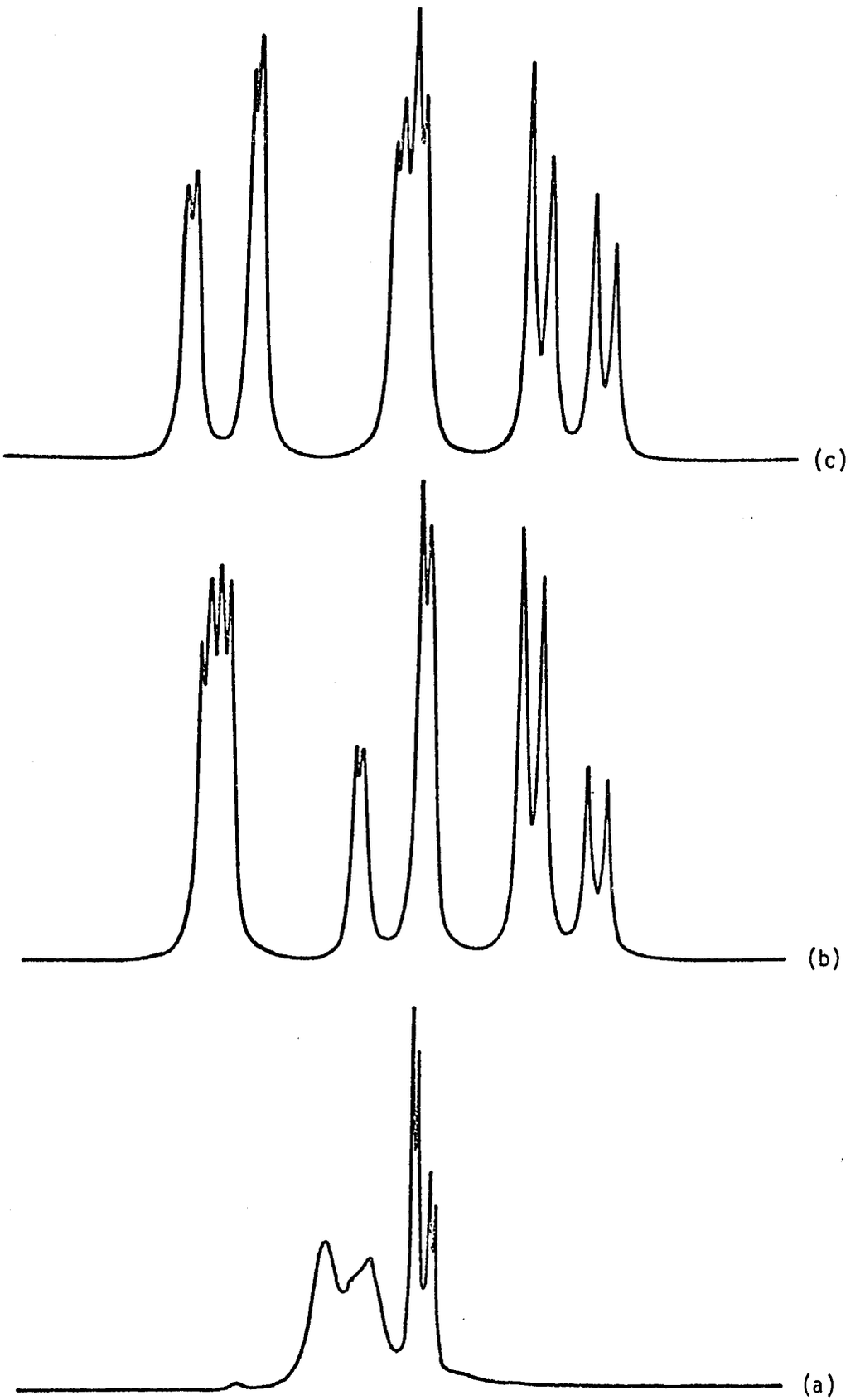

Figure 3. NOE experiment on 2, 2-dichloroacetamide. a) Off-resonance spectrum, b) low-field amide proton saturated, and c) difference spectrum obtained by subtracting b) from a) and multiplied by four to illustrate the NOE at H_{α}. Plot widths are 600 Hz.

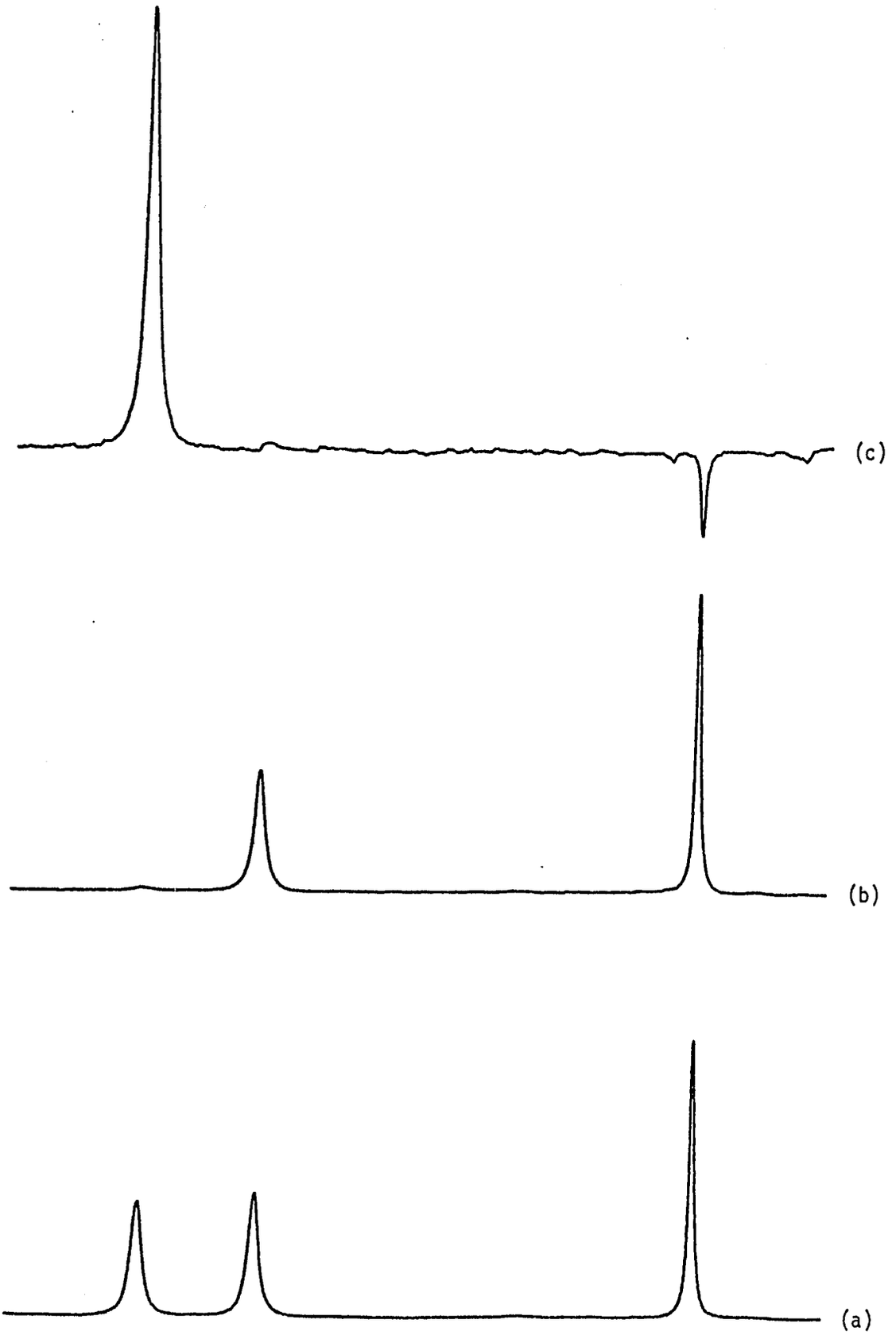

respectively, with the corresponding formyl protons appearing at δ 7.92 and 7.01. Irradiation of the less abundant methyl results in a 5.6 ± 1.2% intensity increase at its formyl proton, while irradiation of the more abundant methyl produces an intensity increase of 2.2 ± 0.4% at its formyl proton. Thus the downfield N-methyl at δ 2.87 is closer to its formyl proton and is therefore the E methyl. K_{EZ}, the equilibrium constant for the ratio of E to Z forms, was measured by direct integration to be 13.5 ± 0.2, somewhat larger than the value of 11.5 reported[63] for neat N-methylformamide.

For N-t-butylformamide in ethylene glycol, the less and more abundant isomeric amide protons appear at δ 8.02 (doublet, J = 12.4 Hz) and 7.72 (broad singlet), respectively, with the corresponding formyl protons at δ 8.24 (J = 12.4 Hz) and 7.15 (J = 2.1 Hz). Saturation of the upfield amide proton produces a 10% intensity increase at its formyl site, as illustrated in Figure 4, while saturation of the downfield amide doublet produces an intensity decrease at its formyl doublet (probably due to non-first-order spin coupling). In N-t-butylformamide, therefore, the upfield proton is H_E (trans to the carbonyl), so that the chemical shifts are reversed relative to other amides. Chemical shifts of the E and Z amide protons in formamide-d_1 are δ 7.73 and 7.37, respectively, so the reversal observed in NBF results solely from a downfield shift of δ 0.65 for H_Z relative to formamide. The signal assignment made on the basis of NOE experiments is consistent with the generalization[65] that the formyl-H_Z

Figure 4. NOE experiment on N-t-butylformamide. a) Off-resonance spectrum, b) irradiation of the upfield amide proton, and c) difference spectrum obtained by subtracting b) from a) to illustrate NOE at the formyl doublet spin-coupled to the irradiated proton. Plot widths are 400 Hz.

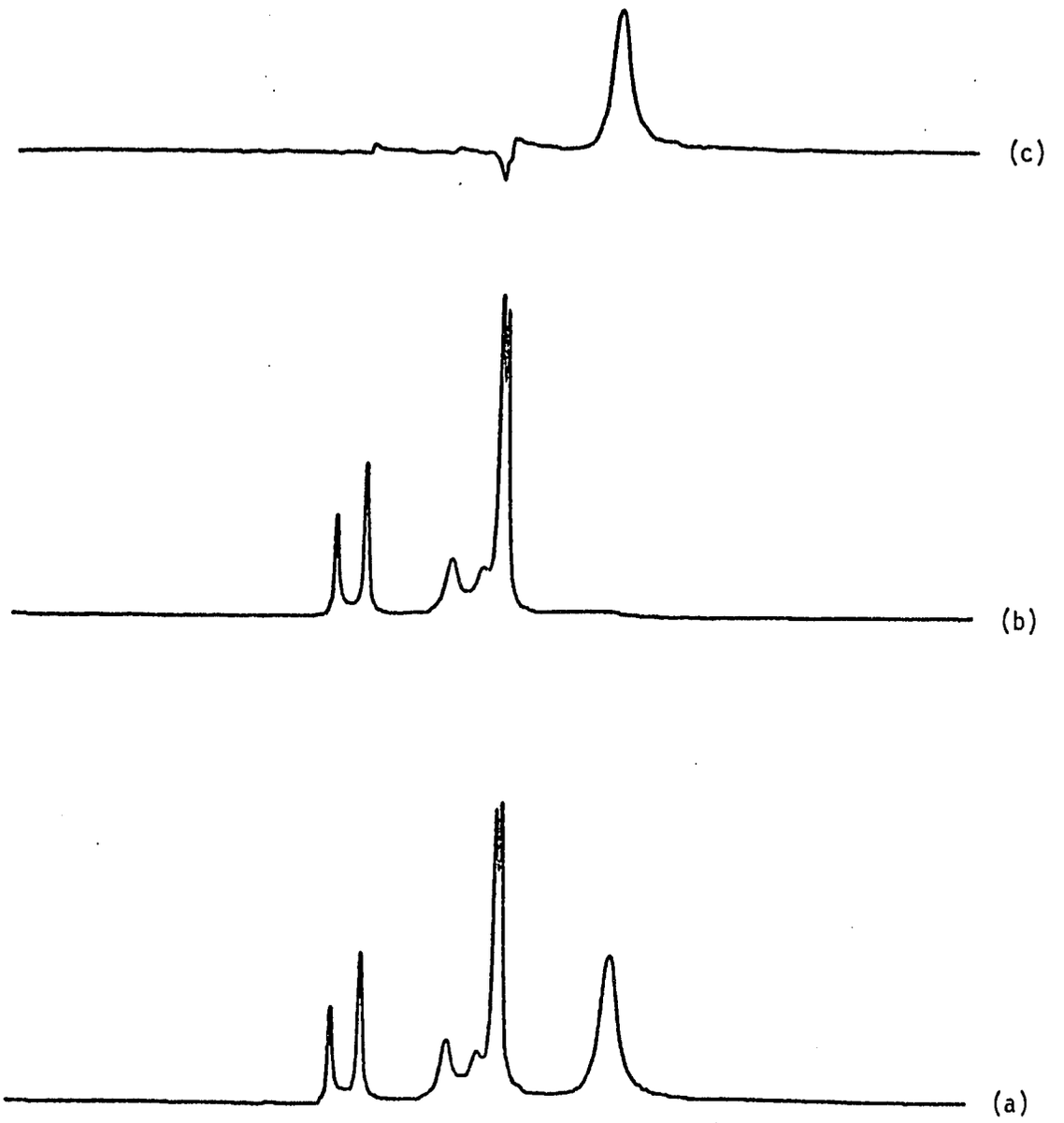

coupling constant is larger than the formyl-H_E coupling constant. K_{EZ} was determined by direct integration of the NMR spectrum to be 2.2, comparable to the value of 2.3 previously reported.[87] In N-t-butylformamide, as in N-methylformamide, the Z (s-trans) form is the more stable stereoisomer. It is very likely that NBF is the sole exception to the general observation that H_E is at lower field; we will assume for the remaining amides in this study that H_E resonates at lower field.

2. Saturation-Transfer Equations for Three-Site Exchange

For amides in ethylene glycol and concentrated sulfuric acid, solvent viscosity decreases scalar relaxation of the N-H protons by the quadrupolar ^{14}N nucleus,[61] so that they appear reasonably sharp, with half-widths of ~8-10 Hz. Nevertheless, lineshape analysis is generally not sufficiently accurate for comparing intramolecular and intermolecular exchange, so we have extended[48] the NMR saturation-transfer technique of Forsén and Hoffman[49] to the determination of all six rate constants of the three-site systems (H_E, H_Z, $H_{solvent}$) studied here. In these experiments, equilibrium intensities and spin-lattice relaxation rates in Fourier transform NMR spectra are measured under conditions of selective saturation. Use of the method has largely been restricted to studies of two-site exchange,[75-81] and the few multi-site systems which have been examined[50,82-85] may be reduced to sets of two-site exchanges, since some of the rate constants are zero. In contrast, all six rate constants are non-zero for

the majority of systems studied here, and the resulting "indirect transfer of saturation" complicates the equations.

Forsén and Hoffman have given the general form of the coupled differential equations describing the time-dependence of exchanging spin systems.[50] For a system consisting of three magnetically non-equivalent sites i, j, and k, with populations p_i, p_j, and p_k, the specific form of this equation is

$$\frac{dI_i}{dt} = -(k_{ij} + k_{ik} + R_i)(I_i - I_i^o) + k_{ji}(I_j - I_j^o) + k_{ki}(I_k - I_k^o) \qquad [1]$$

In Eq. [1], R_i is the spin-lattice relaxation rate for site i, k_{ij} is the first-order rate constant for exchange from site i to site j, I_i is the NMR intensity of site i at time t, and I_i^o is its equilibrium intensity. Analogous equations may be written for j and k. Note that k_{ij} and k_{ji} are related by equilibrium according to $k_{ij} p_i = k_{ji} p_j$. Although Eq. [1] assumes that dipole-dipole relaxation is negligible, this assumption is not necessary to the experiments described here, because we quantitatively account for the dipolar contribution to the observed rate constants as described in the Experimental.

In order to measure all six first-order rate constants, two types of experiments are performed. In saturation-transfer (ST) experiments,[58,86] a given site is saturated, so that its intensity I is zero, and the steady-state intensities (relative to off-resonance equilibrium intensities) at the other sites are measured. When there is exchange, saturation of one site will decrease the intensities at

the other sites, provided rates of exchange and spin-lattice relaxation are comparable. These intensity decreases are defined by

$$t_i(j) = (I_i^o - I_i^o(j))/I_i^o \qquad [2]$$

where $I_i^o(j)$ is the equilibrium intensity of site i when site j is saturated, and I_i^o is its equilibrium intensity without saturating irradiation. This quantity is analogous to the nuclear Overhauser enhancement, $f_i(j)$, which is given by $(I_i^o(j) - I_i^o)/I_i^o$, a positive number when there is enhancement. We define $t_i(j)$ to be greater than zero when there is saturation transfer. Six such values are measured. From Eqs. [1] and [2], and setting $I_i^o/I_j^o = p_i/p_j$, it follows that

$$t_i(j) = \frac{k_{ji}\, p_j + k_{ki}\, p_k\, t_k(j)}{(k_{ij} + k_{ik} + R_i)\, p_i} \qquad [3]$$

where the second term in the numerator is due to the indirect transfer of saturation resulting from chemical exchange from site j to site i via site k.

In T_1 experiments, apparent spin-lattice relaxation rates are measured. While sites j and k are simultaneously saturated, site i is inverted (see Experimental) and the recovery of the steady-state intensity is followed; similar experiments are performed on j and k. Under these conditions of selective saturation, $I_i(j,k)$ approaches $I_i^o(j,k)$ as a single exponential, where $I_i^o(j,k)$ is the steady-state intensity of site i when sites j and k are simultaneously irradiated.

It follows from Eq. [1] that the slope of a plot of $-\ln[I_i^o(j,k) - I_i(j,k)]$ vs time is given by

$$M_i(j,k) = k_{ij} + k_{ik} + R_i \qquad [4]$$

Equations [3] and [4] comprise nine equations that may be solved simultaneously to give expressions for all six rate constants and all three spin-lattice relaxation rates. The general solution for the rate constants is given in Eq. [5], where the second term in the numerator corrects for indirect transfer of saturation from site j to site i via site k.

$$k_{ji} = M_i(j,k) \cdot \frac{t_i(j) - t_i(k)t_k(j)}{1 - t_j(k)t_k(j)} \cdot \frac{p_i}{p_j} \qquad [5]$$

If sites i and k have the same apparent relaxation rate when site j is held saturated [that is, $M_i(j) = M_k(j) \neq M_j(i,k)$], then it is adequate to measure relaxation rates for these sites by a non-selective inversion-recovery experiment while saturating site j only. The suitability of this approximation has been checked in our experiments by verifying that signals i and k pass through the baseline at the same time in a non-selective 180° - τ -90° experiment (see Experimental) when site j is saturated. The quantity $(I_i(j) - I_i^o)/(I_k(j) - I_k^o)$ which appears from Eq. [1] is then time-independent and can be set equal to p_i/p_k. With this approximation, $I_i(j)$ approaches $I_i^o(j)$ as a simple exponential. It follows that the slope of a plot of $-\ln[I_i^o(j) - I_i(j)]$ vs time is

$$M_i(j) = k_{ij} + k_{ik} + R_i - k_{ki}p_k/p_i \qquad [6]$$

and similarly for site k. Solution of the simultaneous equations [3] and [6] gives rate constants for exchange into sites i and k of the form

$$k_{ji} = M_i(j) \cdot \frac{t_i(j) + t_i(k)t_k(j)}{1 + t_i(k) + t_j(k)(t_i(j) - t_k(j))} \cdot \frac{p_i}{p_j} \qquad [7]$$

Since $M_j(i,k)$ is still measured while simultaneously saturating sites i and k, k_{ij} and k_{kj} are given by adaptations of Eq. [5].

In the experiments described here, it proved instrumentally impossible to simultaneously saturate the E (or Z) and solvent sites. We therefore measured apparent relaxation rates of the E and Z sites while saturating only solvent, verifying that they passed through the baseline at the same time in T_1 experiments. The specific forms of Eq. [7] used to calculate rate constants for exchange into the E and Z sites are

$$k_{SE} = M_E(S) \cdot \frac{t_E(S) - t_Z(S)t_E(Z)}{1 - t_E(Z) + t_s(Z)(t_E(S) - t_Z(S)} \cdot \frac{p_E}{p_S} \qquad [7a]$$

$$k_{ZE} = M_E(S) \cdot \frac{t_E(Z) - t_E(S)t_S(Z)}{1 - t_E(Z) + t_S(Z)(t_E(S) - t_Z(S))} \cdot \frac{p_E}{p_Z} \qquad [7b]$$

$$k_{EZ} = M_Z(S) \cdot \frac{t_Z(E) - t_S(E)t_Z(S)}{1 - t_Z(E) + t_S(E)(t_Z(S) - t_E(S))} \cdot \frac{p_Z}{p_E} \qquad [7c]$$

$$k_{SZ} = M_Z(S) \cdot \frac{t_Z(S) - t_Z(E)t_E(S)}{1 - t_Z(E) + t_S(E)(t_Z(S) - t_E(S))} \cdot \frac{p_Z}{p_S} \qquad [7d]$$

A further simplification results when all three sites have the same apparent relaxation rate ($M_i = M_j = M_k$). Then T_1 experiments can be performed without the necessity of saturation during the experiment. It is a good approximation to set the quantities $(I_i - I_i^o)/(I_j - I_j^o)$ in Eq. [1] equal to p_i/p_j. With this approximation, the approach to equilibrium of each site is again governed by a single exponential. Slopes of plots of $-\ln(I_i^o - I_i)$ vs time are given by

$$M_i = k_{ij} + k_{ik} + R_i - \frac{k_{ji}p_j}{p_i} - \frac{k_{ki}p_k}{p_i} \qquad [8]$$

and solution of Eqs. [3] and [8] leads to rate constants

$$k_{ji} = M_i \cdot \frac{t_i(j) - t_i(k)t_k(j)}{1 - t_i(k) + t_j(k)(t_i(j) - t_k(j)) - t_i(j) + t_i(k)t_k(j)} \cdot \frac{p_i}{p_j} \qquad [9]$$

3. Nonexchange Results

At pH ~ 4.7, acid- and base-catalyzed proton exchange of these amides with solvent is slow, so that irradiation of the solvent signal has no effect on the intensities of H_E and H_Z, and vice versa. However, saturation of either amide proton generally produces an intensity decrease at the other site, due to rotation about the C-N partial double bond. Such an experiment, on ^{15}N-labeled benzamide, is illustrated in Figure 5. The results of ST and T_1 experiments for a variety of amides, in ethylene glycol or 60% aq. methanol, and for ethyl acetimidate hydrochloride in aqueous sulfuric acid, are presented in Table 1.

Figure 5. ST experiment on ^{15}N-labeled benzamide in ethylene glycol under non-exchange conditions. a) Off-resonance spectrum, b) with irradiation of both components of H_E, c) with irradiation of both components of H_Z. Calculated rate constants are k_{EZ} = 3.15 sec^{-1}, k_{ZE} = 3.14 sec^{-1} (see Table 1). Plot widths are 500 Hz.

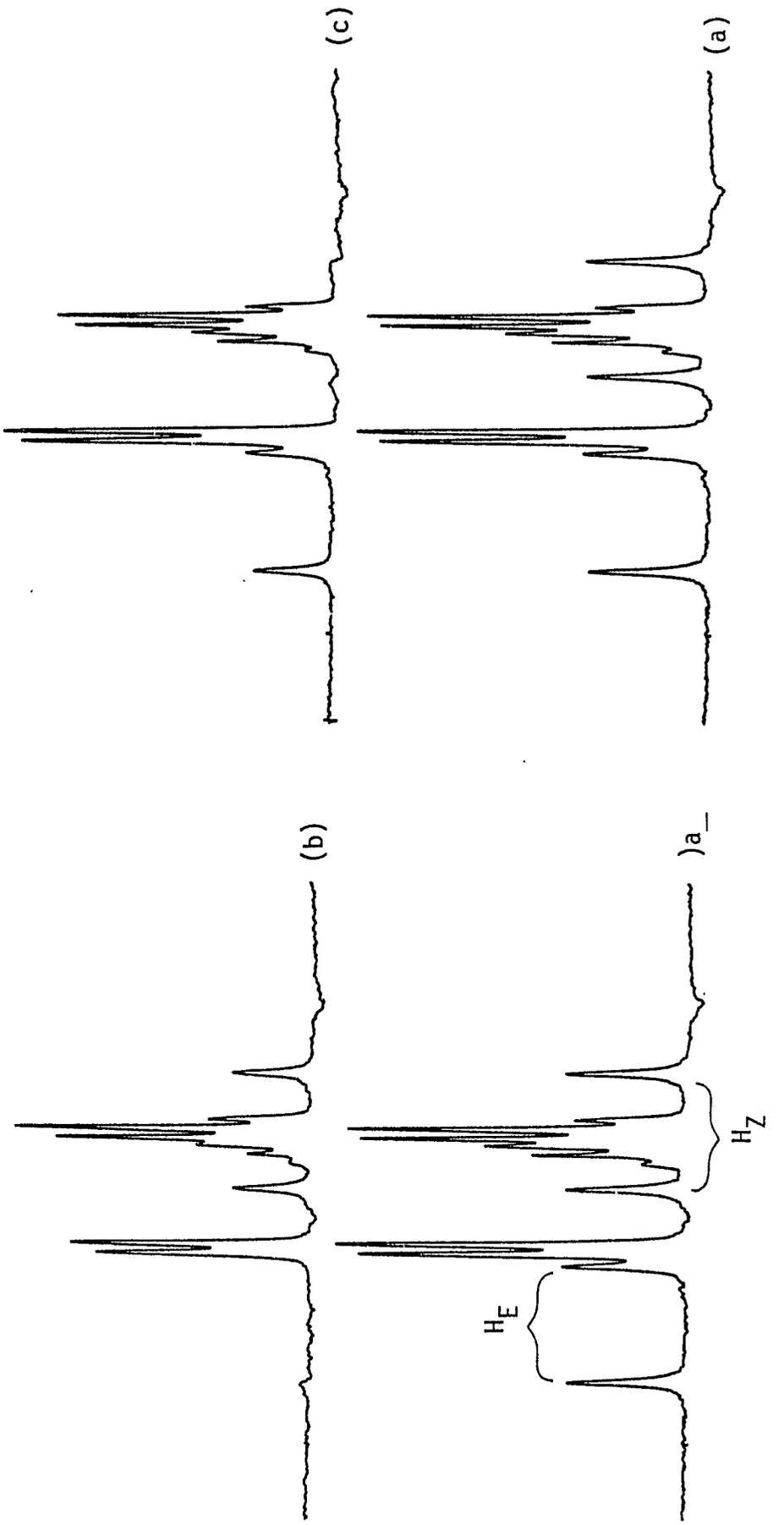

Table 1. Saturation-transfer Results for Rotation about the C-N Bond of RCONHR' (R'= -H, -Me, - +Bu) and Ethyl Acetimidate [a]

	Acetamide	Acetamide-^{15}N	Acetamide	Acrylamide	Methacrylamide	
Solvent	EF	EG	20% fuming H_2SO_4	EG	EG	
$t_E(Z)$	0.13 ±0.007	0.11 ±0.007	0.04 ±0.008 [e]	0.328 ±0.02	0.49[b] ±0.03	0.61[c] ±0.04
$t_Z(E)$	0.14 ±0.008	0.10 ±0.006	0.05 ±0.008 [e]	0.322 ±0.02	0.50 ±0.03	0.61 ±0.04
M_E, sec^{-1}	2.67 ±0.10	3.29 ±0.13	8.74 0.35	2.95 ±0.12	5.00 ±0.19	4.63 ±0.18
M_Z, sec^{-1}	2.46 ±0.10	3.02 ±0.12	8.74 ±0.35	2.82 ±0.12	5.00 ±0.20	4.63 ±0.18
k_{EZ}, sec^{-1}	0.40 ±0.03	0.34 ±0.03	-0.42 ±0.03	1.34 ±0.13	5.00 ±0.64	7.24 ±1.15
k_{ZE}, sec^{-1}	0.41 ±0.03	0.40 ±0.03	-0.34 ±0.02	1.44 ±0.14	4.80 ±0.60	7.24 ±1.15

	Benzamide	Benzamide-^{15}N		Benzamide-^{15}N	Salicylamide	Formamide-d_1
Solvent	EG	EG		60% aq. MeOH	EG	EG
$t_E(Z)$	0.31 ±0.02	0.32 ±0.02	0.32 ±0.02	0.69 ±0.04	0.72 ±0.04	0
$t_Z(E)$	0.31 ±0.02	0.37 ±0.03	0.33 ±0.02	0.71 ±0.04	0.73 ±0.04	0
M_E, sec^{-1}	7.50 ±0.31	6.67 ±0.26	6.25 ±0.25	1.65 ±0.06	7.97 ±0.30	1.61
M_Z, sec^{-1}	7.50 ±0.31	5.36 ±0.21	5.67 ±0.23	1.50 ±0.06	7.93 ±0.29	1.58
k_{EZ}, sec^{-1}	3.37 ±0.32	3.15 ±0.33	2.79 ±0.27	3.67 ±0.77	21.44 ±4.84	0
k_{ZE}, sec^{-1}	3.37 ±0.32	3.14 ±0.30	2.95 ±0.29	3.67 ±0.73	20.49 ±4.47	0

Table 1. Continued

	N-Methylformamide[d]		N-t-Butylformamide	Ethyl Oxamate	Cyanoacetamide	Malonamide
Solvent	H_2O, pH 2.3	H_2O, pH 7.6	EG	EG	EG	EG
$t_E(Z)$			0	0.169 ±0.01 [e]	0.243 ±0.014	0
$t_Z(E)$	0.15 ±0.02	0.12 ±0.02	0	0.173 ±0.01 [e]	0.274 ±0.016	0
M_E, sec^{-1}			-2.42	4.44 ±0.18	3.11 ±0.12	4.30
M_Z, sec^{-1}	0.27 ±0.03	0.32 ±0.02	-1.55	5.10 ±0.20	3.00 ±0.12	4.30
k_{EZ}, sec^{-1}	0.6 ±0.1	0.6 ±0.1	0	-0.75 ±0.06	1.13 ±0.10	0
k_{ZE}, sec^{-1}			0	-0.64 ±0.05	1.00 ±0.09	0

	Chloroacetamide	Dichloroacetamide	Ethyl Acetimidate
Solvent	EG	EG	42% H_2SO_4
$t_E(Z)$	0.251 ±0.016	0.018 ±0.010	0.159 ±0.01 [e]
$t_Z(E)$	0.247 ±0.015	0.023 ±0.011	0.197 ±0.011 [e]
M_E, sec^{-1}	3.20 ±0.13	3.74 ±0.14	6.14 ±0.24
M_Z, sec^{-1}	3.10 ±0.12	3.54 ±0.13	6.34 ±0.25
k_{EZ}, sec^{-1}	1.02 ±0.09	0.08 ±0.04	-1.04 ±0.07
k_{ZE}, sec^{-1}	1.07 ±0.10	0.07 ±0.04	-0.84 ±0.06

[a] At 23°C and pH ~ 4.7 unless otherwise noted. Saturation-transfer resulting from solvent irradiation was ≤2%.

[b] 22°C.

[c] 25°C.

[d] Data for E and Z methyls.

[e] Nuclear Overhauser enhancement.

In all cases, apparent spin-lattice relaxation rates were measured with a non-selective 180°-τ-90° pulse sequence, and rate constants were calculated with Eq. [9]. This equation can be used to calculate k_{EZ} and k_{ZE} because both amide protons have approximately equal rates of relaxation, and there is no saturation transfer from or into solvent. These values represent a lower limit to the true values, since they include negative cross-relaxation terms. Indeed, for ethyl acetimidate hydrochloride, ethyl oxamate, and O-protonated acetamide, where increased double-bond character decreases the rate of uncatalyzed rotation, nuclear Overhauser enhancements are observed in ST experiments, so that the apparent rate constant, which is the difference between the true rate constant and the cross-relaxation term is negative. However, the magnitude of these apparent rate constants implies (see Table 1) that $\sigma_{EZ} \leq 1\ sec^{-1}$, so that the rate constants k_{EZ} and k_{ZE} reported in Table 1 do not differ from the true values by $> 1\ sec^{-1}$.

4. Base-catalyzed Exchange

Saturation-transfer studies of base-catalyzed exchange were undertaken for a variety of primary amides, and the results are presented in Table 2. Typical saturation-transfer experiments, on acrylamide and salicylamide in ethylene glycol, are presented in Figures 6 - 10. For primary amides except malonamide, apparent relaxation rates of the E and Z protons were measured while irradiating solvent, while the solvent relaxation rate was measured with

Figure 6. Saturation-transfer study of base-catalyzed exchange of acrylamide in ethylene glycol at pH 8.21. a) Off-resonance spectrum, b) with irradiation of H_E, c) with irradiation of H_Z. Results are listed in Table 2. Note intensity losses resulting from transfer of saturation. Plot widths are 900 Hz.

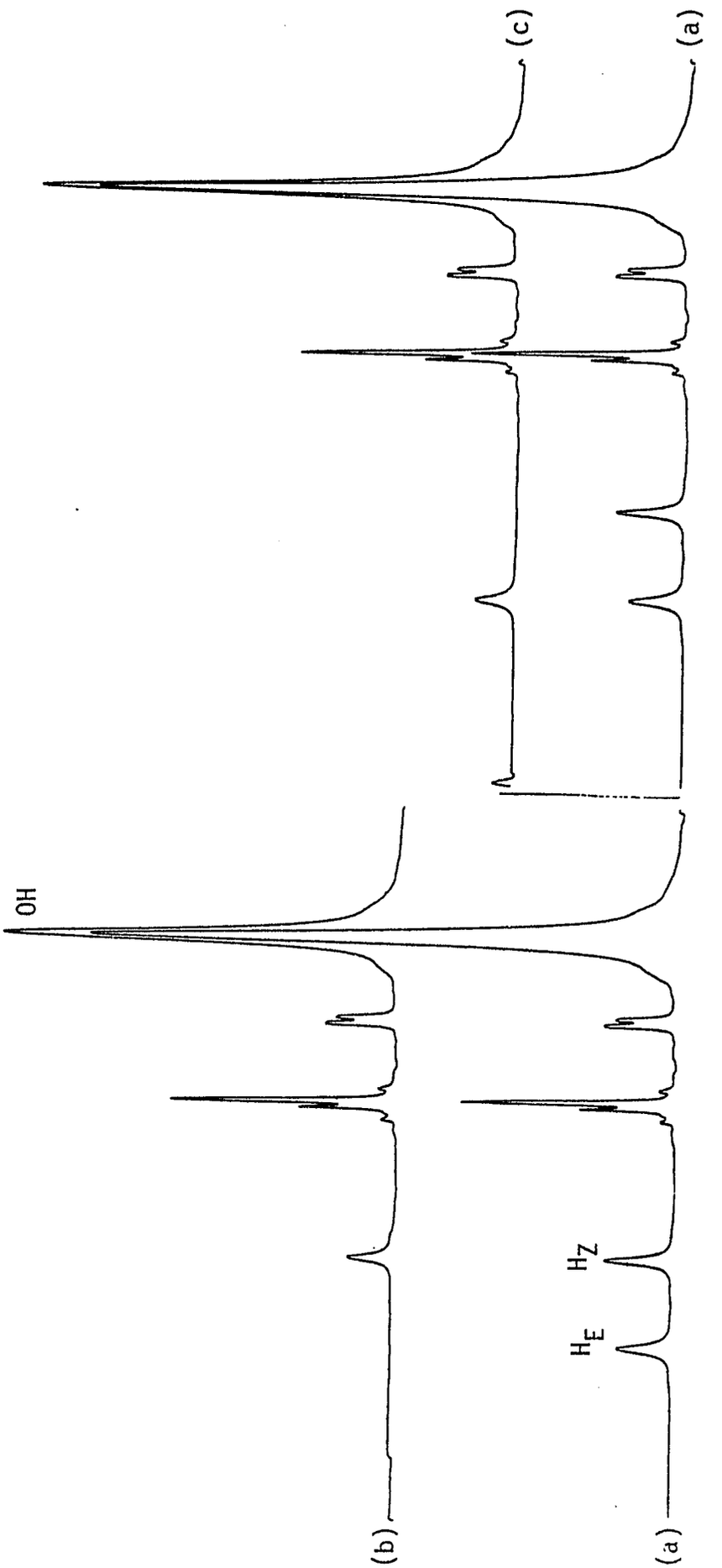

Figure 7. Same acrylamide sample as in Figure 6. a) Off-resonance spectrum, and b) with irradiation of the solvent signal. Note resulting intensity losses at the amide sites. See Table 2 for results. Plot width is 800 Hz.

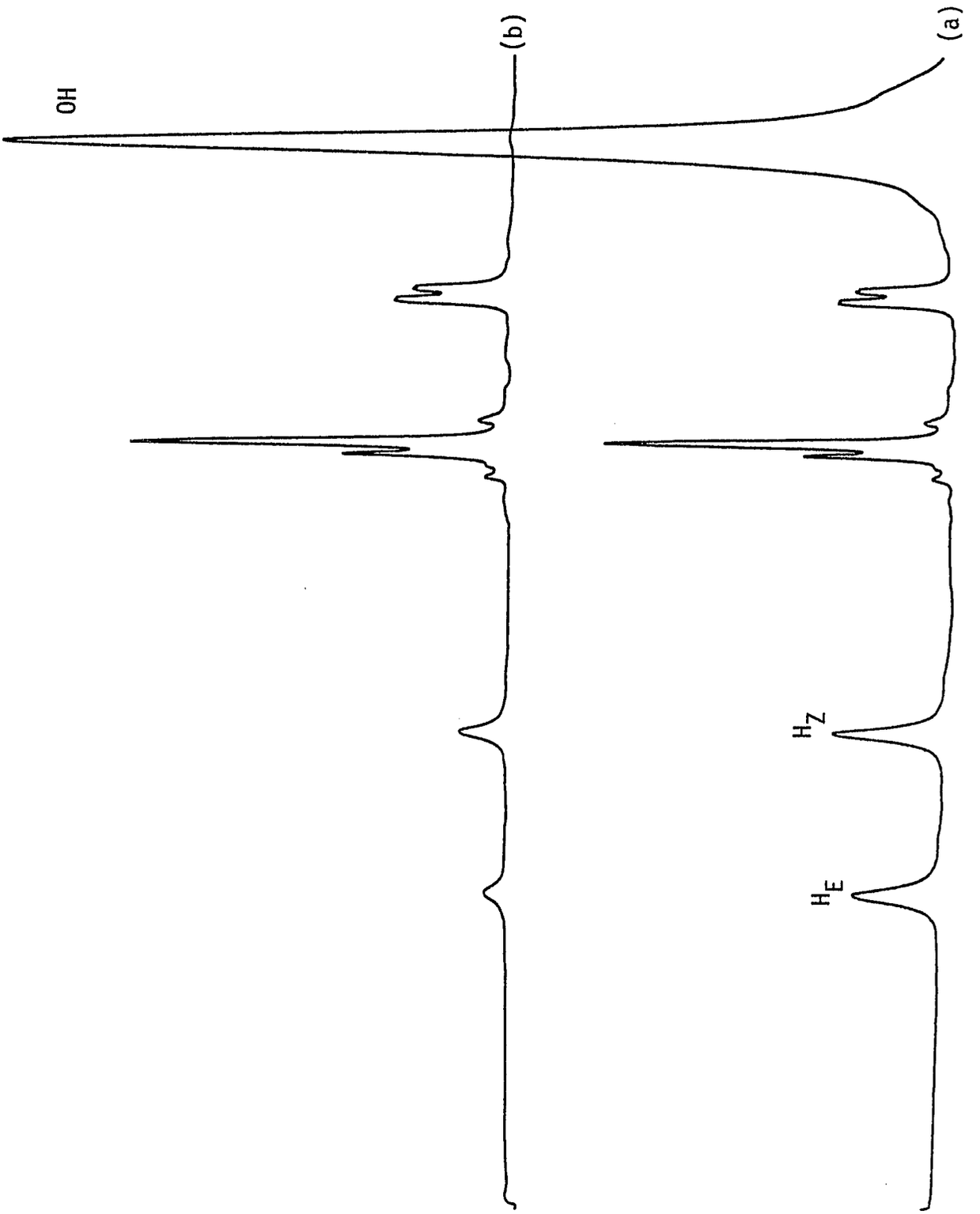

Figure 8. Same acrylamide as in Figure 6. T_1 plot of an inversion-recovery sequence performed on H_E and H_Z while holding solvent saturated. Results are listed in Table 2. Plot width is 300 Hz.

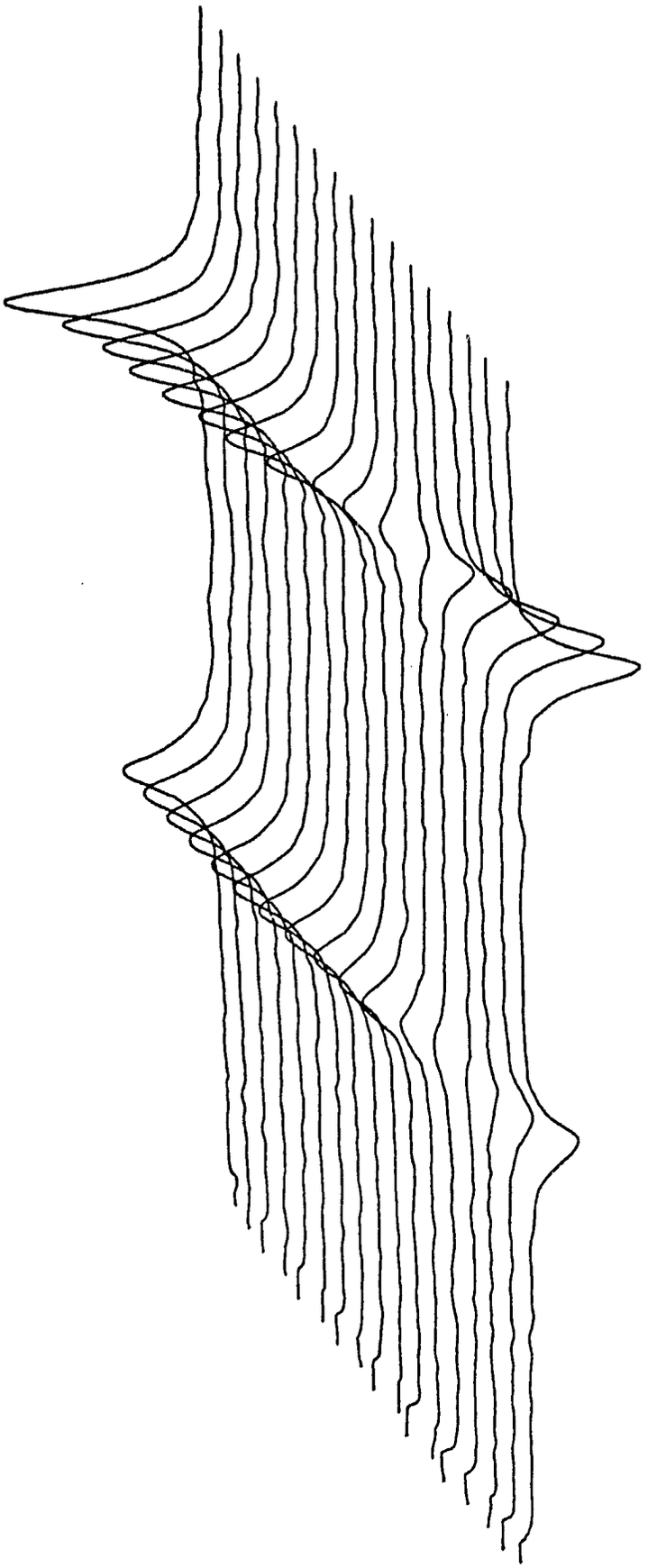

Figure 9. Same acrylamide sample as in Figure 6. T_1 plot of an inversion-recovery sequence performed on the solvent signal while holding H_E and H_Z simultaneously saturated. Results are listed in Table 2. Plot width is 500 Hz.

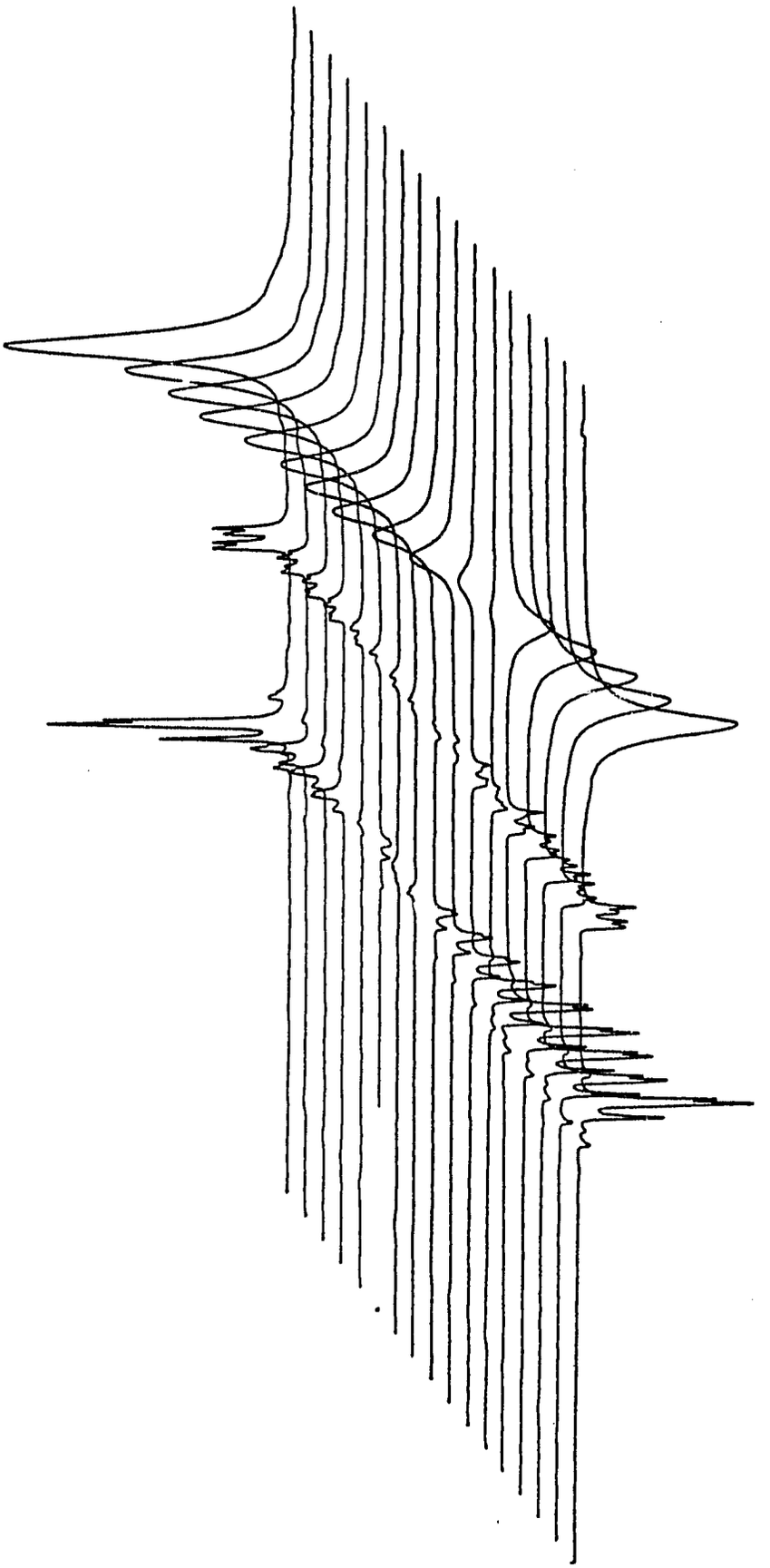

Figure 10. Saturation-transfer study of base-catalyzed exchange of salicylamide in ethylene glycol. pH = 6.95. a) Off-resonance spectrum, b) with irradiation of solvent (not shown), and c) difference spectrum obtained by subtracting b) and a), illustrating equal amounts of saturation transfer from solvent into E and Z sites. Plot widths are 600 Hz.

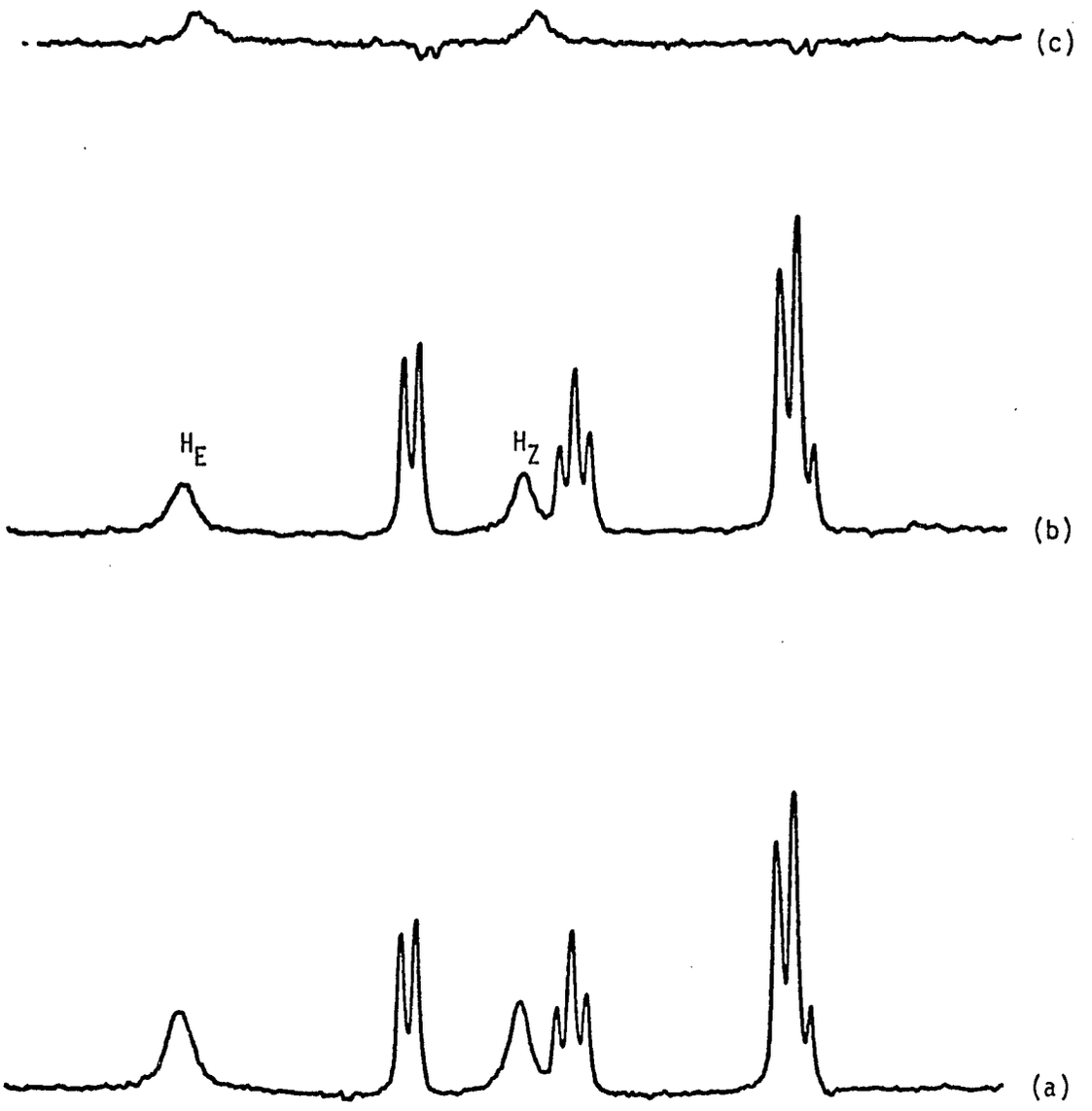

Table 2. Saturation-transfer Results[a] for Base-catalyzed Exchange of E and Z Hydrogens of $RCONH_2$ and HCONHtBu

	Acetamide	Acrylamide	Methacrylamide	Benzamide-^{15}N	Salicylamide
Solvent	EG	EG	EG	EG	EG
pH, measured	8.1	8.21	8.20	8.0	6.95
$[H_S]/[H_{E,Z}]$	11.24	12.22	13.00	59.6	84.8
$t_E(Z)$	0.128 ±0.008	0.205 ±0.010	0.455 ±0.024	0.185 ±0.011	0.638 ±0.037
$t_Z(E)$	0.161 ±0.010	0.273 ±0.017	0.473 ±0.025	0.220 ±0.013	0.640 ±0.038
$t_S(E)$	0.129 ±0.008	0.326 ±0.018	0.207 ±0.012	0.045 ±0.002	0.041 ±0.002
$t_S(Z)$	0.062 ±0.004	0.189 ±0.012	0.191 ±0.011	0.030 ±0.002	0.041 ±0.002
$t_E(S)$	0.554 ±0.033	0.743 ±0.040	0.531 ±0.030	0.434 ±0.024	0.386 ±0.024
$t_Z(S)$	0.332 ±0.02	0.566 ±0.030	0.503 ±0.029	0.341 ±0.019	0.391 ±0.023
$M_E(S), sec^{-1}$	5.07 ±0.20	15.67 ±0.58	11.49 ±0.44	13.50 ±0.50	11.36 ±0.44
$M_Z(S), sec^{-1}$	3.88 ±0.16	8.74 ±0.32	10.56 ±0.40	10.70 ±0.41	11.35 ±0.45
$M_S(E,Z), sec^{-1}$	1.96 ±0.08	3.29 ±0.12	3.00 ±0.12	2.10 ±0.09	2.30 ±0.08
k_{ZE}, sec^{-1}	0.01 ±0.07	-0.22 ±0.37	0.14 ±1.52	-0.11 ±0.39	-0.95 ±5.60
k_{EZ}, sec^{-1}	0.04 ±0.08	-0.18 ±0.34	0.23 ±1.55	0.03 ±0.36	-1.78 ±5.90
k_{ES}, sec^{-1}	2.67 ±0.21	11.69 ±0.98	5.80 ±0.77	5.01 ±0.41	4.86 ±1.15
k_{ZS}, sec^{-1}	1.03 ±0.10	5.20 ±0.58	4.81 ±0.73	2.83 ±0.28	4.89 ±1.15
k_{SE}, sec^{-1}	0.261 ±0.020	0.97 ±0.08	0.485 ±0.07	0.103 ±0.01	0.051 ±0.01
k_{SZ}, sec^{-1}	0.103 ±0.01	0.39 ±0.05	0.392 ±0.06	0.057 ±0.006	0.053 ±0.01

Table 2. Continued

	Formamide-d_1	N-t-butylformamide		Malonamide
Solvent	EG	EG		EG
pH, measured	7.1	8.4	8.5	7.85
$[H_S]/[H_{E,Z}]$	14.96			56.0
$t_E(Z)$	0.130 ±0.007	~0	~0	0.02
$t_Z(E)$	0.089 ±0.005	~0	~0	0.03
$t_S(E)$	0.195 ±0.011	~0	~0	0.037
$t_S(Z)$	0.151 ±0.009	~0	~0	0.03
$t_E(S)$	0.794 ±0.048	0.364	0.445	0.507
$t_Z(S)$	0.679 ±0.042	>0.9	>0.9	0.314
$M_E(S)$, sec^{-1}	7.50 ±0.30	4.10 [d]	4.55 [d]	-- [b]
$M_Z(S)$, sec^{-1}	4.94 ±0.20			-- [b]
$M_S(E,Z)$, sec^{-1}	1.96 ±0.08			-- [b]
k_{ZE}, sec^{-1}	+0.09 ±0.11	0	0	0.18
k_{EZ}, sec^{-1}	-0.24 ±0.07	0	0	0.19
k_{ES}, sec^{-1}	5.39 ±0.41	1.50 ±0.15 [c]	2.02 ±0.2 [c]	4.4 [b, c]
k_{ZS}, sec^{-1}	3.73 ±0.31	12 ±2 [e]	16 ±3 [e]	2.0 [b, c]
k_{SE}, sec^{-1}	0.399 ±0.03	0.11 ±0.01	0.14 ±0.01	0.079
k_{SZ}, sec^{-1}	0.226 ±0.02			0.036

[a] Corrected for E-Z cross-relaxation and C-N bond rotation.
[b] Rate constants were calculated using M_E and M_Z from Table 1.
[c] Calculated from detailed balance.
[d] $M_E(S, Z)$ was measured.
[e] Obtained by total lineshape analysis.

simultaneous saturation of H_E and H_Z. Rate constants for exchange into E and Z sites were then calculated with Eq. [7], while rate constants for exchange into solvent were calculated with Eq. [5]. These rate constants were corrected for E-Z cross-relaxation and isomerization by subtracting from them the appropriate non-exchange rate constants in Table 1. For malonamide, approximate rates of solvent exchange were calculated with Eq. [9] and the intrinsic relaxation rates in Table 1. According to Eq. [8], it follows from detailed balance that M_i measured without irradiation is in fact just equal to R_i, the intrinsic relaxation rate, so it should be possible under these circumstances to calculate rate constants by using intrinsic relaxation rates measured in this manner. Justification for this procedure is presented in Section 1 of the Discussion.

Base-catalyzed proton exchange of N-methylformamide in water was studied by total lineshape analysis. The isomeric N-methyls are split into first-order doublets by their respective N-H protons, so this region may accurately be considered as a four-site system. The N-methyl region of the NMR spectrum of N-methylformamide was recorded as a function of increasing pH. The results are illustrated in Figure 11. The N-methyls sharpen into singlets at still higher pH. The lineshapes were computer-simulated, according to the method described in the Experimental. Program input parameters were fractional site populations calculated from K_{EZ}, the equilibrium constant for the ratio of Z to E forms, doublet

Figure 11. pH-dependence of the N-methyl signals of N-methylformamide basic range. a) pH 6.9, b) 7.0, c) 7.2, d) 7.3, e) 7.4, f) 7.45, g) 7.45, h) 7.55. Measured spectra are to the left and simulated spectra to the right.

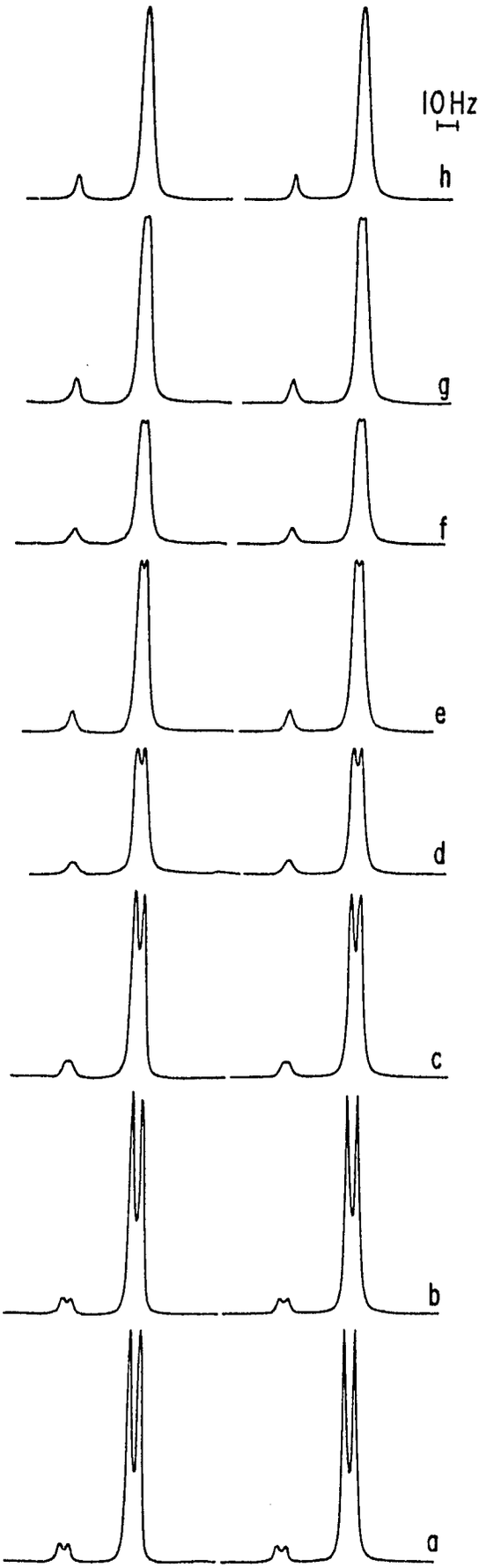

component chemical shifts, and intrinsic T_2 values for the Z and E methyls of 0.23 sec and 0.31 sec, respectively. Different T_2 values were necessary, since the four-bond formyl-methyl coupling constants differ. The values k_{ZS} and k_{ES} were then adjusted to produce the best agreement between experimental and calculated spectra. The simulated spectra are illustrated in Fig. 11, for comparison with the observed ones. It can be seen that collapse of the Z methyl doublet requires higher pH than does collapse of the E doublet, indicating that H_Z undergoes base-catalyzed exchange faster than H_E. Lineshape parameters for the simulated spectra are tabulated in Table 3. Justification for setting $k_{EZ} = k_{ZE} = 0$ in these simulations is that both N-methyls sharpen into separate singlets at a pH higher than that in Figure 11. Plots of log k_{ZS} and log k_{ES} vs pH give second-order rate constants $k_{ZS}^{OH^-} = 1.4 \times 10^8\ M^{-1}sec^{-1}$ and $k_{ES}^{OH^-} = 7.0 \times 10^7\ M^{-1}sec^{-1}$. The latter value, for the dominant stereoisomer, is in excellent agreement with the 25 °C value of $6.78 \pm 0.6 \times 10^7\ M^{-1}$ sec^{-1} reported by Molday and Kallen.[38]

In N-t-butylformamide, rate constants were determined by a combination of saturation-transfer and lineshape analysis methods, and the results are presented in Table 2. First, k_{SE} was measured in a saturation-transfer experiment. Solvent irradiation decreases H_E and largely saturates H_Z, while irradiation of H_Z has no significant effect on either H_E or solvent. Equation [5] was used to calculate k_{SE}, and k_{ES} was calculated from this value from detailed balance.

Table 3. Base-catalyzed Exchange of E and Z Protons of N-methylformamide

pH, measured	k_{ZS}, sec^{-1}	k_{ES}, sec^{-1}
6.9	9.2	4.6
7.0	11.2	5.6
7.2	19.2	9.6
7.3	26.0	13.0
7.4	32.0	16.0
7.45	33.6	16.8
7.45	34.4	17.2
7.55	43.2	21.6

To obtain k_{ZS}, the NMR spectrum under exchange conditions was computer-simulated. Isomeric formyl protons are split into doublets by their respective N-H protons (and vice versa), so the low-field region may be treated as an eight-site system, with solvent constituting the ninth site. Although the formyl-H_Z splitting is not strictly first-order ($J/\Delta\nu \sim 0.25$), it was nevertheless treated as such in the computer simulation. Program input parameters were fractional site populations calculated from K_{EZ}, nine chemical shifts, and intrinsic T_2 values for formyl and amide protons of 0.199 sec and 0.054 sec, respectively. The value of k_{ZS} was then adjusted to produce the best agreement between calculated and experimental spectra. A theoretical spectrum with $k_{ES} = 1.5\ sec^{-1}$, $k_{ZS} = 12\ sec^{-1}$, and $k_{EZ} = k_{ZE} = 0$ is presented in Figure 12 along with the experimental spectrum, which was measured at pH 8.4 in ethylene glycol. The inability of the calculated spectrum to reproduce the inequality of doublet peak heights is due to the assumption of weak coupling. The large value of k_{ZS} is consistent with the observed $t_Z(S)$ of >90% (Eq. [3]). The further observation that the isomeric t-butyl signals remain distinct throughout the basic pH range is verification for setting k_{EZ} and k_{ZE} equal to zero in the simulation.

Figure 12. Base-catalyzed exchange of N-t-butylformamide in ethylene glycol at pH 8.4. a) Measured spectrum and b) calculated spectrum with $k_{ES} = 1.5\ sec^{-1}$, $k_{ZS} = 12\ sec^{-1}$, and $k_{EZ} = k_{ZE} = 0$. Plot widths are 200 Hz.

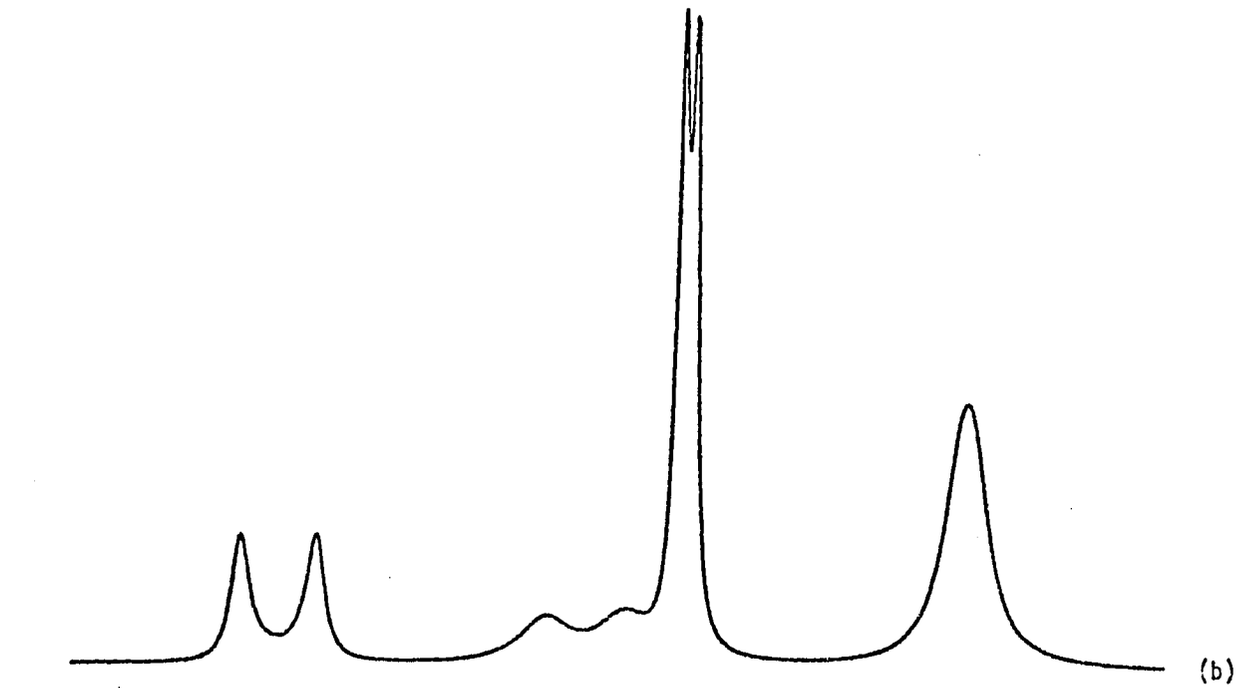

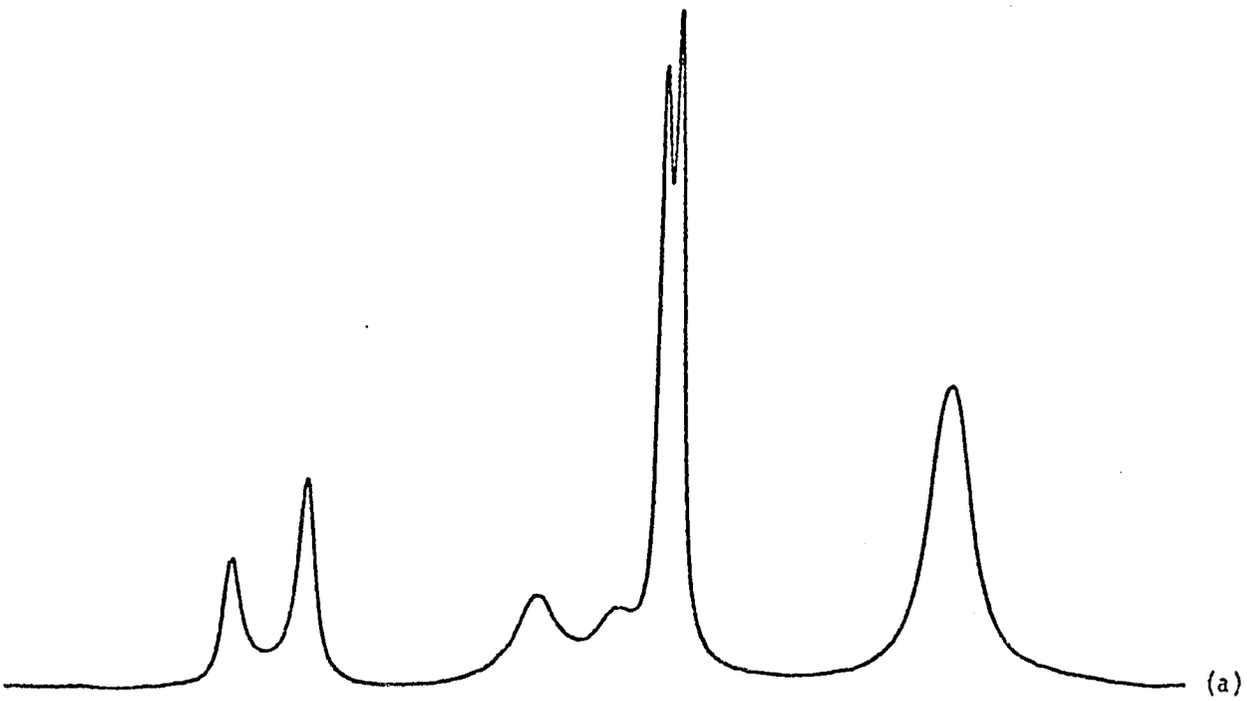

5. Proton Exchange in Imidic Esters

Water-catalyzed exchange in protonated ethyl acetimidate, $CH_3C(OEt)NH_2^+Cl$, was studied by saturation-transfer in 46 wt % aqueous sulfuric acid, where reduced water activity produces proton exchange rates small enough to be measured by saturation-transfer. A typical saturation-transfer experiment is presented in Figure 13. Note the greater transfer of saturation from solvent to the Z site. Rate constants for exchange into E and Z sites were calculated from Eq. [7], while rate constants for exchange into solvent were computed with Eq. [5]. Experimental data and computed rate constants, corrected for cross-relaxation, are presented in Table 4.

It proved impossible to perform the same experiment on protonated 2-iminotetrahydrofuran since at the sulfuric acid concentrations necessary to produce slow exchange, the N-H protons are obscured by the solvent signal. Therefore exchange was studied in wet DMSO-d_6. Addition of 100 µl H_2O to 1 ml solution of the imidate ester hydrochloride in DMSO-d_6 resulted in slow exchange, with H_E being slightly faster to exchange, as judged by relative linewidths or peak heights. Intensity losses at H_E and H_Z upon irradiation of -OH were measured (Table 4), and an approximate ratio of exchange rates was calculated with Eq. [9], assuming that the intrinsic relaxation rates R_E and R_Z were equal, and that cross-relaxation could be neglected. Thus H_E was calculated to exchange with solvent approximately 15% faster than H_Z.

Figure 13. Saturation-transfer experiment on protonated ethyl acetimidate in aqueous sulfuric acid. a) Off-resonance spectrum, and b) with solvent irradiation. Plot widths are 570 Hz.

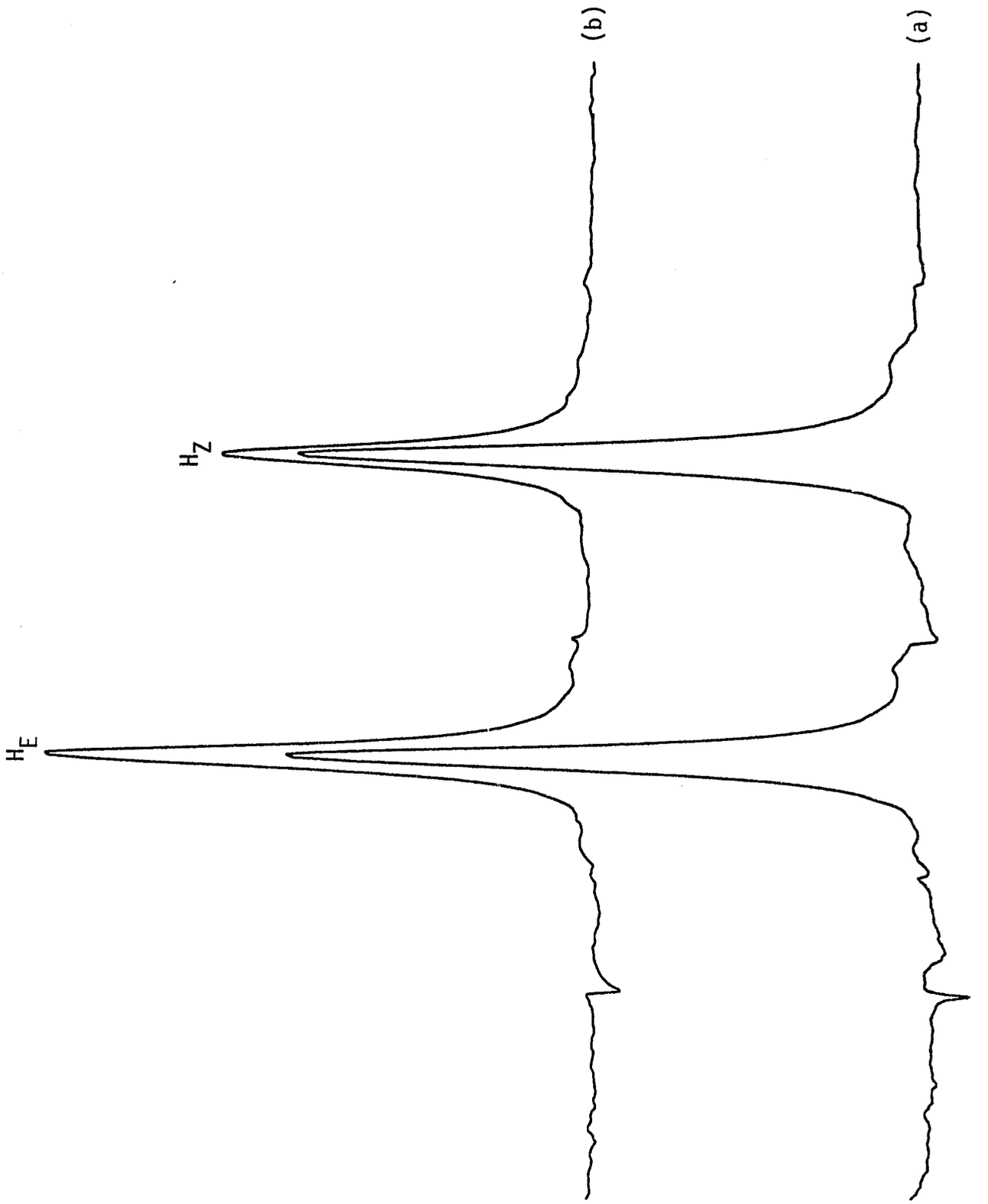

Table 4. Water-catalyzed Exchange of Protonated Ethyl Acetimidate and 2-Iminotetrahydrofuran [a]

	Ethyl Acetimidate	2-Iminotetrahydrofuran·HCl
Solvent	46 wt.% H_2SO_4	Wet DMSO-d_6
$[H_S]/[H_{E,Z}]$	10.65	
$t_E(Z)$	0.137 ± 0.01 [b]	
$t_Z(E)$	0.119 ± 0.007 [b]	
$t_S(E)$	0.025 ± 0.001	0
$t_S(Z)$	0.062 ± 0.004	0
$t_E(S)$	0.105 ± 0.009	0.485
$t_Z(S)$	0.328 ± 0.02	0.450
$M_E(S)$, sec^{-1}	6.62 ± 0.26	
$M_Z(S)$, sec^{-1}	10.34 ± 0.41	
$M_S(E,Z)$, sec^{-1}	4.08 ± 0.16	
k_{ZE}, sec^{-1}	-0.01 ± 0.08	
k_{EZ}, sec^{-1}	-0.13 ± 0.12	
k_{ES}, sec^{-1}	1.43 ± 0.09	
k_{ZS}, sec^{-1}	2.89 ± 0.20	
k_{SE}, sec^{-1}	0.083 ±0.005	
k_{SZ}, sec^{-1}	0.294 ± 0.021	

[a] Corrected for E-Z cross-relaxation.

[b] Nuclear Overhauser enhancement.

6. Proton Exchange in Strong Acid

Saturation-transfer studies of proton exchange in strong acid were also undertaken. Results for acetamide in 9% fuming sulfuric acid are presented in Table 5. Again, Eqs. [7] and [5] were used to calculate rate constants for exchange into amide and solvent sites, respectively, and these rate constants were corrected for cross-relaxation by subtracting from them the apparent rate constants measured under nonexchange conditions in 20% fuming sulfuric acid (Table 1). The data in Table 5 demonstrate that the N-H protons of O-protonated acetamide exchange with solvent at identical rates, and with each other at the same rate.

A similar experiment was performed on 3,5-dinitrobenzamide in 10% fuming sulfuric acid. Here H_E was partially obscured by a phenyl proton singlet, and ST values involving H_E were measured with integrals to compensate for this signal overlap. Consequently, these data are somewhat less accurate, but they nevertheless demonstrate that for O-protonated 3,5-dinitrobenzamide as well, rate constants for intermolecular and intramolecular exchange are all equal, within the considerable experimental error.

Semiquantitative NMR studies were also undertaken for trichloroacetamide and N-methylformamide in fuming sulfuric acid. Both amide protons of trichloroacetamide broaden to the same extent, indicating equal overall rates of exchange (see Table 6). In N-methylformamide, the N-methyl doublets collapse to about the same extent

Table 5. Saturation-transfer Results for Exchange of E and Z Hydrogens of $RCONH_2$ in Strong Acid [a]

	Acetamide	3,5 Dinitrobenzamide [b]
Solvent	9% fuming H_2SO_4	10% fuming H_2SO_4
$[H_S]/[H_{E,Z}]$	10.74	28.1
$t_E(A)$	0.202 ± 0.012	0.56
$t_Z(E)$	0.261 ± 0.015	0.51
$t_S(E)$	0.054 ± 0.003	0.26
$t_S(Z)$	0.052 ± 0.003	0.24
$t_E(S)$	0.356 ± 0.021	0.84
$t_Z(S)$	0.353 ± 0.020	0.76
$M_E(S)$, sec^{-1}	7.84 ± 0.30	
$M_Z(S)$, sec^{-1}	7.81 ± 0.30	28.0
$M_S(E,Z)$, sec^{-1}	6.09 ± 0.24	4.10
k_{ZE}, sec^{-1}	2.14 ± 0.17	
k_{EZ}, sec^{-1}	2.98 ± 0.25	18.6
k_{ES}, sec^{-1}	2.80 ± 0.26	22.2
k_{ZS}, sec^{-1}	2.83 ± 0.25	15.2
k_{SE}, sec^{-1}	0.26 ± 0.02	
k_{SZ}, sec^{-1}	0.26 ± 0.03	0.70

[a] Corrected for E-Z cross-relaxation.

[b] Signal overlap prevented a good assessment of errors.

Table 6. Line-broadening Measurements of Proton Exchange in Amides [a]

Compound	pH, measured	$\Delta\nu^{o}_{1/2}$, Hz	k_E, sec^{-1}	k_Z, sec^{-1}
Benzamide [b]	1.7	10.2	32.0	13.0
	8.6		27.5	7.7
Acrylamide	1.7	10.5	17.8	13.7
	8.2		29.7	9.6
Salicylamide	2.1	14.5	53.4	53.4
	7.0		6.3	6.3
Cyanoacetamide	0.9	9.3	7.2	6.7
			26.3	18.8
Ethyl oxamate	0.7	8.7	11.0	5.9
	0.2 [c]		9.9	22.3
	7.0		14.7	18.9
Chloroacetamide	7.4	11.2	21.0	27.0
Dichloroacetamide	7.0	10.5	32.5	29.6
Trichloroacetamide	0.2	10.8	8.8	13.2
	6.5		21.7	47.1
	10% fuming H_2SO_4		12.9	12.9

[a] In ethylene glycol unless otherwise noted.

[b] 60% aq. MeOH.

[c] In cyclohexanol. Calculated pH.

as a result of proton exchange (as illustrated in Figure 14), and the E methyl simultaneously broadens and appears as a shoulder closer to the Z methyl signal, indicating substantial intramolecular exchange concurrent with proton exchange.

7. Proton Exchange in Dilute Acid

Saturation-transfer results for acid-catalyzed exchange in a variety of primary and secondary amides are presented in Table 7. With several exceptions, to be discussed below, saturation-transfer experiments were performed as detailed in the Experimental, and rate constants for exchange into solvent and amide sites were calculated with Eqs. [5] and [7], respectively. Typical saturation-transfer experiments, on ^{15}N-enriched acetamide and benzamide and on dichloroacetamide in ethylene glycol, are illustrated in Figures 15, 16 and 17.

For benzamide-^{15}N in 60% aqueous methanol, it proved instrumentally impossible to accurately measure amide proton spin-lattice relaxation rates while irradiating solvent, owing to N-H intensity losses and baseline convolutions which perturbed the low-field region of the NMR spectrum. Therefore exchange rates into E and Z sites were calculated with Eq. [9], employing the nonexchange values for M_E and M_Z of 1.65 sec^{-1} and 1.50 sec^{-1}, respectively, listed in Table 1. Justification for this procedure is provided in Section 1 of the Discussion. Rate constants for exchange into solvent were

Figure 14. Spectra of the N-methyl region of N-methylformamide in fuming sulfuric acid. a) 16% fuming sulfuric acid, and b) 10% fuming sulfuric acid. Plots widths are 125 Hz.

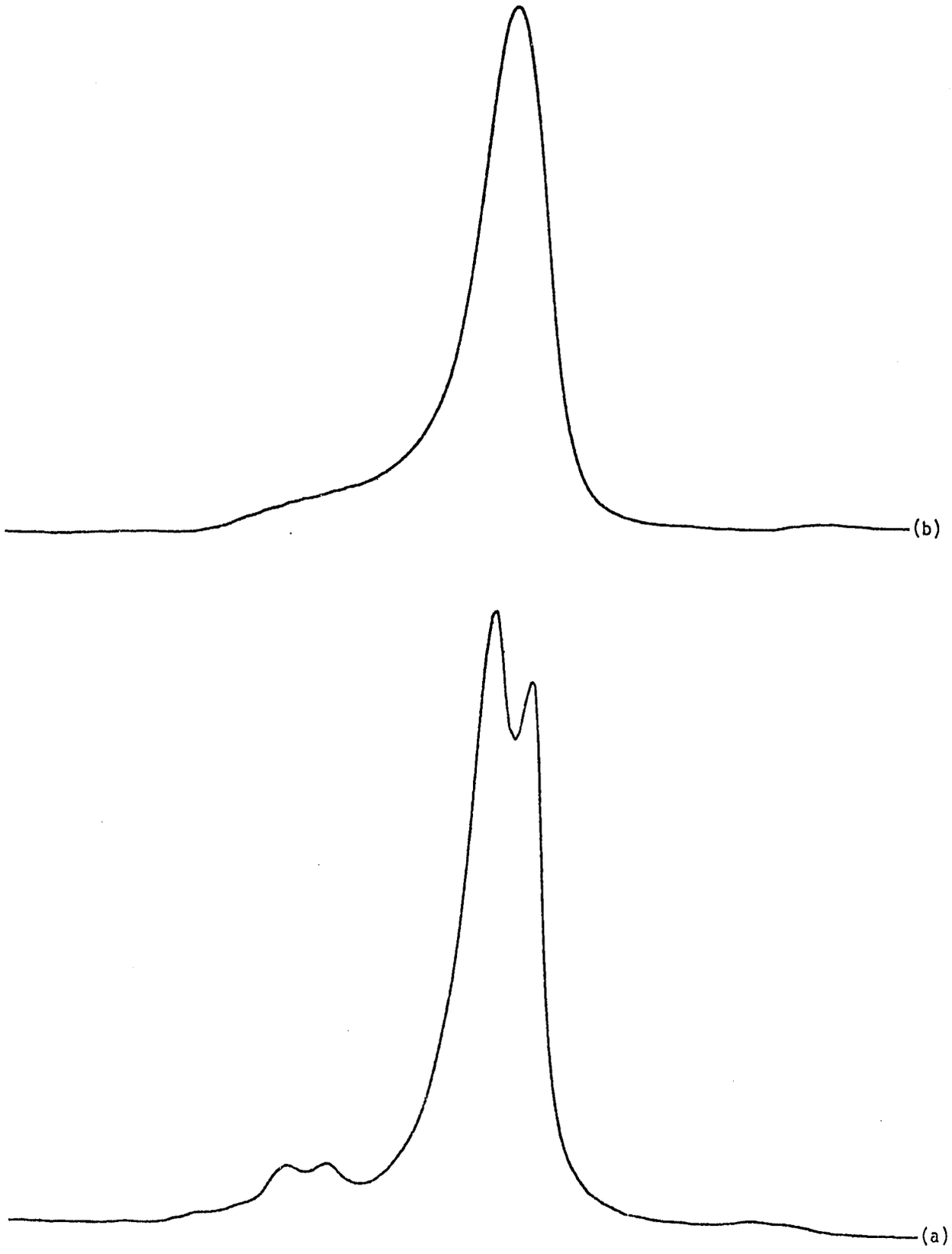

Figure 15. Saturation-transfer experiments on ^{15}N-labeled acetamide in ethylene glycol. pH = 1.8. a) Off-resonance spectrum, b) with irradiation of both components of H_E, c) with irradiation of both components of H_Z, and d) with solvent irradiation. The solvent signal is not shown. Plot widths are 400 Hz.

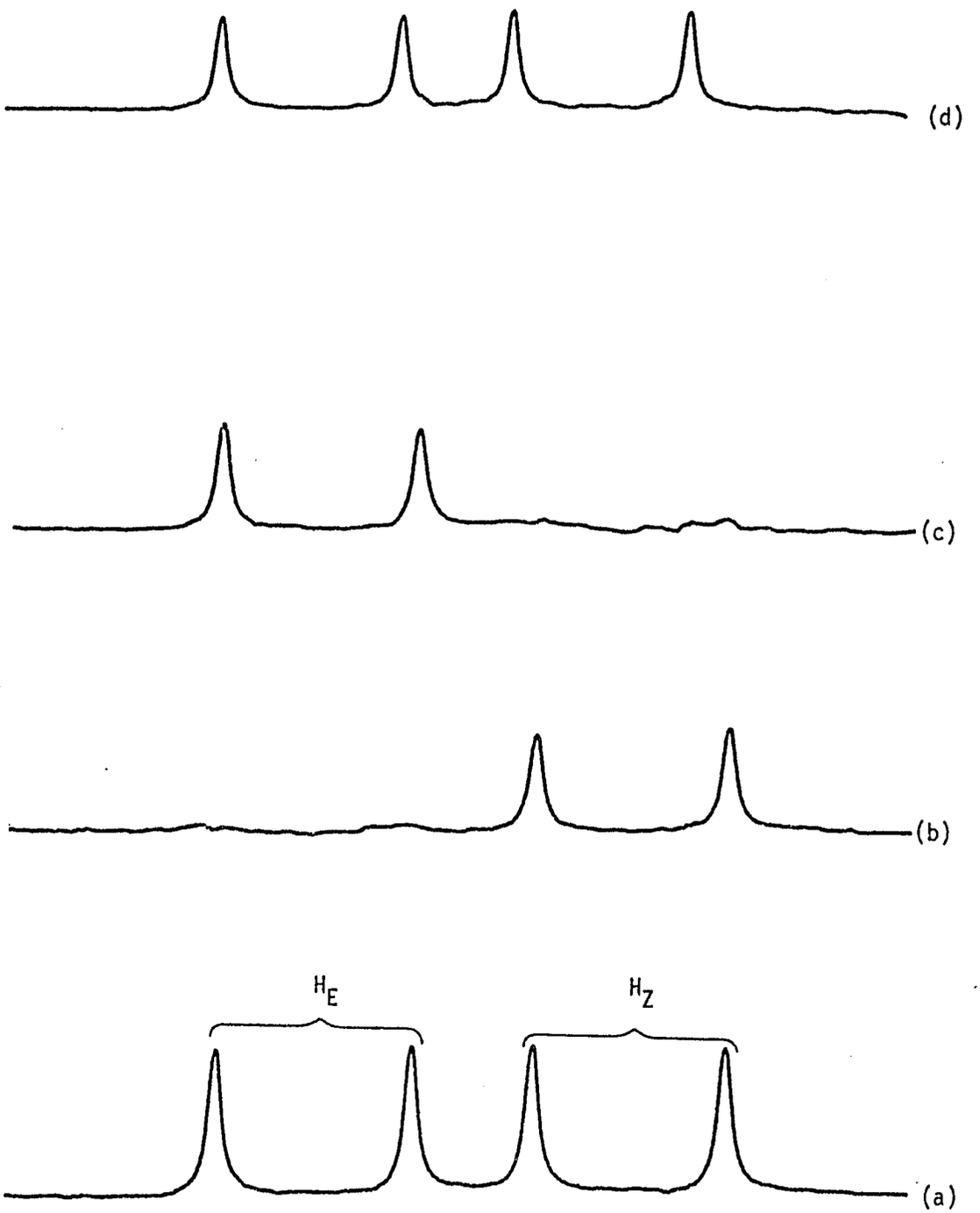

Figure 16. Saturation-transfer experiments on ^{15}N-labeled benzamide in ethylene glycol. pH = 2.0. a) Off-resonance spectrum, b) with irradiation of solvent, c) with irradiation of both components of H_E, and d) with irradiation of both components of H_Z. Plot widths are 500 Hz.

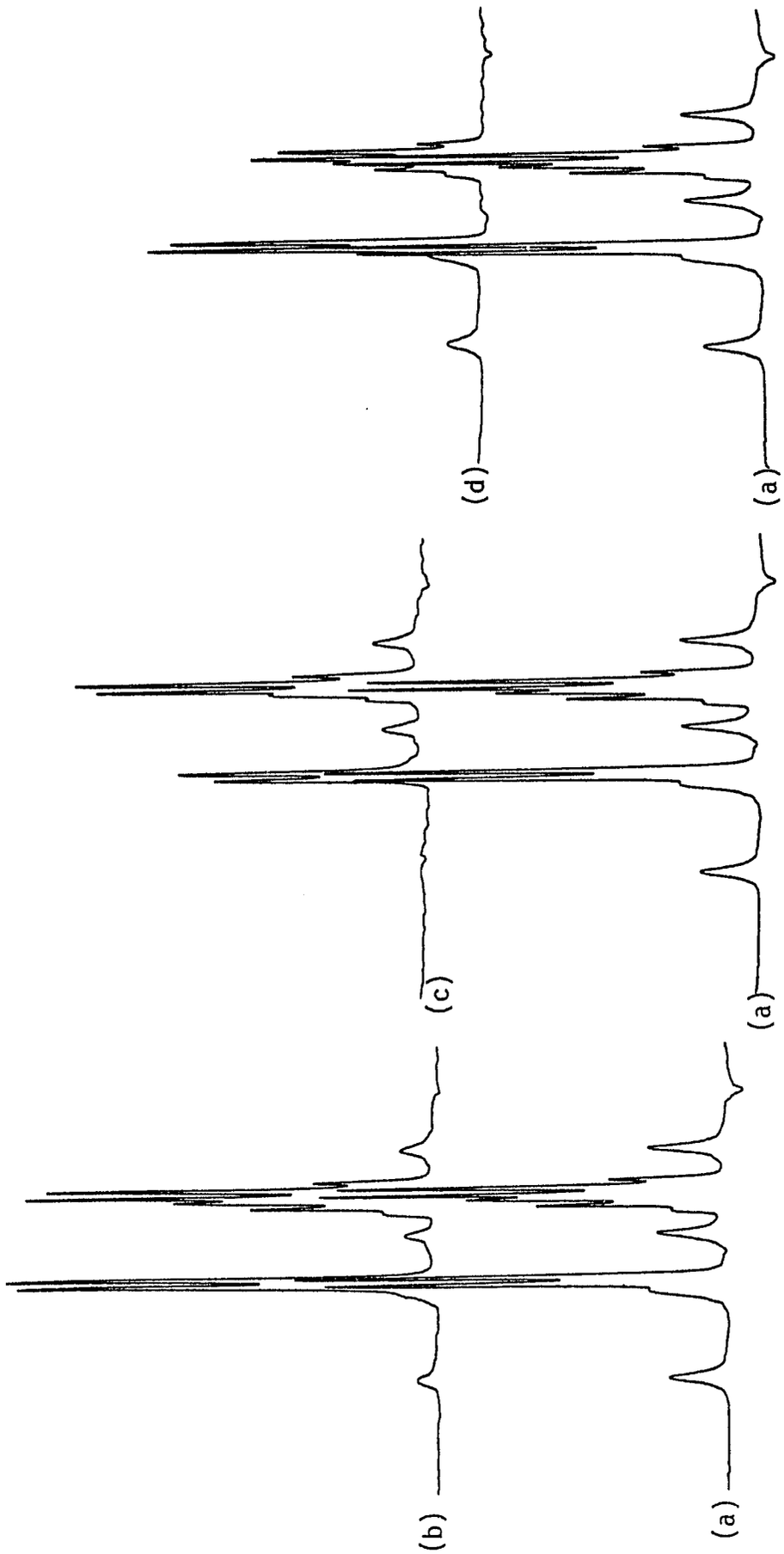

Figure 17. Saturation-transfer study of acid-catalyzed exchange of dichloroacetamide in ethylene glycol at pH 0.4. a) Off-resonance spectrum, b) with irradiation of solvent. Plot widths are 400 Hz.

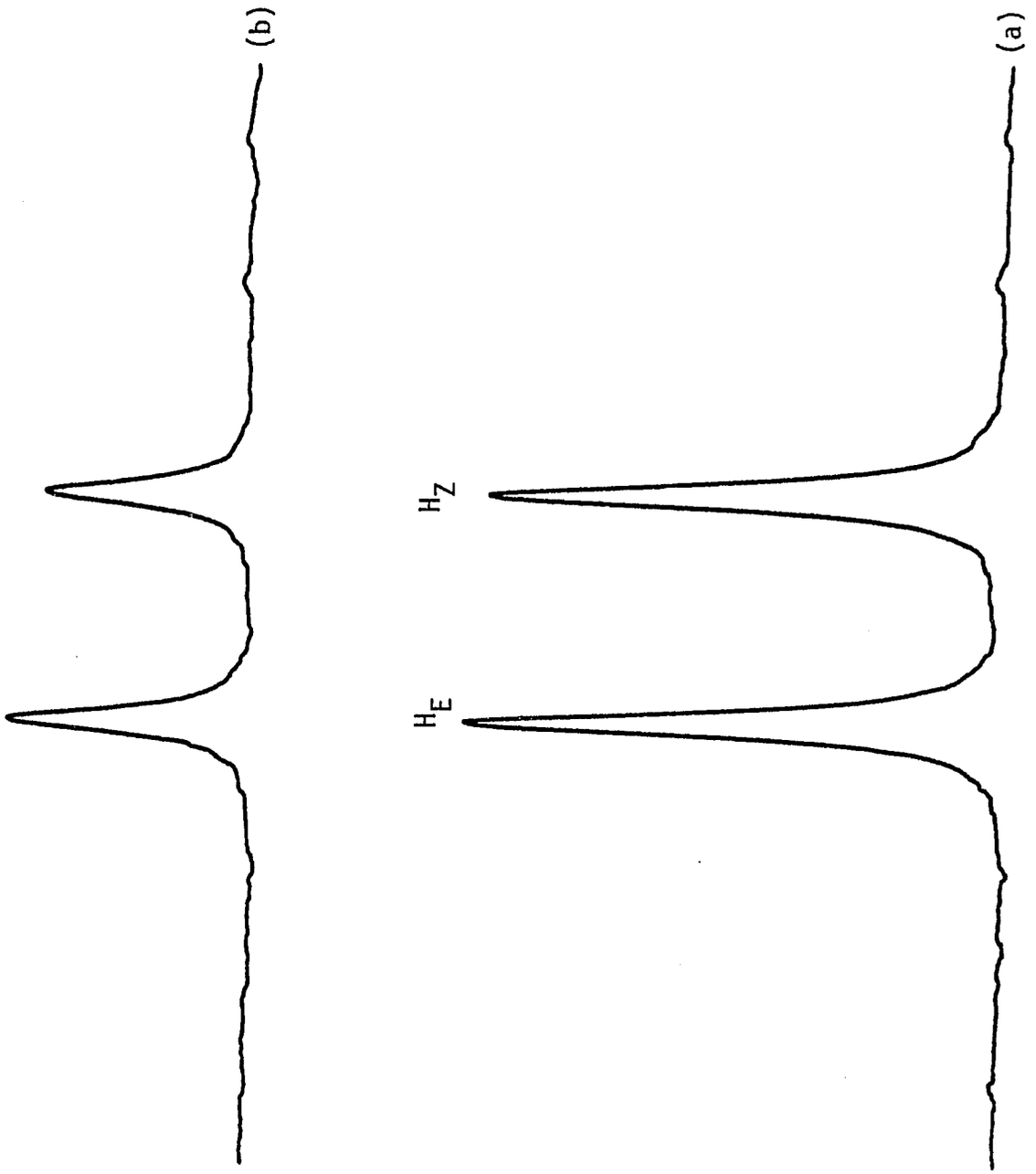

Table 7. Saturation-transfer Results for Dilute Acid-catalyzed Exchange of E and Z Hydrogens of RCONHR′ (R′= -H, -Me, -tBu) [a]

	Acetamide	Acetamide-^{15}N	Acetamide-^{15}N	
Solvent	EG	EG	EG	
pH, measured	1.7	1.8	1.9	
$[H_S]/[H_{E,Z}]$	13.05	14.33	14.33	
$t_E(Z)$	0.354 ±0.019	0.355 ±0.019	0.283 ±0.016	
$t_Z(E)$	0.393 ±0.023	0.364 ±0.020	0.308 ±0.018	
$t_S(E)$	0.158 ±0.009	0.128 ±0.007	0.083 ±0.005	
$t_S(Z)$	0.134 ±0.007	0.118 ±0.007	0.075 ±0.004	
$t_E(S)$	0.605 ±0.035	0.528 ±0.030	0.404 ±0.024	
$t_Z(S)$	0.559 ±0.035	0.508 ±0.030	0.375 ±0.020	
$M_E(S)$, sec^{-1}	7.16 ±0.28	6.53 ±0.25	5.08 ±0.20	2.93 [b]
$M_Z(S)$, sec^{-1}	6.66 ±0.25	6.17 ±0.24	4.83 ±0.19	2.88 [b]
$M_S(E,Z)$, sec^{-1}	2.48 ±0.10	2.14 ±0.08	2.20 ±0.09	2.04 [b]
k_{ZE}, sec^{-1}	2.60 ±0.36	2.55 ±0.34	1.38 ±0.18	1.36
k_{EZ}, sec^{-1}	2.78 ±0.42	2.57 ±0.34	1.60 ±0.20	1.59
k_{ES}, sec^{-1}	3.96 ±0.43	2.99 ±0.33	2.07 ±0.20	1.98
k_{ZS}, sec^{-1}	2.94 ±0.37	2.56 ±0.30	1.78 ±0.19	1.70
k_{SE}, sec^{-1}	0.342 ±0.04	0.245 ±0.03	0.147 ±0.01	0.144
k_{SZ}, sec^{-1}	0.273 ±0.03	0.215 ±0.02	0.122 ±0.01	0.122

[a] [b] Corrected for E-Z cross-relaxation and uncatalyzed C-N bond rotation.
[c] Measured without irradiation of other site(s).
[c] 22°C.
[d] Data for E and Z methyls.
[e] Measured by lineshape analysis.
[f] Calculated from detailed balance.

Table 7. Continued

	Acrylamide	Methacrylamide[c]	Benzamide-^{15}N
Solvent	EG	EG	EG
pH, measured	1.72	1.7	2.0
$[H_S]/[H_{E,Z}]$	10.90	12.17	33.0
$t_E(Z)$	0.410 ±0.024	0.552 ±0.030	0.413 ±0.025
$t_Z(E)$	0.428 ±0.025	0.571 ±0.034	0.423 ±0.024
$t_S(E)$	0.236 ±0.013	0.258 ±0.015	0.180 ±0.011
$t_S(Z)$	0.199 ±0.012	0.232 ±0.015	0.149 ±0.009
$t_E(S)$	0.571 ±0.034	0.542 ±0.032	0.634 ±0.036
$t_Z(S)$	0.535 ±0.031	0.504 ±0.030	0.525 ±0.031
$M_E(S), sec^{-1}$	7.95 ±0.32	9.58 ±0.38	18.0 ±0.7
$M_Z(S), sec^{-1}$	7.19 ±0.29	8.88 ±0.35	15.3 ±0.6
$M_S(E,Z), sec^{-1}$	2.32 ±0.09	2.65 ±0.10	2.13 ±0.08
k_{ZE}, sec^{-1}	2.51 ±0.54	4.14 ±1.54	6.57 ±1.27
k_{EZ}, sec^{-1}	2.51 ±0.55	4.34 ±1.66	6.23 ±1.20
k_{ES}, sec^{-1}	4.63 ±0.52	5.91 ±0.96	10.0 ±1.12
k_{ZS}, sec^{-1}	3.14 ±0.46	4.22 ±0.90	6.40 ±0.97
k_{SE}, sec^{-1}	0.429 ±0.054	0.455 ±0.08	0.38 ±0.04
k_{SZ}, sec^{-1}	0.340 ±0.050	0.339 ±0.07	0.21 ±0.03

Table 7. Continued

	Benzamide-^{15}N	Formamide-d_1	N-methylformamide
Solvent	60% aq. MeOH	EG	H_2O
pH, measured	2.3	1.0	0.9
$[H_S]/[H_{E,Z}]$	150.0	11.31	
$t_E(Z)$	0.40	0.30 ±0.02	
$t_Z(E)$	0.61	0.30 ±0.02	0.51 ±0.04
$t_S(E)$	0.040	0.09 ±0.005	
$t_S(Z)$	0.023	0.08 ±0.005	
$t_E(S)$	0.74	0.46 ±0.03	
$t_Z(S)$	0.65	0.42 ±0.03	
$M_E(S), sec^{-1}$	~ 7.1	2.80 ±0.10	0.3 ±0.03 [b,d]
$M_Z(S), sec^{-1}$	~ 4.6	2.73 ±0.11	0.3 ±0.03 [b,d]
$M_S(E,Z), sec^{-1}$	1.15	1.81 ±0.07	
k_{ZE}, sec^{-1}	1.8	1.05 ±0.11	0.27 ±0.03 [f]
k_{EZ}, sec^{-1}	1.1	1.03 ±0.11	3.6 ±0.4
k_{ES}, sec^{-1}	5.9	1.49 ±0.14	2.8 [e]
k_{ZS}, sec^{-1}	1.6	1.19 ±0.13	8.8 [e]
k_{SE}, sec^{-1}	0.044	0.118 ±0.01	
k_{SZ}, sec^{-1}	0.011	0.097 ±0.01	

Table 7. Continued

	N-t-butylformamide	Ethyl Oxamate	Cyanoacetamide
Solvent	EG	EG	EG
pH, measured	1.5	0.8	1.05
$[H_S]/[H_{E,Z}]$		77.9	27.49
$t_E(Z)$	0.045 ±0.025	0.057 ±0.003	0.235 ±0.014
$t_Z(E)$		0.094 ±0.006	0.234 ±0.015
$t_S(E)$		0.075 ±0.004	0.096 ±0.006
$t_S(Z)$		0.040 ±0.003	0.090 ±0.005
$t_E(S)$	0.13 ±0.02	0.662 ±0.04	0.670 ±0.04
$t_Z(S)$	0.21 ±0.04	0.484 ±0.029	0.626 ±0.038
$M_E(S)$, sec^{-1}	3.03	14.33 ±0.58	10.07 ±0.41
$M_Z(S)$, sec^{-1}	2.07	9.69 ±0.39	9.59 ±0.38
$M_S(E,Z)$, sec^{-1}		1.98 ±0.08	3.58 ±0.14
k_{ZE}, sec^{-1}	0.31	1.10 ±0.08	1.29 ±0.27
k_{EZ}, sec^{-1}		1.38 ±0.10	1.06 ±0.26
k_{ES}, sec^{-1}	0.39	11.05 ±0.83	7.80 ±0.70
k_{ZS}, sec^{-1}	0.44	5.54 ±0.44	7.02 ±0.66
k_{SE}, sec^{-1}		0.123 ±0.009	0.249 ±0.023
k_{SZ}, sec^{-1}		0.059 ±0.005	0.215 ±0.021

Table 7. Continued

	Malonamide	Chloroacetamide	Dichloroacetamide
Solvent	EG	EG	EG
pH, measured	1.58	1.20	0.4
$[H_S]/[H_{E,Z}]$	56.0	28.8	12.81
$t_E(Z)$	0.180 ±0.011	0.294 ±0.012	0.152 ±0.037
$t_Z(E)$	0.157 ±0.010	0.354 ±0.020	0.125 ±0.007
$t_S(E)$	0.047 ±0.003	0.081 ±0.005	0.159 ±0.009
$t_S(Z)$	0.041 ±0.003	0.064 ±0.004	0.185 ±0.010
$t_E(S)$	0.470 ±0.028	0.607 ±0.037	0.540 ±0.037
$t_Z(S)$	0.429 ±0.025	0.583 ±0.035	0.596 ±0.036
$M_E(S), sec^{-1}$	8.33 ±0.33	6.89 ±0.28	11.44 ±0.44
$M_Z(S), sec^{-1}$	8.23 ±0.32	6.08 ±0.24	11.39 ±0.44
$M_S(E,Z), sec^{-1}$	2.00 ±0.08	2.97 ±0.12	3.27 ± 0.12
k_{ZE}, sec^{-1}	1.63 ±0.15	1.41 ±0.28	0.64 ±0.19
k_{EZ}, sec^{-1}	1.34 ±0.12	1.87 ±0.33	0.31 ±0.16
k_{ES}, sec^{-1}	4.68 ±0.38	5.57 ±0.55	5.80 ±0.48
k_{ZS}, sec^{-1}	3.75 ±0.33	3.84 ±0.44	6.87 ±0.56
k_{SE}, sec^{-1}	0.71 ±0.006	0.147 ±0.015	0.479 ±0.04
k_{SZ}, sec^{-1}	0.063 ±0.005	0.121 ±0.014	0.531 ±0.04

calculated with Eq. [5]. To supplement these measurements, acid-catalyzed E-Z saturation-transfer was measured as a function of increasing acidity in 60% aq. methanol, and these results are tabulated in Table 8.

Acid-catalyzed proton exchange of ethyl oxamate was studied by line-broadening in cyclohexanol as well as in ethylene glycol and water. A typical spectrum obtained in cyclohexanol is presented in Figure 18, where H_Z is observed to undergo more rapid exchange (Table 6), contrary to the behavior observed in ethylene glycol and water, where H_E exchanges faster (Tables 7, 10, and 11).

Addition of sulfuric acid to ethylene glycol solutions of N-t-butylformamide resulted in pronounced downfield shifts of the amide protons, as illustrated in Figure 19, in addition to acid-catalyzed exchange broadening. It thus proved impossible to obtain rate constants for solvent exchange and isomerization by total lineshape analysis, as had been intended. Instead, k_{ES}, k_{ZS}, and k_{ZE} were measured in a saturation-transfer experiment in which three saturation-transfer values ($t_E(S)$, $t_Z(S)$, and $t_E(Z)$) and two relaxation rates ($M_E(S)$, $M_Z(S)$) were measured (Figure 15, spectrum d). Exchange into the large excess of solvent is sufficiently slow at this pH that $t_S(E)$ and $t_S(Z)$ are zero. Values of k_{ES} and k_{ZE} listed in Table 7 were calculated with Eq. [7]. Utilizing Eqs. [3] and [6], an expression for k_{ZS} was derived in terms of the above-measured quantities, and is given in Eq. [10].

Figure 18. Acid-catalyzed exchange of ethyl oxamate in cyclohexanol. a) Unbuffered, b) $[H^+]$ = 0.6 M. Plot width is 600 Hz.

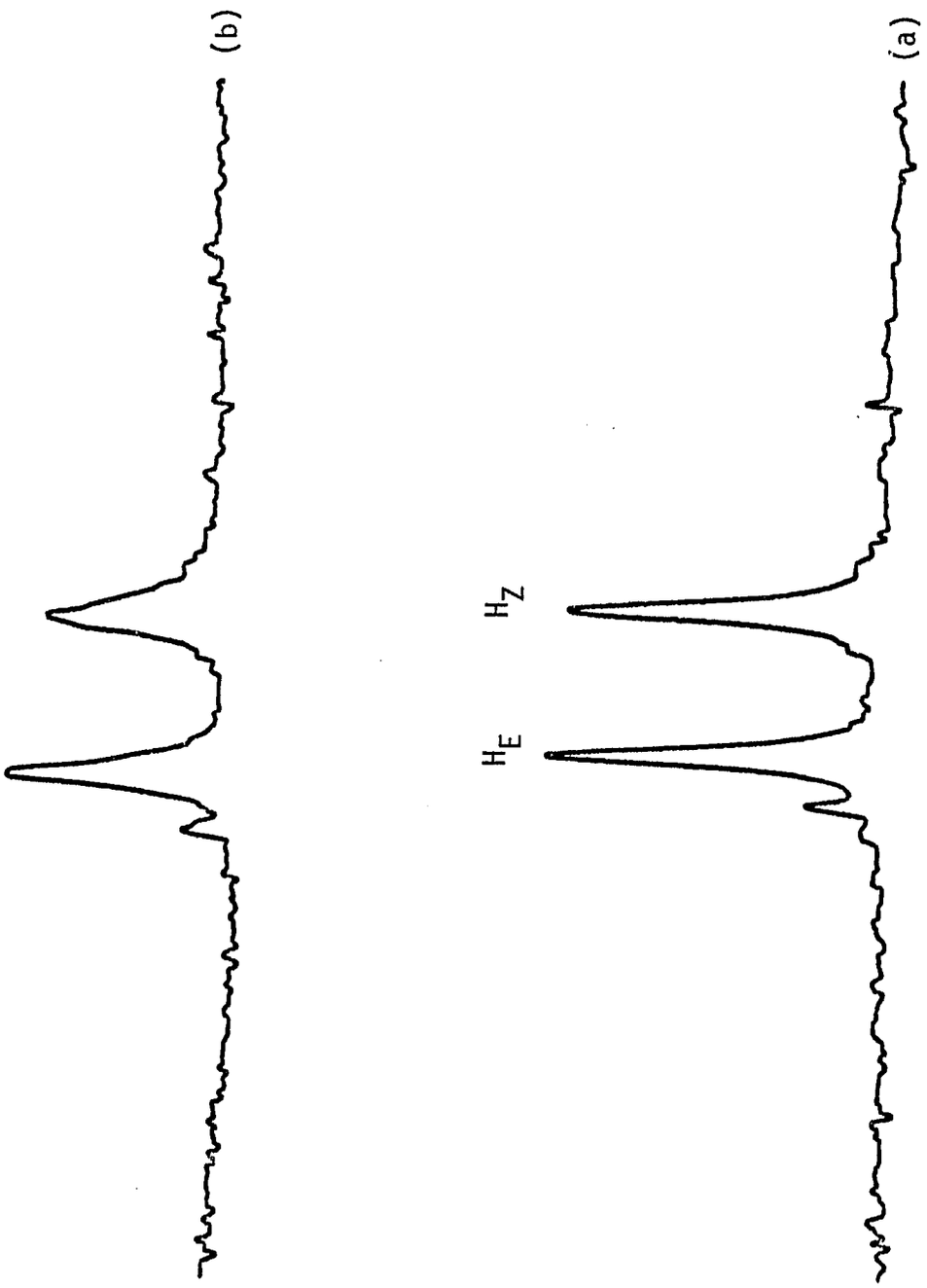

Table 8. Benzamide-^{15}N Acid-catalyzed E-Z Saturation-transfer in 60% Aqueous Methanol

HCl, mM	$t_Z(E)$	$t_E(Z)$
0	0.71 ±0.04	0.69 ±0.03
5	0.59 ±0.03	0.47 ±0.03
10	0.52 ±0.02	0.31 ±0.04
15	0.48 ±0.05	0.29 ±0.05
20	0.49 ±0.02	0.25 ±0.07

Figure 19. Acidity dependence of the low-field region of N-t-butylformamide in ethylene glycol. $[H^+]$ values, mM, are: a) 0, b) 10, c) 20, d) 30, e) 45, f) 60, g) 80, h) 95, i) 125, j) 140. Remaining spectra increase in 18 mM increments. Plot width is 400 Hz.

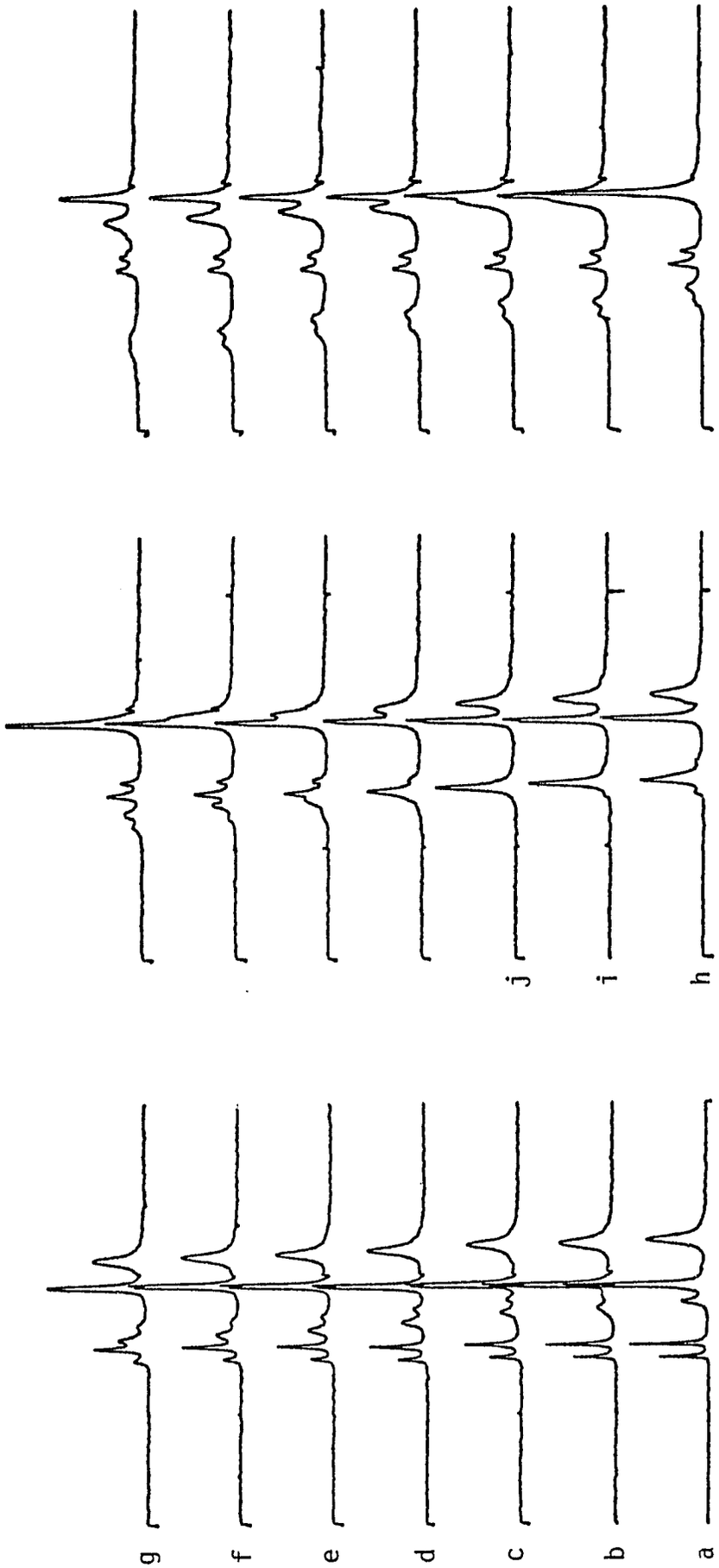

$$k_{ZS} = M_Z(S) \cdot t_Z(S) - M_E(S) \cdot \frac{t_E(Z)(t_E(S) - t_Z(S))}{1 + t_E(Z)} \cdot \frac{p_E}{p_Z} \qquad [10]$$

This expression was then used to calculate the value of k_{ZS} listed in Table 5.

Independent confirmation of the magnitude of k_{ZE} at this pH comes from a lineshape analysis of the t-butyl region of the spectrum as a function of pH. Under non-exchange conditions, the isomeric t-butyls appear as singlets ($\Delta\nu^{o}_{1/2}$ = 1.6 Hz) separated by 2.6 Hz, at 220 MHz, as shown in Figure 20. At an acidity approximately five-fold that of the sample studied by saturation-transfer the t-butyl singlets coalesce (Fig. 20j), in contrast to the behavior observed at basic pH, where they remain distinct, and lineshape simulation of this spectrum affords a rate constant of 3 sec^{-1} for exchange of the E t-butyl into the more abundant Z site. Since the rate of acid-catalyzed t-butyl isomerization, k_{EZ}, occurs at twice the rate of acid-catalyzed proton isomerization, k_{ZE} (as shown later), the rate constant for the latter process in the less acidic sample of Figure 16d is indeed about 0.3 sec^{-1}, as measured by saturation-transfer (Table 7).

Acid-catalyzed proton exchange and isomerization in N-methylformamide (NMF) were studied by a combination of saturation-transfer and lineshape simulation techniques. The effect of acid on the methyl region of the NMR spectrum of NMF is illustrated in Figure 21. As the pH is lowered, the downfield E methyl doublet loses its doublet structure and broadens, eventually coalescing with the Z methyl signal

Figure 20. Acidity dependence of the t-butyl region of N-t-butylformamide in ethylene glycol. Sample acidities are the same as for Figure 15. The upfield singlet is t-butanol, added as standard. Plot width is 400 Hz.

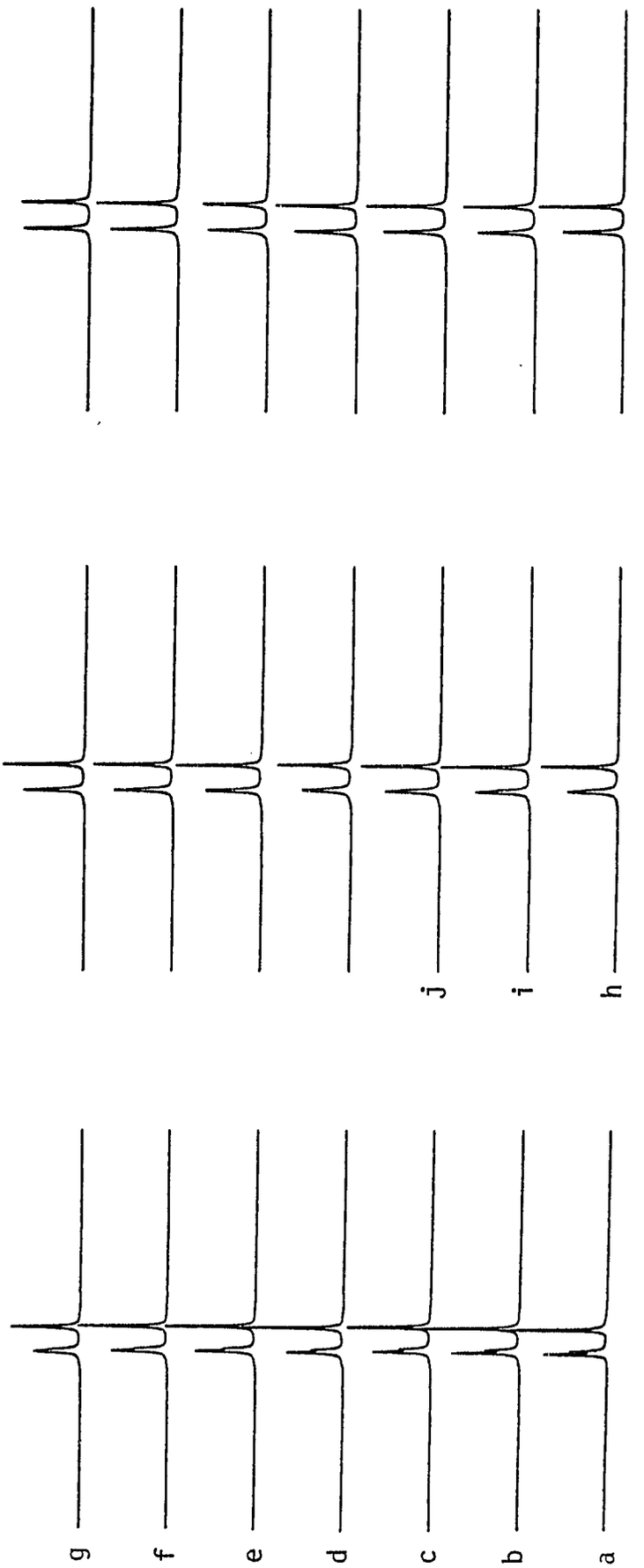

Figure 21. pH-dependence of the N-methyl signals of N-methylformamide in the acidic range. a) pH 1.2, b) 0.85, c) 0.5, d) 0.45, e) 0.4, f) 0.2, g) 0.1. Measured spectra are to the left and calculated spectra to the right.

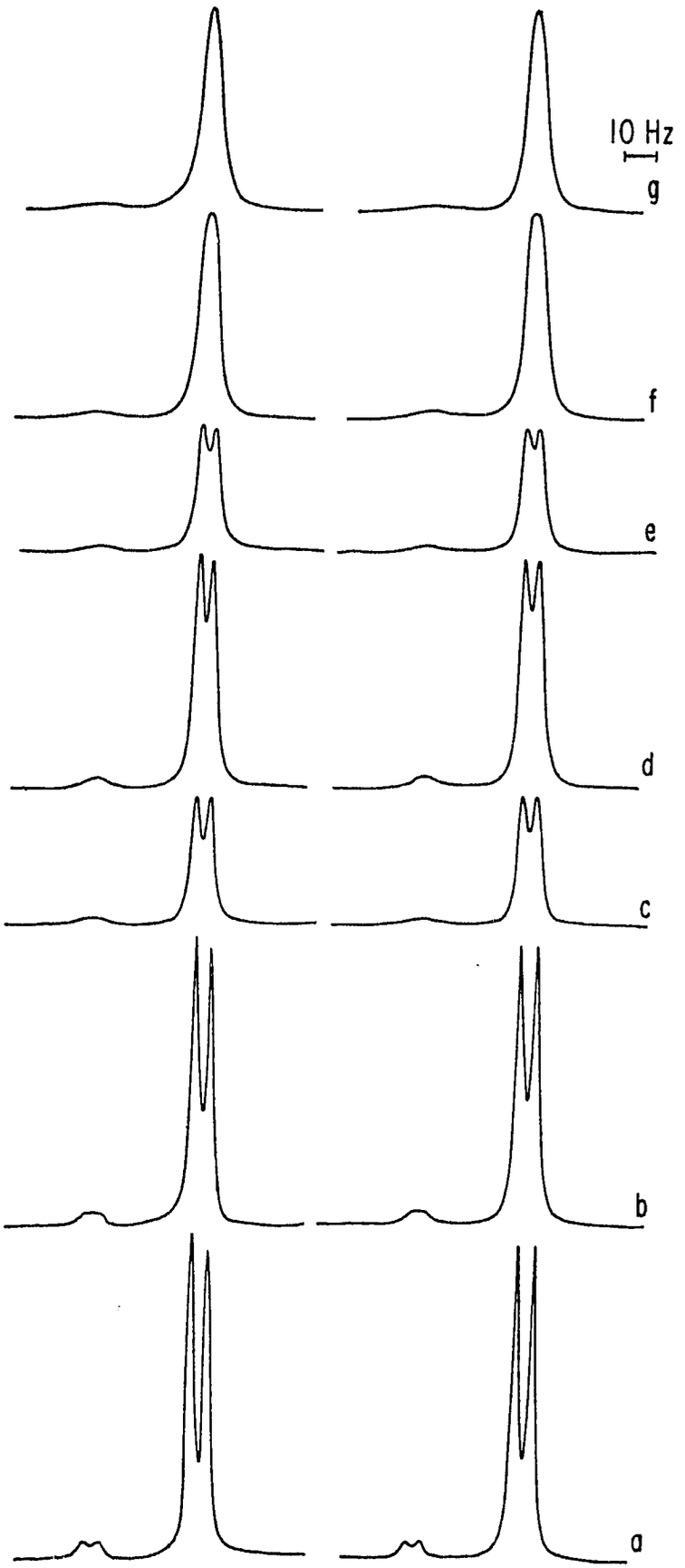

at very low pH, in contrast to the behavior observed at basic pH, where the N-methyls sharpen into separate singlets (Figure 11). The Z methyl likewise loses its doublet structure, but lower pH is required for this than for E doublet collapse. At pH 0.9, irradiation of the less abundant E methyl doublet results in an intensity decrease of 51% at the Z methyl (Table 7), as compared to a 15% decrease at pH 2.3 (Table 1). Thus acid-catalyzed methyl isomerization is occurring, and at pH 0.9 the overall rate constant for this process was calculated with Eq. [9] to be 4.2 sec^{-1}. Of this, 0.6 sec^{-1} is due to uncatalyzed rotation in the amide (Table 1) so k_{EZ}^{R} at this pH is 3.6 sec^{-1}, where the superscript R denotes methyl group isomerization. First-order rate constants for proton exchange were then obtained by lineshape analysis of the N-methyl region of this spectrum (see Figure 21). The rate constant matrix used in the lineshape analysis is given in the Experimental section. Intrinsic T_2 values for the Z and E methyls were 0.18 sec and 0.23 sec, respectively; all other program input parameters were the same as those used for base-catalyzed exchange. Lineshape analysis of this spectrum provided rate constants for proton exchange k_{ZS} and k_{ES} of 8.8 sec^{-1} and 2.8 sec^{-1}, respectively, at pH 0.9. Thus, $k_{ZS}/k_{ES} = 3.2$ and $k_{EZ}^{R}/k_{ZS} = 0.42$. These ratios, in conjunction with calculated sample acidities were used to produce the calculated spectra in the acidic range presented in Figure 21. In these spectra, k_{ZS} was adjusted to produce the best agreement while holding k_{ZS}/k_{ES} and k_{EZ}^{R}/k_{ZS}

fixed at 3.2 and 0.42, respectively. Lineshape parameters for the simulated spectra are tabulated in Table 9. Plots of log k vs -log $[H^+]$ gave second-order rate constants $k_{ZS}^{H^+} = 80\ M^{-1}sec^{-1}$, $k_{ES}^{H^+} = 25\ M^{-1}sec^{-1}$, and $k_{EZ}^{R} = 34\ M^{-1}sec^{-1}$. The value for $k_{ES}^{H^+}$ is in very good agreement with values previously reported: $22.6 \pm 1.6\ M^{-1}sec^{-1}$ [38] and $20 \pm 6\ M^{-1}sec^{-1}$. [17]

8. Relative Exchange Rates

Relative rates of proton exchange are summarized in Tables 10-12 from data presented in Tables 2-9. Ratios measured by saturation-transfer are converted to ratios of total exchange rates, k_E/k_Z, equal to $(k_{ES} + k_{EZ})/(k_{ZS} + k_{ZE})$, so that they may be directly compared to ratios measured by line-broadening. Rate ratio measurements in water were made on a JEOL PFT-100 NMR spectrometer equipped with ^{14}N-decoupling, as detailed in the Experimental.

9. Amide Aggregation

Several experiments were performed to determine whether amide aggregation resulting from intermolecular hydrogen-bonding was significant in the solvents and at the concentrations employed in these studies.

The chemical shifts of the E and Z protons of N-t-butyl formamide were measured in ethylene glycol as a function of amide concentration, since these are expected to be particularly sensitive to interamide hydrogen bonding.[71] No significant changes in chemical

Table 9. Acid-catalyzed Solvent Exchange of E and Z Protons and E-Z Methyl Isomerization in N-methylformamide

$[H^+]$, M	k_{ZS}, sec^{-1}	k_{ES}, sec^{-1}	k^R_{EZ}, sec^{-1}
0.06	5.4	1.7	2.3
0.13	8.8	2.8	3.6 [a]
0.14	11.4	3.6	4.7
0.32	26.0	8.0	10.8
0.36	28.8	9.0	11.8
0.40	32.0	10.0	13.1
0.63	54.4	17.0	22.7
0.80	67.2	21.0	28.0

[a] By saturation-transfer.

Table 10. Relative Total Rates of Base- and Acid-catalyzed Exchange of E and Z Hydrogens in Water[a]

Compound	$k_E^{OH^-}/k_Z^{OH^-}$	$k_E^{H^+}$ $k_Z^{H^+}$
Acetamide	7.4	1.17
Trimethylacetamide	1.50[b]	1.06[b]
Acrylamide	4.05	1.52
Methacrylamide	1.75	1.86
Benzamide	3.57[c,f,g]	2.45[c,f,g] 2.45[c,d,g]
N-methylformamide	0.5[e]	0.31[e]
Ethyl oxamate	0.57	1.08
Cyanoacetamide	3.04	1.15
Trifluoroacetamide	1.86	1.60

[a]Line-broadening measurements in water were made by Mr. Paul Kobrin.

[b]50% aq. MeOH.

[c]60% aq. MeOH.

[d]By saturation-transfer.

[e]By total lineshape analysis.

[f]By line-broadening.

[g]99% ^{15}N-enriched.

Table 11. Relative Total Rates of Base- and Acid-catalyzed Exchange of E and Z Hydrogens in Ethylene Glycol[a]

Compound	$k_E^{OH^-}/k_Z^{OH^-}$	$k_E^{H^+}/k_Z^{H^+}$
Acetamide	2.6	1.09
Acrylamide	2.46, 3.10[b]	1.26, 1.30[b]
Methacrylamide	1.22	1.23
Benzamide-^{15}N	1.79	1.34
Salicylamide	1.0, 1.0[b]	1.0[b]
Formamide-d_1	1.56	1.25
N-methylformamide	0.58	-
N-t-butylformamide	0.125[c]	0.87
Ethyl oxamate	0.78[b]	1.87 0.45[d]
Cyanoacetamide	1.40[b]	1.07
Malonamide	2.2	1.12
Chloroacetamide	0.77[b]	1.42
Dichloroacetamide	1.10[b]	0.84
Trichloroacetamide	0.46[b]	0.67[b]

[a]By saturation-transfer unless otherwise noted.

[b]By line-broadening.

[c]By total lineshape analysis.

[d]In cyclohexanol.

Table 12. Relative Total Rates of Water- or Bisulfate-catalyzed Exchange of E and Z Hydrogens

Compound	k_E/k_Z
Ethyl acetimidate	0.50 [a,d,f]
2-Iminotetrahydrofuran	1.15 [b,d,f]
Acetamide	1.14 ± 0.10 [c,e,f]
3,5-Dinitrobenzamide	1.06 ± 0.10 [c,e,f]
Trichloroacetamide	1.0 ± 0.1 [c,e,g]

[a] In 32% v/v aq. H_2SO_4.

[b] In wet DMSO-d_6.

[c] In fuming sulfuric acid.

[d] Water-catalyzed exchange.

[e] Bisulfate-catalyzed exchange.

[f] By saturation-transfer.

[g] By line-broadening.

shift were observed upon dilution of the amide solution from 2.5 M to 0.15 M.

The relative rates of acid-catalyzed exchange of the E and Z hydrogens of acrylamide were measured by line-broadening in ethylene glycol as a function of amide concentration. The rate ratio k_E/k_Z was 1.21, 1.24, 1.36 and 1.29 at amide concentrations of 2 M, 1 M, 0.5 M and 0.25 M, not significantly different from the value of 1.30 measured at 3 M amide (Table 10).

The relative rates of base-catalyzed exchange of the E and Z hydrogens of acetamide were measured by line-broadening at 0.25 M amide in ethylene glycol. The rate ratio $k_E^{OH^-}/k_Z^{OH^-}$ was found to be 3.0 ± 0.5, not appreciably different from the ratio of 2.6 measured at 3 M amide (see Table 8).

On the basis of these results, and on the basis of a wealth of additional data in the literature,[5,72-74] we conclude that amide aggregation is not significant at or below 3 M concentration in the solvents employed in these studies, so that complications due to dimerization may be neglected.

D. Discussion

1. Error Analysis and Reliability of Data

Errors listed in the data tables are standard deviations determined according to the propagation of errors from the observed standard deviations of repeated ST and T_1 experiments. Although all rate constants are determined independently, the errors are not independent. Rate constants measured in our saturation-transfer experiments typically have standard deviations of ± 10-15%, although rate ratios may be more accurate, since the errors are not independent.

The data in Tables 1, 2, 4, 5, and 7 demonstrate that forward and reverse rates are in every case equal ($k_{ES}[E] = k_{SE}[S]$, $k_{ZS}[Z] = k_{SZ}[S]$, $k_{EZ} = k_{ZE}$) in our experiments, within experimental error, as required by equilibrium. Moreover, the ratio of total exchange rates k_E/k_Z ($= (k_{ES} + k_{EZ})/(k_{ZS} = k_{ZE})$) measured by line-broadening agrees with that measured by saturation-transfer (see Table 10, data for benzamide-^{15}N, and Table 11, data for acrylamide), providing a further measure of the reliability of the saturation-transfer method.

An additional, and compelling, indication of the reliability of the saturation-transfer method is provided by rate data obtained for ^{15}N-acetamide and included in Table 7. First, T_1 experiments were performed on an acidified sample in the usual manner (i.e., by measuring $M_E(S)$, $M_Z(S)$, and $M_S(E, Z)$), and rate constants were

calculated with Eqs. [5] and [7]. Then apparent relaxation rates M_E, M_Z, and M_S were measured on the same sample without selective irradiation (the suitability of this approach being verified as described in the Results section), and rate constants were calculated with Eq. [9]. Apparent relaxation rates measured in this manner are in fact equal to intrinsic relaxation rates (see, e.g., Eq. [8]). Although relaxation rates measured under these two different circumstances are very different, the calculated rate constants agree very well (Table 7). This provides justification for calculating a) malonamide rate constants (Results, Section 5) and b) benzamide ^{15}N rate constants in 60% aq. methanol (Results, Section 8) with intrinsic relaxation rates measured under non-exchange conditions.

Rate ratios measured by the saturation-transfer method are quite reproducible, as the data in Table 7 for acetamide indicate. Although only one set of kinetic data is typically presented in the data tables, experiments were generally performed at least three times to verify the reproducibility of the results.

2. Uncatalyzed Rotation

Rate constants for rotation about the C-N partial double bond of RCONHR′, measured under conditions where solvent exchange is slow, are collected in Table 1. As mentioned in the Results Section, these values are lower limits to the true rate constants. The rate of rotation is very small for formamide, N-methylformamide, N-t-butylformamde, ethyl oxamate, malonamide, and dichloroacetamide,

and slightly larger for acetamide, cyanoacetamide, and chloroacetamide. This trend is in keeping with the rate-retarding effect of electron-withdrawing substituents observed in tertiary amides,[88] where the transition-state for rotation is inductively destabilized.

Very few rotational barriers have been measured in primary amides, owing to the broadness of the amide resonances, and ^{15}N-substituted compounds, which avoid this difficulty, are not commonly available.[89,90] Rate constants for rotation in acetamide of 1.7 sec^{-1} and 4.7 sec^{-1} have been measured[91] in DMF and acetone, respectively, and these may be compared to our measured value of 0.4 sec^{-1} in ethylene glycol. Hydrogen-bonding solvents evidently increase the barrier to rotation. Increased rotational barriers in such solvents have also been observed in tertiary amides.[88]

The rate of rotation is considerably larger in acrylamide, methacrylamide, benzamide, and salicylamide, where the R-group conjugatively stabilizes the transition-state for rotation.[88] Rate constants at 23 °C in ethyleneglycol for rotation in these amides are 1.4, 6.3, 3.4, and 21 sec^{-1}, respectively. The α-methyl group in methacrylamide thus lowers the barrier to rotation relative to acrylamide. A similar trend has been observed in the corresponding N, N-dimethylamides, where a barrier reduction of 2.6 kcal/mole was observed[92] and ascribed to a predominant s-trans conformation in N, N-dimethylmethacrylamide. Likewise, in the s-trans conformation of methacrylamide, non-bonded repulsions between vinylic and

amide hydrogens sterically destabilize the planar ground state, slightly lowering the barrier to rotation by about 0.7 kcal/mole relative to acrylamide. To the extent that such repulsions are smaller than those between vinylic hydrogens and amide N-methyl groups in the tertiary amides, the barrier reduction would be expected to be considerably smaller for the primary amides.

Rotation is considerably faster in salicylamide than in benzamide, since the o-hydroxy substituent is very effective at conjugatively stabilizing the transition state for rotation.

The rate constant for rotation in benzamide was measured in both ethylene glycol and 60% aqueous methanol. The spin-lattice relaxation rates of H_E and H_Z in ^{15}N-enriched benzamide in ethyleneglycol are approximately four times as large as in aqueous methanol, due presumably to increased solvent viscosity which increase the rotational correlation time of the amide and hence the relaxation rate.[61b] The rotation rate, on the other hand, is not appreciably different in these two rather similar solvents.

3. Base-Catalyzed Exchange

a. Primary Amides

To check the reliability of the saturation-transfer method, we have first examined base-catalyzed exchange in a series of amides, for which there is no mechanistic ambiguity.[42] The results of these experiments are assembled in Table 2.

Saturation-transfer data for acetamide are representative. Since the imidate anions resulting from loss of the diastereotopic E and Z hydrogens are expected to be configurationally stable[93] and reprotonated at a diffusion-controlled rate,[38] no base-catalyzed E-Z exchange is expected, and this is indeed confirmed by the kinetic data: k_{EZ} and k_{ZE} are zero, within experimental error (see Table 2). Moreover, H_E exchanges faster, in accord with line-broadeing measurements[42] (Tables 10 and 11). Thus we may have confidence in this saturation-transfer method as an accurate means of measuring intersite rate constants.

Our studies of base-catalyzed exchange in primary amides demonstrate that electron-withdrawing R- groups increase k^{OH^-} (compare, e.g., entries in Table 6 for base-catalyzed exchange of acrylamide and trichloroacetamide), as had been found previously for secondary amides.[38] H_E, the proton trans to oxygen, is removed more rapidly for most of the primary amides studied, owing to lone-pair repulsions which destabilize the E imidate anion resulting from loss of H_Z. A similar effect is operative in carboxylic esters, where the s-trans conformer predominates at equilibrium.[94] The results in Tables 10 and 11 suggest that for those amides where H_E is removed more rapidly, its removal can be subject to a slight steric hindrance by the group R. Thus, the rate ratio is more nearly equal in trimethylacetamide (1.5) than in acetamide (7.4), and is likewise smaller in methacrylamide (1.75), which is s-trans, than in acrylamide (4.05),

which is s-cis.[92] On the other hand, it is difficult to explain the small ratio of 1.56 observed for formamide-d_1, in ethylene glycol on this basis.

Ethyl oxamate, whose Z proton exchanges more rapidly, is an interesting exception to the trend exhibited by most of the other amides. Apparently lone-pair repulsions are worse in 2 than in 3, so that H_E is the slower to exchange.

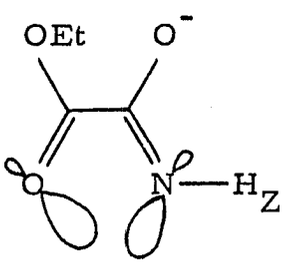

2

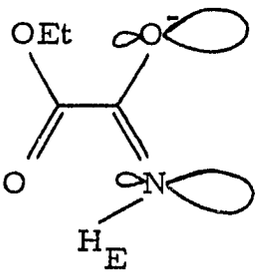

3

Menger and Saito[95] have observed intramolecular catalysis of the base-catalyzed exchange in N-methylsalicylamide. They observed an 8-fold rate enhancement for proton exchange (corresponding to H_E in primary amides) in this compound relative to N-methylbenzamide. They additionally observed that the O-methoxy group in N-methyl-o-anisamide impedes exchange by a factor of six relative to N-methybenzamide, owing to electron release to the amide carbonyl resulting from resonance interaction between the methoxy and amide groups. Thus, despite the electron-donating effect of its ortho hydroxyl, N-methylsalicylamide exchanges considerably faster than N-methyl benzamide. To explain this neighboring-group catalytic effect,

Menger and Saito formulated two mechanisms, as depicted in Figure 22, but were unable to distinguish between them.

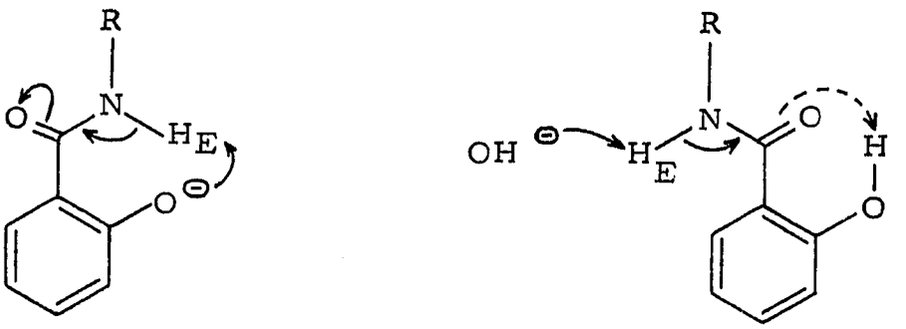

Figure 22. General base and specific base-general acid catalysis of amide proton exchange in salicylamide (R = -H) and N-methylsalicylamide (R = $-CH_3$).

In the first, phenolate anion removes the amide proton; the amide is then reprotonated by the hydroxy group, which in the meantime has exchanged its proton. In the second mechanism, proton exchange is subject to specific base-general acid catalysis, with the developing negative charge on oxygen being stabilized by hydrogen-bonding in the transition-state for exchange.

A distinction between the two mechanisms is possible with the corresponding primary amides (R = $-H_Z$). In the first mechanism, exchange of H_E should be accelerated in salicylamide relative to exchange of this proton in benzamide, whereas exchange of H_Z should show no rate enhancement. In the second mechanism, exchange of both H_E and H_Z should be accelerated. Moreover, to the extent that hydrogen-bonding in the transition-state decreases the electron-

electron repulsion that destabilizes the E-imidate anion, H_E and H_Z should exchange at more nearly equal rates in salicylamide than in benzamide.

The experimental results, collected in Table 2, demonstrate that the E and Z protons of salicylamide undergo base-catalyzed exchange at equal rates, within experimental error (as illustrated in Figure 10). Relative to benzamide exchange rates of not only H_E but also H_Z are accelerated, by 11-fold and 19-fold, respectively. This observation thus conclusively rules out the first mechanism in Figure 18.

There are a number of mysteries concerning the base-catalyzed exchange in primary amides. In both chloro- and trichloroacetamide in ethylene glycol, it is H_Z which is more easily removed, contrary to the behavior observed in dichloroacetamide, where H_E exchanges faster. One possible explanation is that the signal assignment is reversed in the former compounds, but it is secure in both acetamide[40] and dichloroacetamide on the basis of NOE (see Figure 3), and there is no reason to expect a chemical-shift reversal in the mono- and trichloroacetamides. Besides, we have observed that $k_Z^{OH^-}$ exceeds $k_E^{OH^-}$ for two secondary amides. This will be discussed in the following section.

The second-order rate constants for removal of H_E and H_Z in trifluoroacetamide are respectively 3.5×10^{10} $M^{-1}sec^{-1}$ and 2.0×10^{10} $M^{-1}sec^{-1}$ in water.[96] Both these rate constants are in the range

of diffusion-control. Thus hydroxide exhibits intramolecular selectivity in a diffusion-controlled reaction, a remarkable result which is not at present well understood.

There is a viscosity effect on the base-catalyzed exchange. The rate ratios are more nearly unity in ethylene glycol than in water (compare Tables 10 and 11), suggesting that base is less selective in its deprotonating preference in ethylene glycol than in water. The origin of this effect is not well established at this point.

b. Secondary Amides

Hydroxide-catalyzed proton exchange was studied in N-methyl- and N-t-butylformamade, which exist as equilibrium mixtures of E and Z isomers. The equilibrium constants K_{EZ} are 13.5 and 2.2, respectively, with the Z isomer favored. For both amides there is no base-catalyzed E-Z exchange, and H_Z exchanges with solvent faster than H_E, by a factor of 2.0 ± 0.2 for N-methylformamide and 8 for N-t-butylformamide (see Table 2). If reprotonation of the isomeric E and Z imidate anions occurs at the same diffusion-controlled rate,[6] then the measured rate ratios, when corrected for ground-state equilibria, provide a direct measure of anion (product) stabilities. Thus the Z anion is more stable than the E anion by a factor of 6.7 for NMF, whereas the E anion is more stable by a factor of 3.6 for NBF.

The observation that $k_{ZS}^{OH^-}$ exceeds $k_{ES}^{OH^-}$ in both cases is at first puzzling. It had been anticipated by analogy to carboxylic esters

and the majority of primary amides (Discussion, Section 2a), that electron-electron repulsion would further destabilize the E anion, making the equilibrium constant for the anions greater than K_{EZ} and the rate ratio $k_{ZS}^{OH^-}/k_{ES}^{OH^-}$ smaller than one. We propose here that steric hindrance to solvation of the Z anion (and of the transition-state leading to it, where the N-alkyl group is cis to the developing negative charge on oxygen) reduces the anion equilibrium constant relative to K_{EZ}. The effect should be greater the larger the alkyl group, and indeed, in the case of N-t-butylformamide, the E anion is actually more stable.

A value for $k_{ZS}^{OH^-}/k_{ES}^{OH^-}$ of 25 ± 3 (in 80% aqueous ethanol) was recently measured[93] by ^{15}N NMR for the nine-membered ring lactam 1-aza-2-cyclononanone, where K_{EZ} is about one. The authors ascribed the reduced reactivity of H_E to net destabilization of the Z anion, where ring strain results from increased C-N double bond character upon proton removal. As evidence for this effect they cite cyclononene, where the cis isomer is favored by 2.9 kcal/mole.[97] It is not at all clear, however, that cyclononene is a good model for the lactam anion, and in light of the results described here, it is tempting to conclude that the lactam Z anion is less stable because it cannot be as effectively solvated as the E anion. Further evidence against the ring-strain argument is provided by a comparison of proton exchange in 2-pyrrolidone and N-methylacetamide. Two studies agree[7,11] that 2-pyrrolidone, which is locked in the E configuration,

undergoes base-catalyzed proton exchange about ten times faster than N-methylacetamide, which is largely in the Z form.

We have measured the anion equilibrium constant of N-methylformamide in the polar solvent DMSO-d_6 and in the non-polar solvent dioxane. The anion equilibrium constant in DMSO-d_6 saturated with potassium t-butoxide is 5.2, compared to 13.3 without added base, in reasonable agreement with the measured rate ratio of 0.5 in water. This confirms the argument that the exchange rates reflect the relative stabilities of the intermediate imidate anions. More importantly, the anion equilibrium constant in dioxane is 18.8, compared to 12.8 without added base. This result indicates that the E anion is indeed less stable, as expected, but only in non-polar solvents. In polar solvents it is solvated better, and stabilized, because the Z anion suffers steric hindrance to solvation.

We have also measured a k_E/k_Z ratio of 0.65 for base-catalyzed exchange of N-methylformamide in t-butanol. This value is not much larger than the value of 0.5 measured in water. We conclude that, although t-butanol is relatively non-polar, it is nevertheless hydroxylic and capable of solvating the isomeric imidate anions, with the Z anion solvated less effectively, so that the rate ratio is again less than one.

4. Water-Catalyzed Exchange in Imidic Esters

Water-catalyzed proton exchange in two protonated imidic esters was examined, since such exchange serves as a model for the imidic-acid route. Protonated ethyl acetimidate undergoes slow exchange in 46% w/w aqueous sulfuric acid, and the rate constants for this exchange were measured by saturation-transfer. Hydolysis of the imidic ester[33] was negligible in the time necessary to make the measurements. Kinetic data are presented in Table 4. We have found that there is no E-Z exchange, and that H_Z exchanges about twice as rapidly as H_E. No E-Z exchange was expected, owing to the configurational stability of the resulting imidic esters[47] and their rapid rate of reprotonation.[45] Moreover, the observation that H_Z exchanges faster than H_E is consistent with the fact that the E antiperiplanar form (resulting from loss of H_Z) is more stable than the Z_{ap} form, owing to mutual repulsion of the lone-pair dipole moments in the latter.[43-45, 98-100] A similar argument indicates that favoring of the syn-periplanar form should result in H_E exchanging faster. To check this prediction, proton exchange in protonated 2-iminotetrahydrofuran, which is locked in the syn-periplanar configuration, was examined in wet DMSO, and it was found that H_E does indeed exchange approximately 15% faster than H_Z (see Table 12). Thus the Z_{sp} configuration is slightly more stable than the E_{sp} configuration. This result is consistent with the observation that in N-phenyl-2-iminotetrahydrofuran, the Z_{sp} form is favored over the E_{sp} form by a factor of two.[101]

5. Proton Exchange in Strong Acid

Whereas imidic esters undergo proton exchange at rates measurable by NMR in 30% aqueous sulfuric acid, but not in 60% w/w aqueous sulfuric acid, amides undergo proton exchange in these media far too fast to be measured by NMR. Indeed, fuming sulfuric acid is required to reduce the water activity sufficiently to slow proton exchange so that it is measurable by NMR. This fact suggests that there is a second exchange pathway for amides in addition to water-mediated-NH proton removal from the O-protonated amide. To elucidate this mechanism, we undertook saturation-transfer studies of proton exchange in strong acid, where amides are quantitatively protonated on the carbonyl oxygen.[40]

In fuming sulfuric acid, the solvent used for these studies, water activity is extremely low and HSO_4^- is the strongest base available to serve as the proton acceptor. Since the N-H protons of O-protonated amides are not very acidic, direct transfer of an N-H proton to HSO_4^- might be expected to be too energetically costly to compete with an alternative exchange pathway which involves initial O-deprotonation followed by reprotonation on nitrogen. Furthermore, $RCONH_3^+$ ($pK_a \sim -9$)[34] is not a strong acid compared to H_2SO_4 ($H_0 = -12.2$),[130] so that N-H proton transfer to HSO_4^- might not be ultrafast, relative to rotation of the $-NH_3^+$ group. Then it might be expected that H_E and H_Z can become equivalent in the N-protonated amide, and thus exchange at identical rates.

The results of saturation-transfer studies of acetamide, 3,5-dinitrobenzamide and trichloroacetamide in fuming sulfuric acid are collected in Tables 5 and 6, and provide support for this model. The kinetic data indicate that, within experimental error, the N-H protons of these O-protonated amides exchange with solvent at identical rates, and with each other at the same rate. Liler[3] has also favored this mechanism for exchange on the basis of the observation that the N-H NMR signals in O-protonated acetamide appear to coalesce with each other as well as with the solvent NMR signal. Her conclusion is not firm, however, and these saturation-transfer experiments represent the first conclusive evidence that proton exchange in strong acid occurs via the N-protonated form.

In the experiments described here, no NMR signal due to -O<u>H</u> in $RC(OH)NH_2^+$ is observed, indicating rapid exchange of this proton with solvent. At -90°C, however, the -OH signal of O-protonated acetamide in fluorosulfuric acid is visible but broad, owing to exchange with solvent at a rate of approximately 60 sec^{-1}.[102] At 25°C, where we have found the rate of acetamide -NH proton exchange in fuming sulfuric acid to be about 2 sec^{-1} (see Table 5), the rate of -OH proton exchange can be estimated with these data to be about 2×10^6 sec^{-1}. Thus -OH proton exchange exceeds -NH proton exchange by a factor of about 10^6.

The greater rate of -OH over -NH proton exchange in these O-protonated amides may be accounted for by an additional pathway for

-OH exchange alone to occur. We suggest that -OH protons may undergo additional acid-catalyzed exchange via the dication, $RC(OH_2^+)=NH_2^+$, which is formed in kinetically significant amounts by protonation of $RC(OH)=NH_2^+$. By analogy to protonated amidines,[103] where $RC(NH_2)=NH_2^+$ is more stable than $RC(NH_3^+)=NH$, $RC(OH_2^+)=NH_2^+$ is expected to be more stable than the other possible dication, $RC(NH_3^+)=OH^+$. It has been established[103] that acid-catalyzed exchange in amidinium ions, $RC(NH_2)=NH_2^+$, which are isoelectronic with O-protonated amides, occurs by way of the dication $RC(NH_3^+)=NH_2^+$, providing precedent for our mechanism of -OH proton exchange.

It is also possible that -OH proton exchange is concerted, involving simultaneous -O-H bond-making and bond-breaking in the transition-state. Although the dication $RC(OH_2^+)=NH_2^+$ thus may not be an actual intermediate in these proton transfer reactions, we cannot at present exclude it as an intermediate.

6. Proton Exchange in Dilute Acid

a. Primary Amides

Two possibilities exist for dilute acid-catalyzed proton exchange in amides: 1) direct protonation on nitrogen (Eq. [11]), and 2) protonation on oxygen, followed by proton abstraction from nitrogen to generate the imidic acid (Eq. [12]).[37,39]

$$H^+ + RCONH_2 \rightleftharpoons RCONH_3^+ \qquad [11]$$

$$\Big\downarrow\Big\uparrow$$

$$RC(OH)NH_2^+ \rightleftharpoons RC(OH)NH + H^+ \qquad [12]$$

In order to distinguish between these mechanisms, we have used our saturation-transfer method to study such exchange in ten primary amides, and the results are collected in Table 7. In all cases, H_E and H_Z exchange with solvent at significantly different rates. This result would seem to exclude the N-protonation mechanism (Eq. [11]), since protonation on nitrogen, to produce $RCONH_3^+$, should make the E and Z protons equivalent. However, this cation is a strong acid ($pK_a \sim -9$),[34,104] and undergoes diffusion-controlled[46] proton transfer to water. Therefore its lifetime is only on the order of 10^{-12} sec.[105] This is comparable to 0.5×10^{-12} sec, the measured lifetime[106] of a conformer of the isoelectronic species CH_3COCH_3, and hydrogen bonding of $-NH_3^+$ might further raise the barrier to rotation about the C-N single bond. Thus it is not unlikely that rotation and deprotonation occur at competitive rates, thereby preserving the inequivalence of H_E and H_Z. In order to quantitatively interpret the results of our saturation-transfer experiments, we must first explore the kinetic consequences of restricted rotation about the C-N bond in $RCONH_3^+$.

Protonation of the nitrogen lone pair of $RCONH_2$ produces a Boltzmann distribution of the conformers of $RCONH_3^+$, so that the predominant conformation is close to the most stable one (4)[107-110]

(see Figure 23). Conformer $\underset{\sim}{4}$ may then rotate, with a first-order rate constant k_r, to either conformer $\underset{\sim}{5}$ or $\underset{\sim}{6}$ before deprotonation. A given conformer then loses either highly acidic ($pK_a \sim -9$)[34] proton gauche to the R-group at a diffusion-controlled rate characterized by the first-order rate constant k_d. Abstraction of the proton <u>syn</u> to the carbonyl, however, should be negligibly slow in comparison, since this proton is estimated to have a pK_a of approximately $\underset{\sim}{6}$.[111]

However, torsional oscillation of 45° or more in conformers $\underset{\sim}{4}$ - $\underset{\sim}{6}$ can be shown to result in the proton <u>syn</u> to the carbonyl being lost at the same diffusion-controlled rate as for the other two (oscillation of ±60° being required to surmount the threefold energy barrier to the other conformation), since the neutral amide, rotated by 45°, plus hydronium ion is isoenergetic with the N-protonated amide. At equilibrium, the rate of proton loss from the N-protonated amide, rotated by 45°, must be equal to the rate of protonation of the neutral amide, also rotated by 45°. The rate of the latter process is negligible at room temperature (due to the vanishingly small concentration of neutral amide rotated by ≥45°) and microscopic reversibility then requires that if a proton does not enter into the position that eclipses oxygen, it cannot leave from that position. Therefore, we make little error in assuming that the proton <u>syn</u> to oxygen may not be removed by water. Alternatively, one may calculate the amount of N-protonated amide rotated by ≥45°. For a threefold potential of 1 kcal/mole, only 6.5% of the N-protonated population is rotated by ≥ 45°, and may be safely neglected.

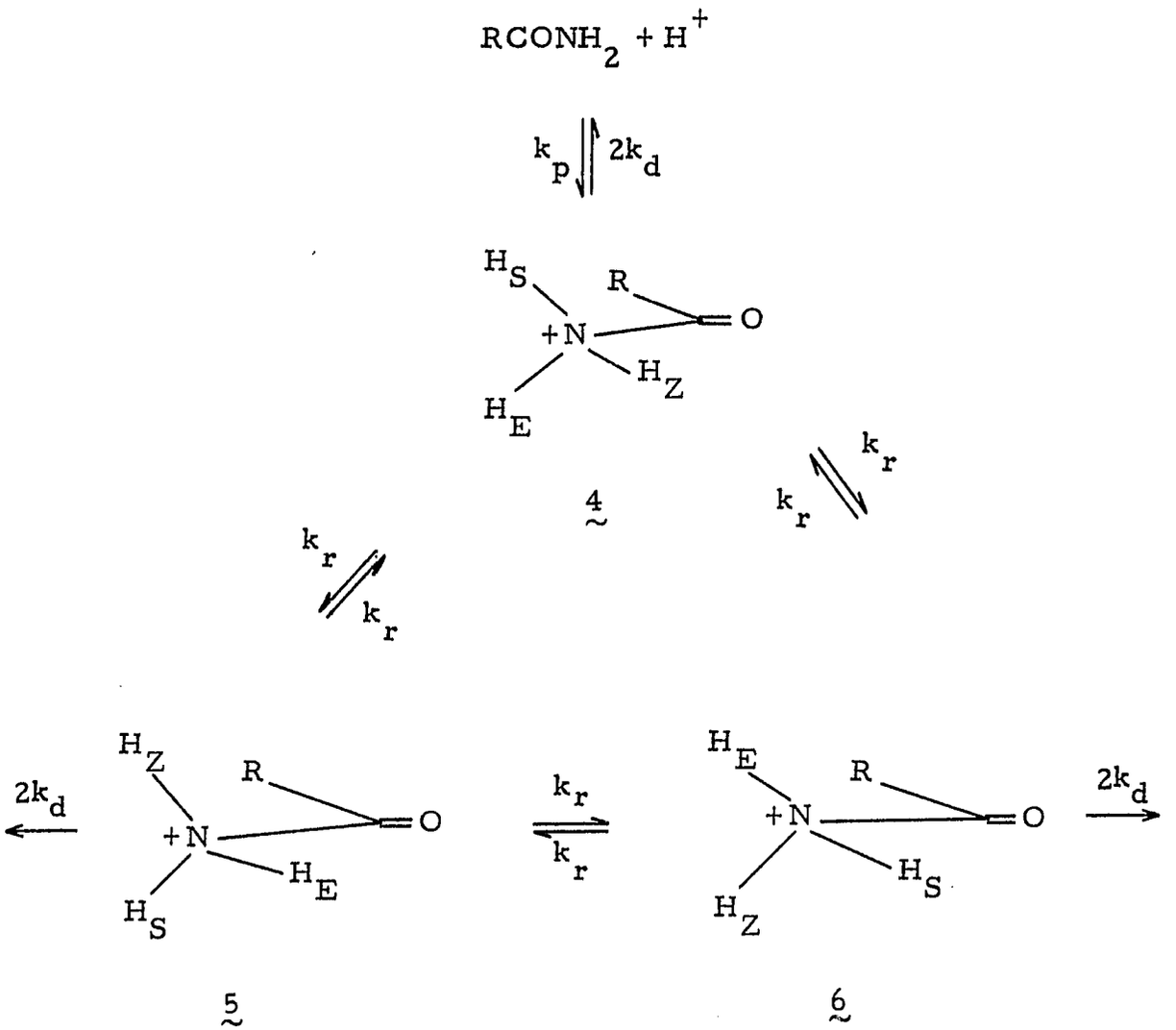

Figure 23. Kinetic scheme for proton exchange in primary amides via N-protonation. H_S denotes the proton from solvent.

Since loss of H_Z requires rotation to $\underset{\sim}{5}$ or $\underset{\sim}{6}$, whereas loss of H_E does not, we may expect that H_E might exchange faster, if rotation and deprotonation are competitive. This intuitive notion can be quantified in the following manner. Application of the steady-state approximation to conformers $\underset{\sim}{4}$, $\underset{\sim}{5}$, and $\underset{\sim}{6}$ within the context of Figure 23 allows us to solve for the steady-state concentrations of these conformers in terms of k_r, k_d, and k_p, the pseudo-first-order rate constant for protonation of $RCONH_2$. The results are

$$[4] = \frac{k_r + 2k_d}{2k_d(3k_r + 2k_d)} \cdot k_p\,[\text{amide}] \qquad [13]$$

$$[\underset{\sim}{5}] = [\underset{\sim}{6}] = \frac{k_r}{2k_d(3k_r + 2k_d)} \cdot k_p\,[\text{amide}] \qquad [14]$$

The first-order rate constants for exchange measured in these NMR experiments are independent of [amide] and are simply:

$$k_{ES} = k_d([\underset{\sim}{4}] + [\underset{\sim}{6}]) = \frac{(k_r + k_d)}{(3k_r + 2k_d)} \cdot k_p \qquad [15]$$

$$k_{ZS} = k_d([\underset{\sim}{5}] + [\underset{\sim}{6}]) = \frac{k_r}{(3k_r + 2k_d)} \cdot k_p \qquad [16]$$

$$\left.\begin{aligned} k_{ZE} &= k_d([\underset{\sim}{5}] + [\underset{\sim}{6}]) \\ k_{EZ} &= 2k_d([\underset{\sim}{5}]) \end{aligned}\right\} = \frac{k_r}{(3k_r + 2k_d)} \cdot k_p \qquad [17]$$

where Eqs. [15]-[17] have been obtained by appropriate substitution of Eqs. [13] and [14]. Equations [15]-[17] show that $k_{EZ} = k_{ZE}$, as required by equilibrium, and that protonation on nitrogen results in acid-catalyzed intramolecular exchange of H_Z with H_E at a rate equal to the rate at which it exchanges with solvent, because exchange of H_Z requires rotation, whereupon it exchanges with equal probability into the solvent and E sites. Moreover, to the extent that the lifetime of $RCONH_3^+$ is too short to permit rotational equilibration about the C-N single bond, H_E will exchange faster with solvent than H_Z. The ratio of solvent exchange rates is

$$\frac{k_{ES}}{k_{ZS}} = 1 + \frac{k_d}{k_r} \qquad [18]$$

and the ratio of <u>total</u> exchange rates for H_E and H_Z is

$$\frac{k_E}{k_Z} \equiv \frac{(k_{ES} + k_{EZ})}{(k_{ZS} + k_{ZE})} = 1 + \frac{k_d}{2k_r} \qquad [19]$$

If exchange can be demonstrated to proceed by N-protonation, Eqs. [18] and [19] then provide a measure of k_r relative to k_d.

In the primary amides studied here, H_E and H_Z are diastereotopic, and we have measured each of their exchange rates separately. A distinction between the N-protonation and imidic-acid pathways (Eqs. [11] and [12]) is provided by comparing rate constants for intermolecular and intramolecular exchange. In contrast to the behavior

elucidated above for the N-protonation pathway, which requires that $k_{ZS} = k_{ZE}$, the imidic-acid pathway requires that k_{EZ} and k_{ZE} be zero, since the configurational stability[47] of the imidic acids precludes acid-catalyzed intramolecular exchange. The distinction between the imidic-acid and N-protonation routes thus depends on whether k_{ZE} is zero or equal to k_{ZS}, respectively.

Kinetic data for acid-catalyzed exchange in ethylene glycol (see Table 7) demonstrate that for acetamide, acrylamide, methacrylamide, benzamide, and formamide, k_{ZE} differs from k_{ZS} by less than one standard deviation. We therefore conclude that exchange in these amides proceeds predominantly via the N-protonation route, although we cannot rule out a small fraction of exchange via the imidic acid. Moreover, k_{ES} and k_{SE} are significantly greater than k_{ZS} and k_{SZ}, respectively, for all of these amides. This result is consistent with line-broadening measurements (Ref. 42 and Table 11), which show that H_E exchanges faster than H_Z in the acid-catalyzed reaction.

The data in Table 8 provide further evidence that $k_{ZE} = k_{ZS}$ for benzamide-^{15}N in 60% aqueous methanol. In the limit where exchange dominates the intrinsic relaxation rate and uncatalyzed rotation, the saturation-transfer quantities $t_Z(E)$ and $t_E(Z)$ reduce to $k_{ZE}/(k_{ZE} + k_{ZS})$ and $k_{EZ}/(k_{EZ} + k_{ES})$, respectively (see Eq. [3]). For benzamide-^{15}N, the limiting value of $t_Z(E)$ approaches 0.49 ± 0.02 at the highest acidity, indicating that k_{ZE} equals k_{ZS}. Furthermore, since $k_{EZ} = k_{ZE} = k_{ZS}$, a value for k_{ES}/k_{ZS} of 3.0 ± 0.9 can

can be estimated from the measured limiting value for $t_E(Z)$ of 0.25 ± 0.07 (Table 8). This value agrees with the value of 3.9 ± 0.2 measured in a full saturation-transfer experiment at lower acidity in this solvent (Table 7).

Further qualitative support for the conclusion that N-protonation is the sole exchange pathway in acrylamide is provided by an analysis of the NMR lineshape of the N-H region at intermediate rates of exchange. Acid-catalyzed intramolecular exchange of H_E and H_Z at a rate equal to the rate at which H_Z exchanges with solvent should cause the N-H signals to coalesce with each other, and to move upfield towards solvent as well. For a non-exchanging sample in ethylene glycol at 90 MHz, the chemical-shift difference of H_E and H_Z is 52 Hz. Successive acidification of the solution progressively broadens the N-H lines, but does not affect either their chemical shifts or their separation. When the solution is further acidified to pH $\sim$ 0.3, extensive exchange-broadening of the N-H resonances occurs, and they do appear closer to each other by about 10 Hz, suggestive of intramolecular exchange via N-protonation. A rough value of k_{EZ} may be calculated from this result with Eq. [20] [59]:

$$k_{EZ} = \frac{\pi}{\sqrt{2}} (\Delta\nu^{o2} - \Delta\nu^2)^{1/2} \qquad [20]$$

where $\Delta\nu^o$ and $\Delta\nu$ are the chemical-shift differences in the absence and presence of chemical exchange, respectively. Using values of 52

and 42 Hz, k_{EZ} is about 70 sec^{-1}. According to the results in Table 7, H_Z is also exchanging with solvent at this rate, and H_E is exchanging with solvent at 1.5 times this rate. Thus, the total exchange rates necessary to produce a 10 Hz lessening in chemical-shift difference are 175 sec^{-1} and 140 sec^{-1} for H_E and H_Z. Mort importantly, the N-H signals have not shifted significantly upfield towards solvent, which is about 200 Hz upfield of H_Z. On the basis of Eq. [20], we expect this result, since the chemical-shift difference between solvent and N-H sites is too big to produce noticeable upfield shifts at these rates.

An alternative argument, namely that exchange occurs through the imidic-acid route, but that because k_{ES} exceeds k_{ZS} the chemical-shift difference between H_E and H_Z lessens, can be discounted since substantial upfield shifts are required for both H_E and H_Z with H_E shifting faster, and these are not observed. We therefore conclude that the observed lineshape behavior is additional evidence in favor of the N-protonation pathway in acrylamide. Calculated lineshapes using the lineshape simulation program DNMR3[113] bear out the conclusions reached with Eq. [20].

Bovey and Tiers[41] were unable to observe any lessening of chemical-shift difference for the N-H protons in acidified aqueous solutions of polyacrylamide, and so concluded that exchange and C-N bond rotation do not occur via a common intermediate. They were, however, working at 40 MHz, where the amide signals appeared on the

shoulder of the large water peak, and it is probable that in their experiments the amide protons would be broadened and lost in the solvent envelope at the fairly rapid exchange rates which we have found necessary to produce a detectable lessening in chemical-shift difference.

Having established that proton exchange in acetamide, acrylamide, methacrylamide, benzamide, and formamide (and almost certainly trimethylacetamide and salicylamide as well, although saturation-transfer experiments were not conducted on these compounds) proceeds entirely by N-protonation, we can use the rate ratios collected in Tables 10 and 11 in conjunction with Eq. [19] to obtain further insight into the rotational barriers in these N-protonated amides.

Since the rate of deprotonation of $RCONH_3^+$ is diffusion-controlled and constant for all of these amides, the observed values of $k_E^{H^+}/k_Z^{H^+}$ in Tables 10 and 11 provide a measure of k_r, with larger ratios corresponding to larger rotational barriers. We have observed that acrylamide, methacrylamide, benzamide, and formamide show rate ratios appreciably greater than one, whereas acetamide, trimethylacetamide, and salicylamide exhibit ratios near one. We can then rationalize this dichotomy in terms of the effect of R on the barrier.[42] The barrier should be lower when R = $-CH_3$ or $-C(CH_3)_3$, since these groups have their steric bulk above and below the O-C-N plane, and thus raise the energy of the preferred conformation (7) of $RCONH_3^+$. The barrier in CH_3COCH_3, which is isoelectronic to

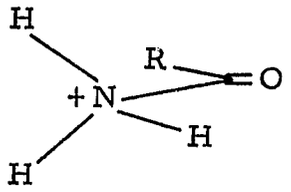

7

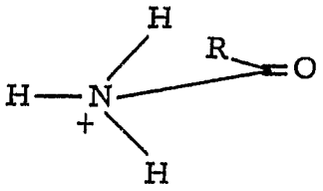

8

$CH_3CONH_3^+$, is in fact lower than that in $HCOCH_3$.[107] This argument has also been used[112] to rationalize the lowered barrier in cis-butene, as compared to propene or trans-butene. In contrast, groups that have their steric bulk in the O-C-N plane may be expected to raise the barrier by destabilizing 8, the transition-state for rotation. Indeed, the barrier in $CH_2=CHCOCH_3$, which is isoelectronic to $CH_2=CHCONH_3^+$, is higher than that in $HCOCH_3$.[107] For those groups that lower the barrier, $k_E^{H^+}/k_Z^{H^+}$ is close to unity, but for $CH_2=CH^-$, $CH_2=CMe-$, and $C_6H_5^-$, there is a greater barrier to exchange of H_Z, so the ratio is somewhat greater than unity.

Measurement of the exchange rate ratio for benzamide and salicylamide in ethylene glycol (Table 11) indicates that, whereas H_E exchanges about 34% faster than H_Z in benzamide, they exchange at equal rates in salicylamide. The effect of the O-hydroxy group is thus opposite to that expected on the basis of steric effect arguments. We tentatively ascribe the equality of exchange rates in the latter compound to hydrogen bonding in the transition state for rotation (9), which lowers the barrier and allows H_E and H_Z to become equivalent in the lifetime of the N-protonated cation.

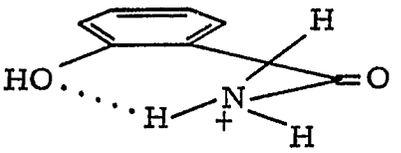

9

It is possible to estimate the barrier to rotation in these N-protonated amides with Eq. [19], subject to making some assumption concerning the magnitude of k_d, the first-order rate constant for diffusion-controlled deprotonation. For definiteness we adopt[105, 114] a value for k_d of 10^{12} sec^{-1} in aqueous solution. Then, for example, values of k_r for $CH_3CONH_3^+$ and $CH_2=CHCONH_3^+$ of $3 \cdot 10^{12}$ sec^{-1} and $1 \cdot 10^{12}$ sec^{-1} can be calculated with the rate ratios in Table 10. Using the expression[106] $k_r = 1.3 \times 10^{13} \exp(-V_o/RT)$, barriers to rotation V_o of 0.9 and 1.5 kcal/mole are arrived at for N-protonated acetamide and acrylamide, respectively. These values are quite close to the barrier heights of 0.8 and 1.25 kcal/mole measured[107] for the isoelectronic ketones in the gas phase. A barrier height of 0.9 kcal/mole has also been measured[106] for acetone in the pure liquid. The close agreement indicates that hydrogen bonding of solvent to the $-NH_3^+$ group[115] does not raise the barrier to rotation. There is some evidence in support of this tentative conclusion. The correlation time of NH_4^+ in aqueous solution has been estimated to be $\sim 10^{-12}$ sec,[116] not much longer than that for liquid CH_4, which is ca. 2×10^{-13} sec.[129] It has been concluded[117] that there is free

rotation in $CH_3NH_3^+$, although this could be due to methyl rotation while the $-NH_3^+$ group is "anchored" within a solvent shell. Most recently, Levy et al.[118] have concluded, on the basis of ^{13}C and ^{15}N T_1 measurements, that there is free rotation in $C_6H_5NH_3^+$ in CF_3SO_3H, but that rotation is hindered ($k_r \sim 10^{10}$ sec^{-1}) in water, methanol, and acetonitrile. It is difficult, however, to see why rotation should be hindered in the latter solvent.

The absence of a solvation effect on rotation in the N-protonated amide can be rationalized by assuming that the $-NH_3^+$ group carries solvent with it as it rotates, so that strong hydrogen bonds need not be broken. Such a model then predicts that k_r should depend on solvent viscosity. Therefore, to gain better insight into the nature of the rotational process, we have estimated the dependence of k_r on solvent viscosity by measuring k_E/k_Z for benzamide-^{15}N in ethylene glycol and in 60% aqueous methanol. The measured rate ratio should reflect the viscosity dependence of both k_r and k_d, according to Eq. [19], but we can independently estimate the latter dependence.

The rate ratio in 60% aqueous methanol, as measured by both saturation-transfer and line-broadening, is 2.45 (Table 10). The rate ratio measured in ethylene glycol, however, is only 1.34 (Table 11), so k_d/k_r has been reduced in this more viscous solvent. With Eq. [19], the ratio of k_d/k_r in 60% aqueous methanol to that in ethylene glycol can be calculated with these values to be about 4.3, and it remains to assess the ratio of k_d in 60% aqueous methanol to k_d in

ethylene glycol in order to estimate the k_r ratio for these two solvents.

Since the rate-limiting step in the amide deprotonation actually involves translational or rotational diffusion of hydronium ion away from the amide,[114,119] the k_d ratio might be expected to be proportional to the ratio of solvent viscosities. But it is an oversimplification to take k_d as proportional to the macroscopic viscosity, and it would seem that a better measure of the k_d ratio is provided by the ratio of the proton limiting conductance in the two solvents. This quantity has been measured in both 60% aq. methanol[120] and ethylene glycol,[121] values of 116 and 27.7 $cm^2/ohm \cdot mol$, respectively, being obtained. We thus take the k_d ratio to be 4.2, and the fourfold increase in k_d then completely accounts for the fourfold increase in (k_d/k_r) in aqueous methanol relative to ethylene glycol. Therefore k_r is the same in both solvents, and this suggests that rotation of $-NH_3^+$ occurs <u>within</u> a solvent shell, with hydrogen bonds to solvent being simultaneously made and broken. This conclusion is independent of our choice for k_d.

The k_d/k_r ratios for acetamide and benzamide can be calculated with Eq. [19] and the data in Table 10 to be 0.34 and 2.9, respectively. Thus k_r exceeds k_d for acetamide but is smaller than k_d for benzamide. Since exchange of H_Z requires rotation of the N-protonated amide, we have the remarkable result that the rate-limiting step for exchange of H_Z in benzamide is largely rotation

about the C-N single bond, occurring with a rate constant of approximately 3.5×10^{11} sec^{-1}. In acetamide, where k_r exceeds k_d, rotation is only partially rate-limiting.

The results of Cox[122] are consistent with this picture. He has measured deuterium isotope effects of 1.25 and 1.06 for the acid-catalyzed isomerization of dimethylacetamide and dimethylbenzamide, respectively. Such exchange must occur by protonation on nitrogen, and isomerization then requires rotation. To the extent that the proton is more fully transferred in the transition-state for rotation in dimethylbenzamide (where, by analogy to benzamide, rotation is largely rate-limiting) than in dimethylacetamide, a smaller deuterium isotope effect is expected for dimethylbenzamide, as observed.

The kinetic data in Table 7 demonstrate that for ethyl oxamate, cyanoacetamide, malonamide, and chloroacetamide, k_{ZE} is considerably smaller than k_{ZS}, indicating that exchange occurs predominantly through the imidic pathway. Some exchange via N-protonation is nevertheless occurring, since k_{EZ} and k_{ZE} are non-zero. For H_Z, the fraction of exchange occurring through N-protonation is simply k_{ZE}/k_{ZS}, or 20%, 18%, 43%, and 37% for ethyl oxamate, cyanoacetamide, malonamide, and chloroacetamide, respectively. For H_E, the N-protonation exchange fraction is $\geq k_{EZ}/k_{ES}$ (since $k_{EZ} \leq k_{ES}$ in the N-protonation pathway), or at least 12%, 14%, 29%, and 34%, respectively, of the total intermolecular exchange. For dichloroacetamide, where k_{EZ} and k_{ZE} are zero, within

experimental error, proton exchange occurs entirely by the imidic-acid pathway. The effect of electron-withdrawing groups, then, is to produce a changeover in mechanism from N-protonation to the imidic-acid pathway. This observation will be rationalized later.

We had expected that H_E and H_Z should exchange at different rates in the imidic-acid pathway, since they remain diastereotopic in the conjugate acid 10 and since the intermediates (11-Z, 11-E) are expected to be configurationally stable.[47] Moreover, by analogy with imidic esters,[43] 11-E should be more stable than 11-Z. To the extent that the transition states reflect the relative stabilities of the intermediates, H_Z should then exchange faster with solvent than

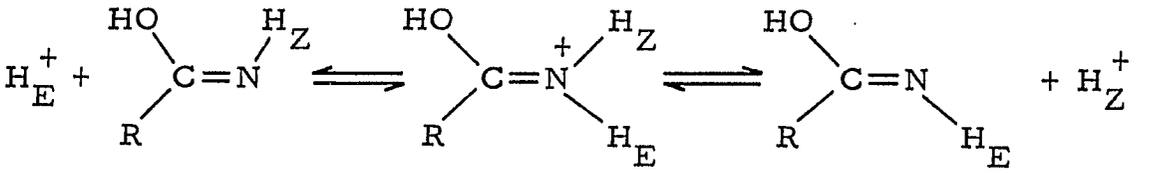

11-Z 10 11-E

H_E. Indeed, k_{ZS} exceeds k_{ES} in protonated ethyl acetimidate (Table 6). Several additional lines of experimental evidence[99,100] also support these relative stabilities in imidic esters. The theoretical consensus regarding the relative configurational stabilities of formimidic acid, though, is less clear: one calculation concludes that the E_{ap} form is most stable,[44] while another[123] suggests that the Z_{sp} form is most stable.

H_Z was also observed to exchange about 20% faster than H_E in dichloroacetamide (Tables 7, 11, Figure 21), whereas in the remaining

four amides where the imidic-acid mechanism is predominant, k_{ES} is somewhat larger than k_{ZS} (Tables 7, 11). This might be rationalized (despite the analogy to imidic esters) if the syn-periplanar form (O-H syn to -R in 11-Z and 11-E) is more stable than the anti-periplanar form in these imidic acids, so that 11-Z_{sp} is more stable than 11-E_{sp}, owing to mutual lone pair repulsion of lone pair dipole moments in the latter. Indeed, in protonated 2-iminotetrahydrofuran, which serves as a model for the syn periplanar configuration, we have found that H_E exchanges about 15% faster than H_Z (Table 12).

An alternative, and more likely, possibility is simply that 11-Z, being more polar, is preferentially solvated, so that it is in fact more stable than 11-E in the polar, protic solvents used in this study. A similar solvent polarity effect has been observed in the imidic esters MeC(OMe)NPh and +BuC(OMe)NMe, where the E/Z diastereomer ratios decrease from 2.2 and ′.7, respectively, in CCl_4 to 1.3 and 2.5 in methanol.[43]

If solvation of the imidic acids is a significant factor in determining their relative stability, the E form might be expected to be more stable than the Z form in less polar solvents, so that H_Z should exchange faster than H_E. To this end, acid-catalyzed hydrogen exchange in ethyl oxamate was studied in cyclohexanol, which has a dielectric constant of 15 (compared to 37 and 81 for ethylene glycol and water, respectively). For ethyl oxamate in ethylene glycol and water, imidic-acid exchange is predominant, but H_E exchanges faster

than H_Z. In cyclohexanol, however, as illustrated in Figure 18, H_Z exchanges significantly faster than H_E, indicating that the E imidic acid is more stable in this less polar solvent.

It seems, then, that although the E_{ap} configuration is favored in imidic esters, the E and Z configurations of the imidic acids are much closer in energy. Indeed, the 20%-faster exchange rate of H_Z in dichloroacetamide corresponds to a free-energy difference of only 110 cal/mole favoring 11-E over 11-Z, so very small solvation and polarity effects might be sufficient to produce stability reversals. H_Z also exchanges faster than H_E in trichloroacetamide (Table 11), indicating exchange through the imidic acids, yet in trifluoroacetamide, which almost certainly exchanges through the imidic-acid pathway as well, H_E exchanges about 60% faster than H_Z (Table 10). The results reported here provide the first experimental evidence that polar, protic solvents are capable of reversing the stabilities of the imidic acid stereoisomers.

b. Secondary Amides

The relative contributions of the N-protonation and imidic-acid pathways to exchange have also been assessed for N-methyl and N-t-butylformamide. In order to make this assessment, it is first necessary to determine the kinetic consequences for proton exchange and isomerization resulting from protonation at the amide nitrogen.

The N-protonation route for acid-catalyzed proton exchange in secondary amides is detailed in Figure 24. Protonation on nitrogen

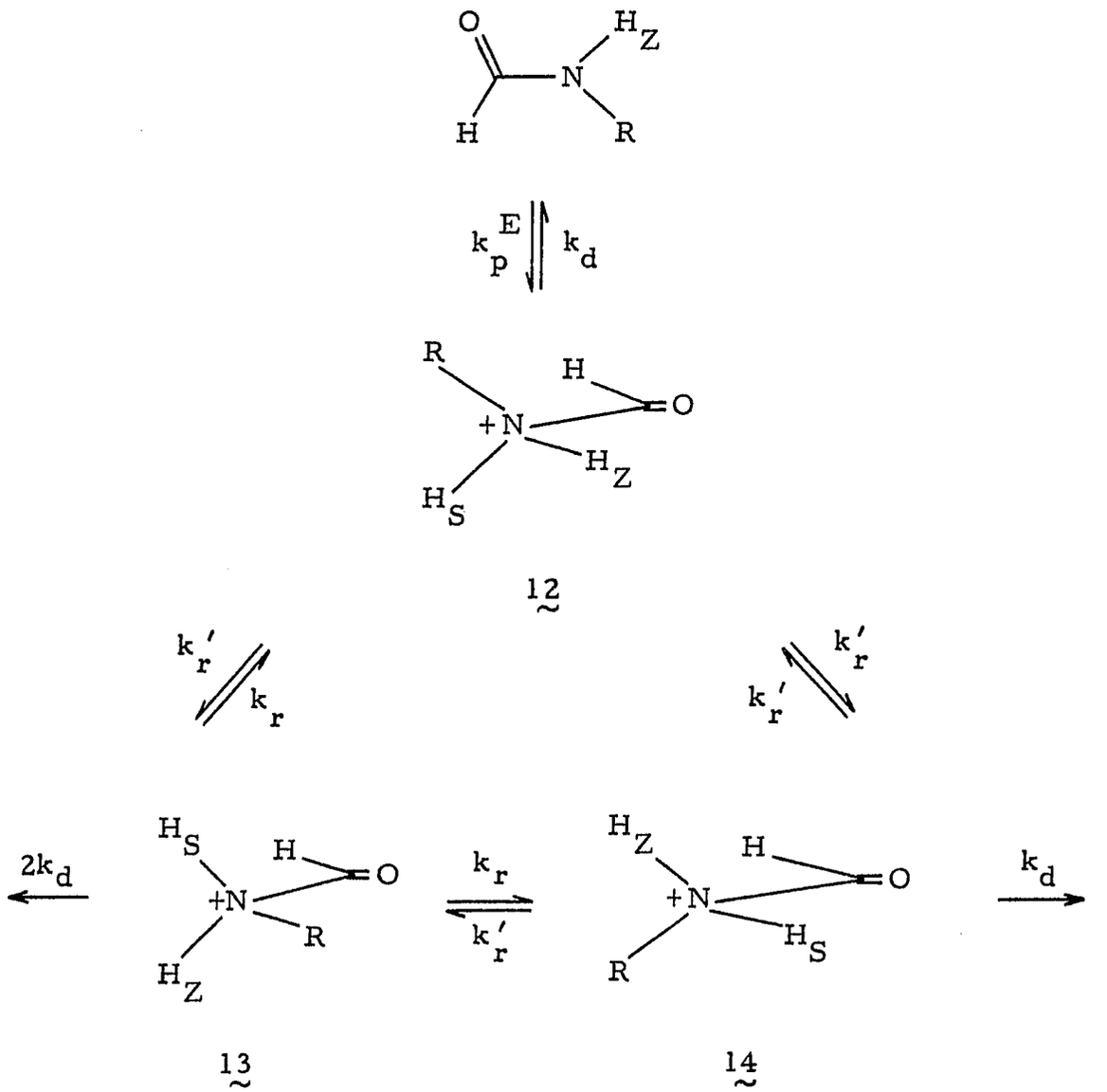

Figure 24. Proton exchange and isomerization in the E isomer of secondary formamides by protonation on nitrogen. H_S denotes the solvent proton.

of the E isomer (with pseudo-first-order rate constant k_p^E) produces conformer 12 (or its mirror image), which may then convert into conformers 13 and 14 with a rotational rate constant k_r', as shown.[124] The rotameric equilibrium constant, K_r, is defined by k_r/k_r', and can be estimated from model compounds. Strictly, three independent rate constants are necessary to describe the rotations, since 13 and 14 are probably not formed from 12 at the same rate. However, this scheme is simpler, and it avoids introducing an extra rate constant that we cannot measure. As previously discussed for primary amides, the proton syn to oxygen in a given conformer may not be removed by solvent, while the proton gauche to oxygen is removed at a diffusion-controlled rate characterized by the first-order rate constant k_d.

Rate expressions for exchange of H_Z and isomerization of the -R group may in the less abundant E isomer be derived, in a manner completely analogous to that used for primary amides, by applying a steady-state approximation to the three conformers and solving for the concentrations of these species in terms of k_p^E, k_r, k_r', and k_d. Thus

$$[12] = \frac{k_p^E k_r'(3k_r + 2k_d) \cdot [\text{E-amide}]}{2k_d(3k_r' + k_d)(k_r + k_r' + k_d)} + \frac{k_p^E \cdot [\text{E-amide}]}{(3k_r' + k_d)} \qquad [21]$$

$$[13] = \frac{k_r' k_p^E [\text{E-amide}]}{2k_d(k_r + k_r' + k_d)} \qquad [22]$$

$$[14] = \frac{k'_r k_p^E (3k_r + 2k_d) \cdot [\text{E-amide}]}{2k_d (3k'_r + k_d)(k_r + k'_r + k_d)} \qquad [23]$$

These concentrations may be checked in the appropriate limits: when deprotonation is much faster than rotation, the concentrations of [13] and [14] are vanishingly small, whereas when rotation exceeds deprotonation, the concentrations of [12] and [14] are equal, as expected, and the ratio of 12 (or 14) to 13 is given by k_r/k'_r.

The exchange rate of H_Z into solvent is simply $k_d[13] + k_d[14]$. The isomerization rate of the -R group from the E into the Z site (denoted by k_{EZ}^R) is equal to $2k_d$ [13], whereas the rate constant for isomerization of H_Z into the H_E site (denoted by k_{ZE}) is equal to k_d[13], or one-half k_{EZ}^R since H_Z may exchange not only into the H_E site but also into solvent, whereas the -R group cannot. Appropriate substitution of Eqs. [21]-[23] yields for these processes the first-order rate constant expressions.

$$k_{ZS} = \frac{3k_p^E k'_r}{2(3k'_r + k_d)} \qquad [24]$$

$$k_{EZ}^R = \frac{k_p^E k'_r}{(k_r + k'_r + k_d)} \qquad [25]$$

$$k_{ZE} = \frac{k_p^E k'_r}{2(k_r + k'_r + k_d)} \qquad [26]$$

where the superscript R in Eq. [25] denotes R-group isomerization. Similarly, by the steady-state method, the rate constant for exchange with solvent of H_E, in the predominant Z configuration of the amide, is simply equal to

$$k_{ES} = \frac{k_p^Z}{2} \qquad [27]$$

one-half the first-order rate constant for protonation of the Z isomer.

The three rate constant ratios of interest in the studies described here are the ratios of R-group and proton isomerization to proton exchange in the less stable E isomer, and the ratio of proton solvent exchange rates in the E and Z isomers of the secondary amide. These ratios, for exchange via the N-protonation mechanism, are given in Eqs. [28] - [30]

$$\frac{k_{EZ}^R}{k_{ZS}} = \frac{2(3k_r' + k_d)}{3(k_r + k_r' + k_d)} \sim \frac{2}{K_r + 1} \qquad [28]$$

$$\frac{k_{ZE}}{k_{ZS}} = \frac{(3k_r' + k_d)}{3(k_r + k_r' + k_d)} \sim \frac{1}{K_r + 1} \qquad [29]$$

$$\frac{k_{ZS}}{k_{ES}} = \frac{3k_r'}{3k_r' + k_d} \cdot \frac{k_p^E}{k_p^Z} \sim K_r \cdot K_{EZ} \qquad [30]$$

where the approximate expressions have been obtained by assuming that rotation is fast relative to deprotonation, and by appropriate substitution of the ground-state and rotameric equilibrium constants

K_{EZ} and K_r. Since isomerization and exchange in the E isomer both require rotation, we make little error in Eqs. [28] and [29] by assuming rapid rotation. Since rotation probably exceeds deprotonation in any event for the substituted formamides examined here (as judged from the kinetic data for $DCONH_2$ in Table 11, where $k_r = 2k_d$), this assumption can reasonably be made in Eq. [30] as well.

1. N-Methylformamide

In order to discuss exchange and isomerization in N-methylformamide, it is necessary at the outset to determine the relative stabilities of conformers 12-14 in Figure 23. By analogy to propionaldehyde,[125] which is isoelectronic with $HCONH_2Me^+$, conformers 12 and 14 are about 800 cal/mole less stable than 13, corresponding to a rotameric equilibrium constant K_r ($= k_r/k_r'$) of 0.26. The ground-state equilibrium constant K_{EZ} is 13.5 (see Results).

Equation [28] thus demonstrates that for exclusive N-protonation exchange, methyl isomerization should exceed exchange of H_Z with solvent by 60%. Equation [30] indicates that k_{ZS} should exceed k_{ES} by a factor of 3.5.

The data in Table 9 give measured values for k^R_{EZ}/k_{ZS} and k_{ZS}/k_{ES} of 0.42 and 3.2, respectively. These values, coupled to the values in Eqs. [28] and [30] expected for exchange only via N-protonation, permit an assessment of the relative contributions of the imidic-acid and N-protonation mechanisms to exchange in N-methylformamide.

The imidic-acid pathway requires that k^R_{EZ} be zero, since the configurational stability[47] of the imidic acids precludes acid-catalyzed isomerization. Isomerization can occur only by N-protonation, so that k^R_{EZ} provides a measure of the contribution of this pathway. The amount of exchange of H_Z occurring through N-protonation is just 0.42/1.6, or 26%. The remainder, or 74%, must then occur through the imidic-acid route. The amount of exchange of H_E occurring through N-protonation can be estimated with Eqs. [28] and [30] and the measured ratios from Table 9 to be $(0.42 \times 3.2)/(1.6 \times 3.5)$, or 24%, the remaining 76% proceeding through the imidic-acid route. Thus the latter route is the predominant mode of proton exchange for both isomers of N-methylformamide. The ratio of exchange rates of H_Z and H_E via the imidic-acid route is then just $(0.74/0.76) \times 3.2$, or 3.1.

Since reprotonation of the imidic acids is expected to be diffusion-controlled for both isomers,[33,46] the solvent exchange rate ratio of 3.1 for this pathway directly reflects the stability difference of the imidic acids. Therefore, the relative exchange rates imply that the stabilities of the isomeric imidic acids parallel the stabilities of the amide tautomers, with the Z imidic acid more stable. The equilibrium constant is just $K_{EZ}/3.1$, or 4.4. Here as well, as in the case of ethyl oxamate, malonamide, and cyano- and chloroacetamide, the relative stability of the isomeric imidic acids appears to be opposite to that observed for imidic esters.

A fundamental aspect of the imidic-acid pathway is that, unlike the N-protonation pathway, it should be subject to general-acid catalysis. We have sought to establish the presence of general-acid catalysis in N-methylformamide by varying buffer concentrations at constant pH. Three samples were buffered at pH 1.3 with trichloroacetate buffers, and the results are presented in Figure 26. For the three spectra presented in Figure 26, the total concentration of trichloroacetic acid was 0.16 M, 0.3 M and 0.43 M, respectively, with increasing acid concentration producing increasing doublet collapse of the N-methyl signals resulting from proton exchange. Thus proton exchange in NMF is subject to general acid catalysis, providing further evidence in favor of the imidic-acid pathway. We have also verified the existence of general-acid catalysis in N-methylformamide with phosphate and oxalate buffers by observing increased proton exchange with increasing concentration of the general acid in a pH range where the specific-acid catalyzed reaction is not significant.

Further qualitative evidence in support of our conclusion of predominant imidic-acid exchange in N-methylformamide in dilute acid lies in a comparison of the lineshape in strong and dilute acid (see Figures 14 and 21). In strong acid, where the exchange mechanism is entirely via N-protonation (Discussion, Section 5), the E methyl appears as a shoulder on the Z methyl, indicating substantial isomerization concurrent with proton exchange. In contrast, in dilute acid the E methyl, although broadened, always remains distinct from

the Z methyl. Thus isomerization is not as fast relative to proton exchange in dilute acid, due to incursion of the imidic-acid mechanism.

The relative stabilities of the N-conjugate and imidic acids of N-methylformamide are summarized in Figure 25.

Martin[39] has accounted for greater rates of proton exchange in the Z isomer of N-methylacetamide, N-methylbenzamide, and N-methylformamide over isomerization in the corresponding tertiary amides in terms of predominant exchange via the imidic-acid route for all three secondary amides. However, on the basis of the results previously presented for primary amides, where electron-donating -R groups such as methyl and phenyl favor N-protonation exchange, it seems probable that both N-methylacetamide and N-methylbenzamide exchange entirely by N-protonation, although this cannot be verified because only one isomer is detectable by NMR. The sixfold greater rate of protonation of N-methylacetamide over N, N-dimethylacetamide measured by Martin[39] might then be due simply to steric hindrance to solvation of the more highly substituted tertiary N-conjugate acid, the factor of six then being typical of an effect of this nature. For N-methylbenzamide as well, Martin's results yield an identical factor of six for the benzamide series when corrected for hindered rotation in the N-protonated tertiary amide.

In contrast, the predominant Z isomer of N-methylformamide undergoes proton exchange 24 times as fast as acid-catalyzed isomerization occurs in N, N-dimethylformamide. This larger difference

Figure 25. Relative energies of the N-conjugate and imidic acids of N-methylformamide.

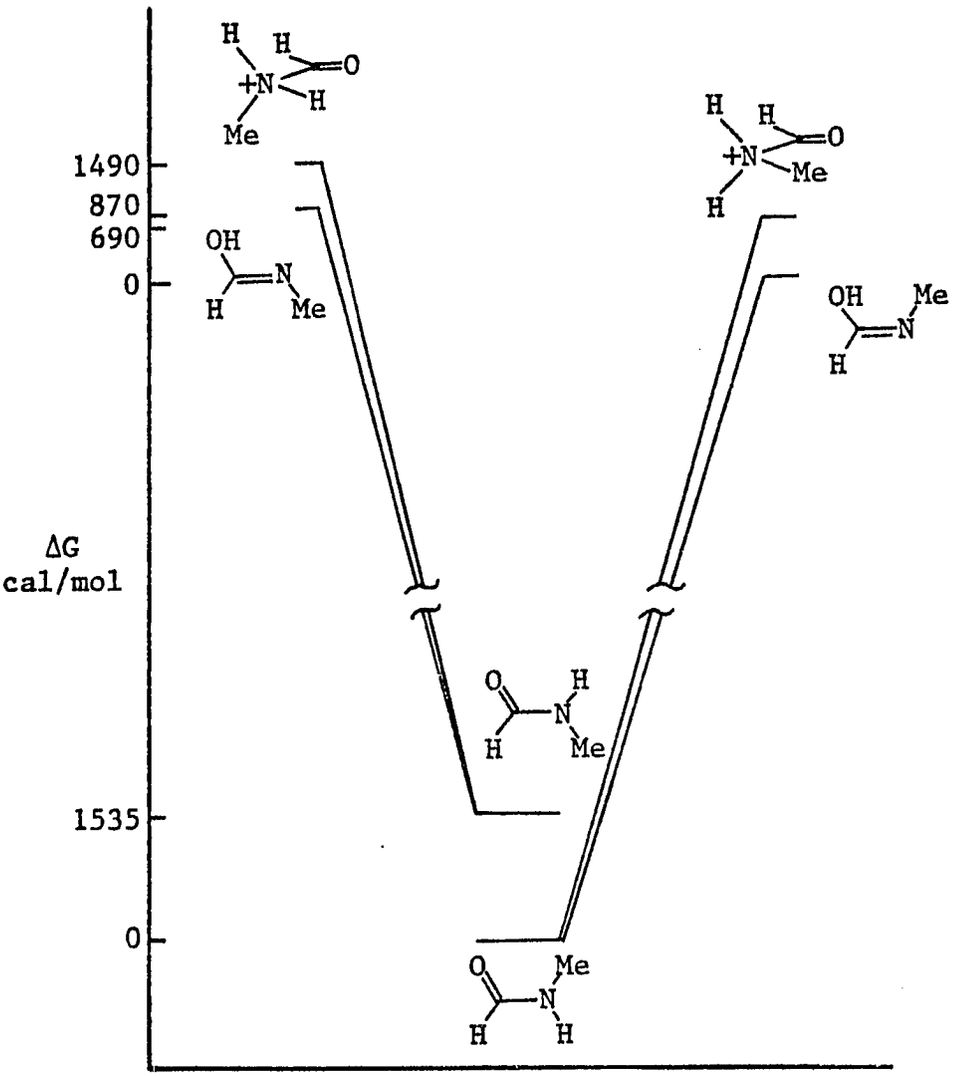

Figure 26. General-acid catalysis of N-methylformamide proton exchange. See text for details. Plot width is 150 Hz.

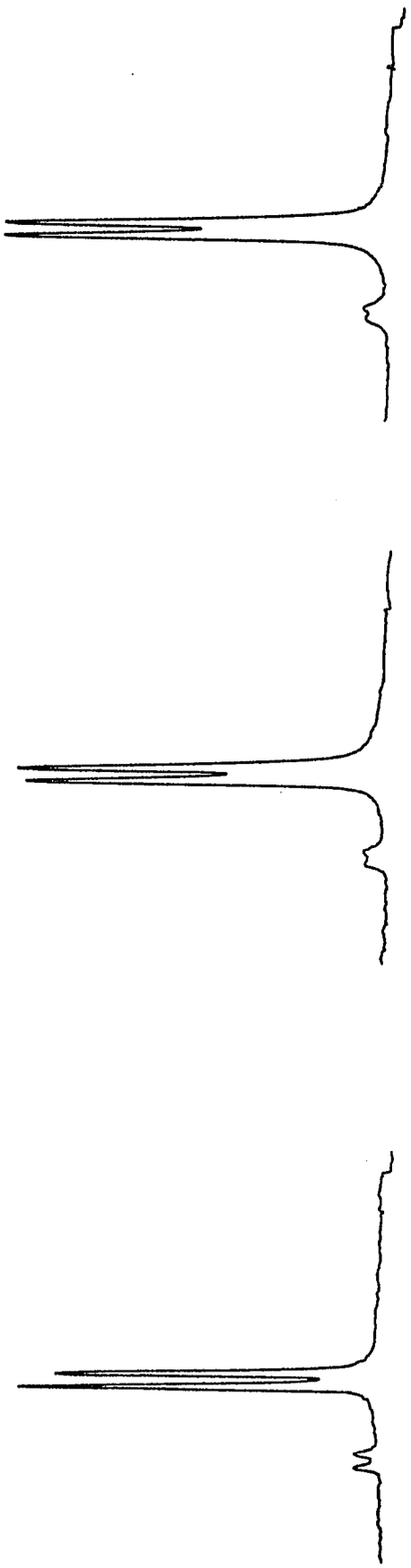

cannot be attributed to a steric effect, but is suggestive of predominant O-protonation exchange in N-methylformamide, and it is tempting to conclude that the percentage of N-protonation exchange for N-methylformamide is just 6/24, or 25%, as we have observed.

2. N-t-butylformamide

Rate constants for acid-catalyzed exchange and isomerization were also measured for N-t-butylformamide by saturation-transfer. Values for k_{ZS}, k_{ES}, and k_{ZE} of 0.44 sec^{-1}, 0.39 sec^{-1}, and 0.31 sec^{-1}, respectively, were obtained at pH 1.5 (see Table 7). These values correspond to second-order rate constants of about 15, 13, and 10 $M^{-1}sec^{-1}$, respectively. According to Eq. [29], since $K_r \geq 0$ in the N-protonation route, and k_{ZE} is zero for the imidic-acid route, solvent exchange of H_Z will always be greater than or equal to isomerization into the H_E site regardless of mechanism.

The measured values of k_{ZE}/k_{ZS} and k_{ZS}/k_{ES} can be computed from the results in Table 7 to be 0.7 and 1.1, respectively. Karabatsos and Hsi[125] have measured a value of K_r of 1.5 for $HCOCH_2tBu$, which is isoelectronic with N-protonated N-t-butylformamide. Using this value, k_{ZE}/k_{ZS} would be expected to be 0.4, and the fraction of exchange of H_Z due to N-protonation is then 0.7/0.4, or greater than 100%. This discrepancy cannot be rationalized by incursion of the imidic-acid mechanism, nor can it be rationalized by slow rotation in the N-protonated amide, since k_{ZE}/k_{ZS} approaches one-third in that limit (Eq. [29]). This overly

large value, taken together with the observation of substantial Z-E isomerization, leads us to conclude that exchange of H_Z occurs entirely through N-protonation and that the K_r value for $HCOCH_2tBu$ is not appropriate to $HCONH_2tBu^+$. Subject to this assumption of 100% N-protonation, $1/(K_r + 1)$ must equal the measured ratio of 0.7 (according to Eq. [29]), giving an estimated value for K_r of about 0.45. This value of K_r is quite different from the value of 1.5 measured for $HCOCH_2tBu$,[127] and corresponds to the anti form 13 of N-protonated N-t-butylformamide being more stable by ~480 cal/mol than the gauche form 12 (or 14) (see Figure 24). Using the measured values of k_{ZS}/k_{ES} and k_{ZE}/k_{ZS}, and taking K_r and K_{EZ} to be 0.45 and 2.2, respectively, the amount of exchange of H_E occurring through N-protonation can then be estimated with Eqs. [29] and [30] to be $(1 + 0.45)(0.7 \times 1.1)/(0.45 \times 2.2)$, or 100% as well.

It is difficult to see why the imidic-acid route does not contribute to proton exchange in N-t-butylformamide, as it does in N-methylformamide. Proton exchange is slower in the former compound, judging from the second-order rate constants. It may well be that the imidic acids are sterically destabilized relative to the conjugate N-acids in N-t-butylformamide.

In formamide itself, proton exchange occurs only through N-protonation, although here as well, the estimated second-order rate constants are smaller than for N-methylformamide (see Table 7). It is possible that this is due to stabilization of the imidic acids of

N-methylformamide by methyl substitution relative to the unsubstituted formimidic acids, much as alkenes are stabilized by alkyl substitution.

We have, however, observed specific-acid catalysis of proton exchange in N-t-butylformamide, and have verified that there is no general-acid catalysis by phosphate buffers. This contrasts with our observation of such catalysis by this buffer in N-methylformamide, and is consistent with our conclusion of pure N-protonation exchange in N-t-butylformamide, since the N-protonation mechanism is expected to be subject only to specific-acid catalysis.

Our conclusions concerning these secondary amides are subject to a number of assumptions. We have assumed that the rotameric equilibrium constant K_r measured for $HCOCH_2Me$ is appropriate to $HCONH_2Me^+$, even though such a transferability does not hold for $HCONH_2tBu^+$. We have also assumed that 12 interconverts to 13 and 14 at the same rate, even though it is probable that 12 rotates to 14 faster than to 13 (Figure 23). We have also assumed, in our kinetic analysis, that rotation is fast compared to deprotonation in these N-protonated secondary amides, and it is conceivable that a large -R group in $HCONH_2R^+$ could slow rotation considerably. Nevertheless, in an expanded N-protonation model where the above assumptions are not made, the experimental data for N-t-butylformamide provide realistic k_d/k_r ratios, whereas the data for N-methylformamide do

not. We therefore feel that the central conclusions of our analysis of exchange in these secondary amides are correct.

7. Unification of Acid-catalyzed Results for Primary Amides

A general scheme unifying our results pertaining to acid-catalyzed proton exchange in primary amides can be constructed in the following manner. For simplicity, we neglect statistical factors and hindered rotation in the N-protonation pathway, and the slight rate differences observed for H_E and H_Z in the imidic-acid pathway.

Exchange pathways in acid media are depicted in Figure 27.

$$H^+ + RCONH_2 \underset{k_2}{\overset{k_1}{\rightleftharpoons}} RCONH_3^+ \qquad K_a^N$$

$$k_3 \Big\downarrow \Big\uparrow k_4 K_a^O$$

$$RC(OH)NH_2^+ \underset{k_6}{\overset{k_5}{\rightleftharpoons}} RC(OH)NH + H^+ \qquad K_a^I$$

Figure 27. Exchange pathways in acid media.

K_a^I, K_a^O, and K_a^N are acidity constants for proton loss from nitrogen and oxygen in the O-protonated amide and from nitrogen in the N-protonated amide, respectively.

Proton exchange by N-protonation occurs at a steady-state rate v_N equal to

$$v_N = k_1[H^+][RCONH_2] = k_2[RCONH_3^+] = \frac{k_2}{K_a^N} \cdot [H^+] \cdot \frac{K_a^O}{K_a^O + [H^+]} \cdot C_A \qquad [31]$$

where C_A is the total concentration of amide. Exchange via the imidic-acid pathway occurs at a steady-state rate v_I given by

$$v_I = k_5[RC(OH)NH_2^+] = k_6[RC(OH)NH][H^+] = k_6 K_a^I \cdot \frac{[H^+]}{K_a^O + [H^+]} \cdot C_A \qquad [32]$$

We now examine the behavior of these rate expressions as the acidity of the medium is varied.

a. Dilute Acid

In dilute acid, where $[H^+] \ll K_a^O$, Eqs. [31] and [32] simplify to

$$v_N = \frac{k_2[H^+]}{K_a^N} \cdot C_A \qquad [33]$$

and

$$v_I = \frac{k_6 K_a^I[H^+]}{K_a^O} \cdot C_A \qquad [34]$$

In dilute acid, the ratio of N-protonation to imidic-acid exchange rates then equals

$$\frac{v_N}{v_I} = \frac{k_2}{k_6} \cdot \frac{K_a^O}{K_a^I \cdot K_a^N} \qquad [35]$$

and is independent of pH. Since k_2 and k_6 are estimated to be 10^{12} sec^{-1}, [105,114] and 10^{10} $M^{-1}sec^{-1}$, [46] respectively, if we know K_a^I, K_a^O, and K_a^N, it is possible to estimate the amount of exchange occurring by each pathway. For example, for acetamide, $K_a^O = 10^{+0.9}$, [126] K_a^N has been estimated to be $10^{+9.0}$, [34] and K_a^I may be approximated by that for ethyl acetimidate, which is $10^{-7.6}$. [127] Using these values in Eq. [35], V_N/V_I is estimated to be 30, so that proton exchange in acetamide should occur almost entirely through the N-protonation pathway, as observed.

Alternative expressions for v_N/v_I can be derived by noting that the quantity $K_a^O/K_a^I K_a^N$ in Eq. [35] is equal to K_T^+/K_a^I, K_T/K_a^N, or $K_T K_T^+/K_a^O$, where K_T and K_T^+ are tautomeric equilibrium constants for the ratio of N- to O-protonated amide and the ratio of neutral amide to imidic acid, respectively. Thus

$$\frac{v_N}{v_I} = \frac{k_2}{k_6} \cdot \frac{K_T^+}{K_a^I} = \frac{k_2}{k_6} \cdot \frac{K_T}{K_a^N} = \frac{k_2}{k_6} \cdot \frac{K_T K_T^+}{K_a^O} \qquad [36]$$

To the extent that the tautomeric equilibrium constants K_T and K_T^+ are less sensitive to R-group substitution than the acidity constants are, we may expect that electron-withdrawing -R groups, which increase K_a^I, K_a^O, and K_a^N, should favor the imidic-acid mechanism, whereas electron-donating groups should favor the N-protonation pathway. Qualitatively this is reasonable, since the transition-state for the imidic-acid mechanism resembles the uncharged imidic-acid

(reprotonation of this species being diffusion-controlled) whereas the transition-state for the N-protonation mechanism resembles the cation, $RCONH_3^+$ (deprotonation of which is also diffusion-controlled). Eqs. [33] and [34] further show that whereas the proton exchange rate in the N-protonation mechanism depends on $1/K_a^N$, the exchange rate in the imidic-acid pathway depends on the ratio of acidity constants K_a^I/K_a^O. Since the effect of electron-withdrawing groups is to increase all three acidity constants, the rate of the N-protonation mechanism should show the greater sensitivity to substituent effects.

Cyano-, chloro-, and dichloroacetamide, with pK_a^O values of -3.7, -2.8, and -4.2,[126] are considerably less basic than acetamide ($pK_a^O = -0.9$),[126] acryalmide ($pK_a^O = -0.3$),[127] or benzamide ($pK_a^O = -1.7$)[128] and exchange largely or entirely through the imidic-acid route. Likewise, ethyl carbethoxyimidate, $EtOCOC(OEt)NH_2^+$, which serves as a model for O-protonated ethyl oxamate, has a $pK_a^I < 5.2$,[127] and is considerably more acidic than ethyl acetimidate ($pK_a^I = 7.6$),[127] which serves as a model for O-protonated acetamide. Thus ethyl oxamate and malonamide (which is structurally analogous), as well as chloro- and dichloroacetamide, may also be expected to exchange via the imidic-acid route in dilute acid.

b. Strong Acid ($pK_a^O > H_0 > pK_a^N$)

In strong acid, where the acidity of the N-protonated amide nevertheless still exceeds that of the medium, we may replace $[H^+]$ in Eqs. [31] and [32] by h_0, where h_0 characterizes the (non-ideal)

acidity of the medium. Although the H_A acidity function is appropriate for primary amides,[130] it pertains to O-protonation. The acidity function for N-protonation is unknown, but the closest analogy is to primary nitroanilines, and therefore to H_0. It is also not known which acidity function to use to describe the rate of protonation of an imidic acid. For definiteness, we will choose H_0 throughout, although the choice will not matter.

Under these conditions, h_0 far exceeds K_a^O, so that, from Eqs. [31] and [32]

$$v_N = k_2 \cdot \frac{K_a^O}{K_a^N} \cdot C_A \qquad [37]$$

$$v_I = k_6 h_0 \cdot \frac{K_a^I}{h_0} \cdot C_A \qquad [38]$$

Both k_2 and $k_6 h_0$ are first-order diffusion-controlled rate constants (ca. 10^{12} sec^{-1}), and we may set them equal to each other. Then the ratio v_N/v_I in strong acid is equal to

$$\frac{v_N}{v_I} = \frac{K_a^O}{K_a^I K_a^N} \cdot h_0 \qquad [39]$$

According to Eq. [37], exchange by N-protonation is independent of the acidity of the medium, since as the acidity increases, the decrease in the concentration of free amide is exactly compensated by

an increase in its rate of protonation. On the other hand, Eq. [38] demonstrates that v_I decreases with increasing acidity, since N-H proton removal from O-protonated amide (k_5) requires water, whose activity decreases with increasing h_0. No rate advantage is gained here once the amide is substantially O-protonated. Equation [39] is again a consequence of the fact that the transition states for exchange resemble $RCONH_3^+$ and RC(OH)=NH, respectively, so that increasing acidity therefore favors the transition state bearing the additional proton.

c. Very Strong Acid ($H_0 \leq pK_a^N$)

Under conditions where medium acidity exceeds that of the N-protonated amide, exchange via O-protonation is of course insignificant, and furthermore, k_1h_0 and k_3h_0 now become diffusion-limited. The rate of N-protonation exchange is given from Eq. [31] by

$$v_N = k_1 h_0 [RCONH_2] \qquad [40]$$

The concentration of free amide may be obtained with the steady-state approximation given in Eq. [41]

$$\frac{d[RCONH_2]}{dt} = 0 = k_4[RC(OH)NH_2^+] - (k_1 + k_3)h_0[RCONH_2] \qquad [41]$$

and substituted in Eq. [40] to give

$$v_N = k_4 \cdot \frac{k_1}{k_1 + k_3} [RC(OH)NH_2^+] \qquad [42]$$

Unless $k_3 > k_1$, the rate-limiting step under these conditions is k_4, the rate of O-deprotonation. The free amide is then reprotonated at a diffusion-controlled rate on either oxygen or nitrogen, with a selectivity specified by the unknown ratio $k_1/(k_1 + k_3)$. Only protonation on nitrogen leads to proton exchange.

The acidity dependence of k_4 is solved for by setting

$$k_4[RC(OH)NH_2^+] = k_3 h_0 [RCONH_2] \qquad [43]$$

as required by equilibrium. Rearranging Eq. [43] to solve for k_4 and substituting this result in Eq. [42] gives

$$v_N = k_3 h_0 \cdot \frac{K_a^O}{h_0} \cdot \frac{k_1}{k_1 + k_3} \cdot C_A \qquad [44]$$

When acid is solvent, $k_3 h_0$ approaches the diffusion-controlled limit of 10^{12} sec^{-1}. With $k_3 h_0$ so limited, proton exchange even by the N-protonation mechanism decreases with increasing acidity, as observed.

The foregoing discussion is summarized in Figures 27 and 28. In Figure 27 is presented a free-energy diagram for N-protonation and imidic-acid exchange routes as a function of medium acidity. The bottom curve depicts the energetic situation for proton exchange in dilute acid, with N-protonation shown as having the smaller energetic requirement. In dilute acid, v_N and v_I are both directly proportional to $[H^+]$, as illustrated in Figure 28. As the acidity of the medium

Figure 27. Free-energy diagram for N-protonation and imidic-acid exchange pathways as a function of medium acidity.

Figure 28 Plot of v_N, v_I against medium acidity.

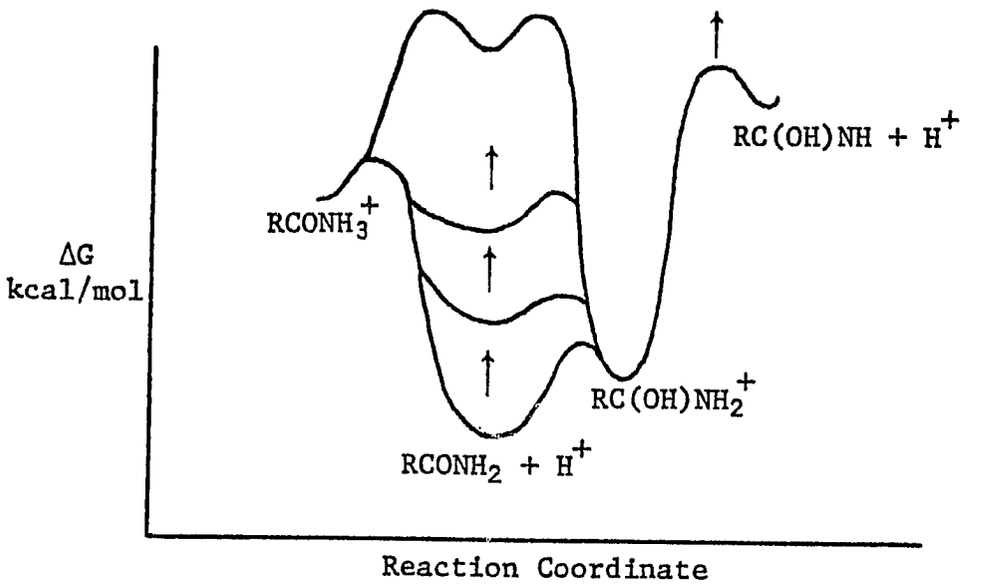

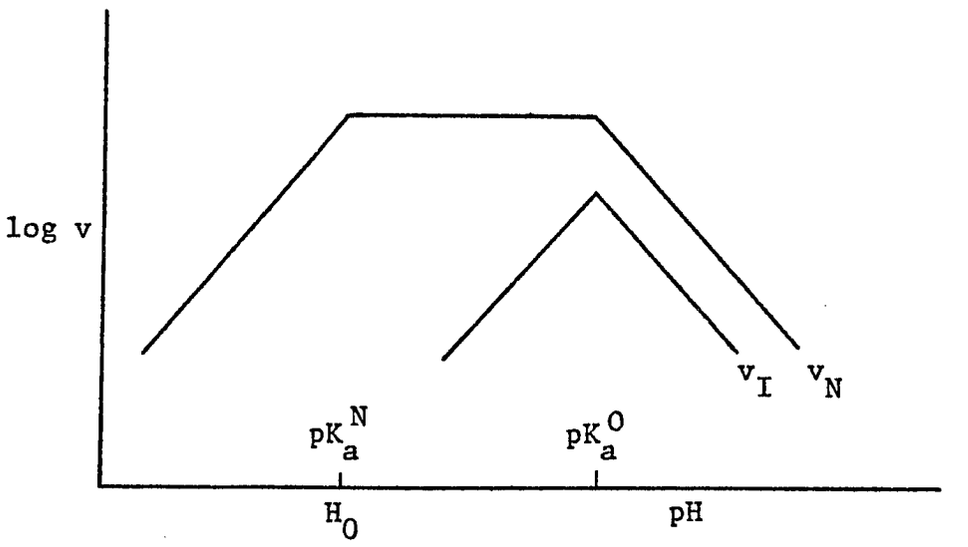

increases (symbolized by arrows in Figure 27), $RCONH_2$ and RC(OH)NH are increasingly destabilized relative to their conjugate acids, which remain unaffected except perhaps for small solvation effects. At intermediate acidities, when the amide is quantitatively O-protonated and $RCONH_2$ lies between $RCONH_3^+$ and $RC(OH)NH_2^+$ in energy, the barrier height for No-protonation exchange is unchanging, so that v_N is constant, while decreasing water activity causes v_I to drop rapidly. Finally, when the medium becomes more acidic than $RCONH_3^+$, $RCONH_2$ lies higher in energy than $RCONH_3^+$, so that the rate-limiting step for exchange is O-deprotonation. This process becomes more costly with increasing acidity, so that v_N as well finally decreases.

References

1. M. S. Miller and I. M. Klotz, J. Am. Chem. Soc., 95, 5694 (1973).

2. D. L. Hunston and I. M. Klotz, J. Phys. Chem., 75, 2123 (1971).

3. M. Liler, J. Chem. Soc., Perkin Trans. 2, 720, 816 (1972).

4. L. C. Martinelli, C. D. Blanton, and J. F. Whidby, J. Am. Chem. Soc., 93, 5111 (1971), J. Phys. Chem., 75, 1895 (1971).

5. R. L. Vold, E. S. Daniel, and S. O. Chan, J. Am. Chem. Soc., 92, 6771 (1970).

6. M. Sheinblatt, J. Am. Chem. Soc., 92, 2505 (1970).

7. C. Y. S. Chen and C. A. Swenson, J. Am. Chem. Soc., 2505 (1970).

8. T. Schleich, R. Gentzler, and P. H. von Hippel, J. Am. Chem. Soc., 90, 5954 (1968).

9. J. E. Bundschuh and N. C. Li, J. Phys. Chem., 72, 1001 (1968).

10. I. M. Klotz and B. H. Frank, J. Am. Chem. Soc., 87, 5103 (1966).

11. I. M. Klotz and P. L. Feidelseit, J. Am. Chem. Soc., 88, 5103 (1966).

12. A. Huidt and R. Corett, J. Am. Chem. Soc., 92, 5546 (1970).

13. O. Bensaude, M. Dreyfus, G. Dodin, and J. E. Dubois, J. Am. Chem. Soc., 99, 4438 (1977).

14. O. Bensaude, J. Aubard, M. Dreyfus, G. Dodin, and J. E. Dubois, J. Am. Chem. Soc., 100, 2823 (1978).

15. M. Dreyfus, O. Bensaude, G. Dodin, and J. E. Dubois, J. Am. Chem. Soc., 98, 6338 (1976).

16. K.-C. Chang and E. Grunwald, J. Am. Chem. Soc., 98, 3737 (1976).

17. M. Takeda and E. O. Stejskal, J. Am. Chem. Soc., 82, 25 (1960).

18. I. M. Klotz, J. Coll. and Interface Sci., 27, 804 (1968).

19. S. W. Englander, N. W. Downer, and H. Teitelbaum, Ann. Rev. Biochem., 41, 903 (1972), and references cited therein.

20. R. S. Molday, S. W. Englander, and R. G. Kallen, Biochem., 11, 150 (1972).

21. S. W. Englander and A. Poulson, Biopolymers 7, 379 (1969).

22. J. S. Svaupa, D. D. Mueller, and I. M. Klotz, J. Am. Chem. Soc., 89, 6024 (1967).

23. B. Leichtling and I. Klotz, Biochemistry 5, 4026 (1966).

24. S. W. Englander and J. J. Englander, Methods in Enzymology, Vol. 49, Part G, 1978.

25. D. G. Cross, A. Brown, and H. F. Fisher, J. Biol. Chem., 251, 1785 (1976).

26. D. G. Davis and B. F. Gisin, J. Am. Chem. Soc., 101, 3755 (1979).

27. G. Fraenkal and C. Franconi, J. Am. Chem. Soc., 82, 4478 (1960).

28. A. J. Kresge, P. H. Fitzgerald, and Y. Chiang, J. Am. Chem. Soc., 96, 4698 (1974).

29. M. Liler, Chem. Commun., 115 (1971).

30. C. R. Smith and K. Yates, J. Am. Chem. Soc., 94, 8811 (1972).

31. R. A. McClelland, J. Am. Chem. Soc., 97, 5281 (1975).

32. A. Williams, J. Am. Chem. Soc., 98, 5645 (1976).

33. T. C. Pletcher, S. Koehler, and E. H. Cordes, J. Am. Chem. Soc., 90, 7072 (1968).

34. A. R. Fersht, J. Am. Chem. Soc., 93, 3504 (1971).

35. W. W. Bachovchin and J. D. Roberts, J. Am. Chem. Soc., 100, 8041 (1978).

36. J. Kraut, Ann. Rev. Biochem., Vol. 46, 331 (1977).

37. A. Berger, A. Loewenstein, and S. Meiboom, J. Am. Chem. Soc., 81, 62 (1959).

38. R. S. Molday and K. G. Kallen, J. Am. Chem. Soc., 94, 6739 (1972).

39. a) R. B. Martin, Chem. Commun., 793 (1972). b) R. B. Martin and W. C. Hutton, J. Am. Chem. Soc., 95, 4752 (1973).

40. W. E. Stewart and T. H. Siddall, III, Chem. Rev., 70, 517 (1970).

41. F. A. Bovey and G. V. D. Tiers, J. Polym. Sci., Part A-1, 849 (1963).

42. C. L. Perrin, J. Am. Chem. Soc., 96, 5628 (1974).

43. C. O. Meese, W. Walter, and M. Berger, J. Am. Chem. Soc., 96, 2259 (1974).

44. L. Radom, W. J. Hehre, and J. A. Pople, J. Am. Chem. Soc., 93, 289 (1971).

45. A. C. Satterthwait and W. P. Jencks, J. Am. Chem. Soc., 96, 7045 (1974).

46. M. Eigen, Angew. Chem. Int. Ed., 3, 1 (1964).

47. R. M. Moriarty, C.-L. Yeh, and P. W. Whitehurst, J. Am. Chem. Soc., 92, 6360 (1970).

48. C. L. Perrin and E. R. Johnston, J. Magn. Reson., 33, 619 (1979).

49. S. Forsen and R. A. Hoffman, J. Chem. Phys., 39, 2892 (1963).

50. S. Forsen and R. A. Hoffman, J. Chem. Phys., 40, 1189 (1964).

51. A. L. Van Geet, Anal. Chem., 42, 679 (1970).

52. C. A. MacKenzie, G. A. Schmidt, and L. R. Webb, J. Am. Chem. Soc., 73, 4990 (1951).

53. T. C. Pletcher, S. Koehler, and E. H. Cordes, J. Am. Chem. Soc., 90, 7072 (1968).

54. H. Nohira, Y. Nishikawa, Y. Furuya, and T. Mukaiyama, Bull. Chem. Soc. Japan, 38, 897 (1965).

55. G. Asknes and J. E. Prue, J. Chem. Soc., 1959, 103.

56. ITRCAL, Copyright 1973, Nicolet Instrument Corporation, Madison, WI 53711.

57. R. M. Silverstein and G. C. Bassler, Spectrometric Identification of Organic Compounds, John Wiley and Sons, New York (1963), p. 144.

58. J. Noggle and R. Schirmer, The Nuclear Overhauser Effect, Academic Press, New York, 1972.

59. C. S. Johnson, Jr., Advan. Mag. Resonance, 1, 33 (1965).

60. L. W. Reeves and K. N. Shaw, Can. J. Chem., 48, 3641 (1970).

61. J. Farrar and E. Becker, Pulse and Fourier Transform NMR, Academic Press, New York, 1975, a) p. 60, b) Chapter 4.

62. Reference 37, Appendix A.

63. L. A. LaPlanche and Max T. Rogers, J. Am. Chem. Soc., 85, 3728 (1963); ibid., 86, 337 (1964).

64. A. H. Lewin and M. Frucht, Org. Mag. Res., 7, 206 (1975).

65. L. H. Piette, J. D. Ray, and R. A. Ogg, Jr., J. Mol. Spectroscopy, 2, 66 (1958).

66. C. Rabiller, J. P. Renou, and G. J. Martin, J. Chem. Soc., Perkin II, p. 536 (1977).

67. J. R. Dyer, Applications of Absorption Spectroscopy of Organic Compounds, Prentice-Hall, 1965, pp. 77-78.

68. R. B. Homer and C. D. Johnson, in The Chemistry of Amides, J. Zabicky, Ed., John Wiley and Sons, New York, 1970, p. 187.

69. L. R. Isbrandt and Max T. Rogers, Chem. Commun., 1971, p. 1378.

70. R. F. Butterworth, A. G. Pernet, and S. Hanessian, Can. J. Chem., 49, 981 (1971).

71. B. Birdsall, J. Feeney, and P. Partington, J. Chem. Soc., Perkin II, p. 2145 (1973).

72. I. M. Klotz and J. S. Franzen, J. Am. Chem. Soc., 84, 3461 (1962).

73. H. Susi and J. S. Ard, Arch. of Biochem. and Biophys., 117, 147 (1966).

74. H. Susi, S. N. Timasheff, and J. S. Ard, J. Biol. Chem., 239, 3051 (1964).

75. B. E. Mann, Prog. in NMR Spectroscopy, 11, 95 (1977) and references cited therein.

76. B. E. Mann, J. Magn. Reson., 25, 91 (1977).

77. R. K. Gupta, S. H. Koenig, and A. G. Redfield, J. Magn. Reson., 7, 66 (1972).

78. K. J. Karel and M. Brookhart, J. Am. Chem. Soc., 100, 1619 (1978).

79. P. D. Johnston and A. G. Redfield, Nucl. Acids Res., 4, 3599 (1977).

80. S. Waelder, L. Lee, and A. G. Redfield, J. Am. Chem. Soc., 97, 2927 (1975).

81. I. D. Campbell, C. M. Dobson, R. G. Ratcliffe, and R. J. P. Williams, J. Magn. Reson., 29, 397 (1978).

82. J. W. Faller, in Determination of Organic Structures by Physical Methods, F. C. Nachod and J. J. Zuckerman, Eds., Academic Press, New York, 1973, Chapter 2 and references cited therein.

83. B. E. Mann, Chem. Commun., 626 (1977).

84. V. I. Mamatyuk, B. G. Derendyaev, A. N. Detsina, and V. A. Koptyug, Russ, J. Org. Chem., 10, No. 12, 2487 (1974).

85. J. W. Faller and J. W. Sibert, J. Organomet. Chem., 31, C5-C8 (1971).

86. R. A. Hoffman and S. Forsén, Prog. in NMR Spectroscopy, 1, 15 (1966).

87. W. Walter and G. Maerten, Justus Liebigs Ann. Chem., 712, 58 (1968).

88. L. M. Jackman, "Rotation about Partial Double Bonds," in Dynamic Nuclear Magnetic Resonance Spectroscopy, L. Jackman and F. Cotton, Eds., Academic Press, 1975.

89. T. Drakenberg, K. I. Dahlquist, and S. Forsén, J. Phys. Chem., 76, 2178 (1970).

90. W. Walter, E. Schaumann, and H. Rose, Org. Mag. Res., 5, 191 (1973).

91. T. Drakenberg, Tetrahedron Letters, 1743 (1972).

92. R. F. Hobson and L. W. Reeves, J. Magn. Reson., 10, 243 (1973).

93. I. Yavari and J. D. Roberts, J. Am. Chem. Soc., 100, 5217 (1978).

94. R. Huisgen and H. Ott, Tetrahedron, 6, 253 (1959).

95. F. M. Menger and G. Saito, J. Am. Chem. Soc., 95, 6838 (1973).

96. P. Kobrin, unpublished data.

97. R. B. Turner and W. R. Meador, J. Am. Chem. Soc., 79, 4133 (1957).

98. M. Kandel and E. H. Cordes, J. Org. Chem., 32, 3061 (1967).

99. H. Lumbroso and D. M. Bertin, Bull. Soc. Chim. Fr., 1728 (1970).

100. O. Exner and O. Schindler, Helv. Chem. Acta 55, 1921 (1972).

101. H. Saitô and K. Nukada, Tetrahedron, 22, 3313 (1966).

102. R. J. Gillespie and T. Birchall, Can. J. Chem., 41, 148 (1963).

103. C. L. Perrin, J. Am. Chem. Soc., 96, 5631 (1974).

104. A. J. Kresge, Acc. Chem. Res., 8, 354 (1975).

105. Z. Luz and S. Meiboom, J. Am. Chem. Soc., 86, 4768 (1964).

106. J. R. Lyerla, Jr., and D. M. Grant, J. Phys. Chem., 76, 3213 (1972).

107. J. P. Lowe, Prog. Phys. Org. Chem., 6, 1 (1968).

108. Topics in Stereochemistry, E. Eliel and N. Allinger, Eds., Academic Press, Vol. 5, pp. 167-205 (1970).

109. W. J. Hehre and L. Salem, Chem. Commun., p. 754 (1973).

110. W. J. Hehre, D. Cremer, J. S. Binkley, and J. A. Pople, J. Am. Chem. Soc., 96, 6900 (1974).

111. H. Pracejus, Chem. Ber., 92, 988 (1959).

112. W. G. Dauben and K. S. Pitzer, in Steric Effects in Organic Chemistry, M. S. Newman, Eds., Wiley, New York, 1956, p. 58.

113. DNMR3, by D. A. Kleier and G. Binsch, Available from the Quantum Chemistry Program Exchange, Indiana University, Bloomington, Indiana. Program No. 165.

114. E. Grunwald and M. S. Puar, J. Phys. Chem., 71, 1842 (1967).

115. E. M. Arnett, et al., J. Am. Chem. Soc., 94, 4724 (1972).

116. Water, A Comprehensive Treatise, F. Franks, Ed., Vol. 3, Chap. 7, p. 385.

117. S. Albert and J. A. Ripmeister, J. Chem. Phys., 58, 541 (1973).

118. G. C. Levy, A. D. Godwin, J. M. Hewitt, and C. Sutcliffe, J. Magn. Reson., 29, 553 (1978).

119. N. A. Bergman, Y. Chiang, and A. J. Kresge, J. Am. Chem. Soc., 100, 5955 (1978).

120. T. Shedlovsky and R. L. Kay, J. Phys. Chem., 60, 151 (1956).

121. Physical Chemistry of Organic Solvent Systems, A. K. Carrington and T. Dickinson, Eds., Plenum Press, London, 1973, p. 654.

122. B. G. Cox, J. Chem. Soc., B, p. 1780 (1970).

123. J. Teyssey̆re, et al., Bull. Chem. Soc. Belgique, 85, 39, (1976).

124. Internal Rotation and Inversion, by D. G. Lister, J. N. MacDonald, and N. L. Owen, Academic Press, New York, 1978, p. 8.

125. G. J. Karabatsos and N. Hsi, J. Am. Chem. Soc., 87, 2864 (1965).

126. M. Liler, J. Chem. Soc., B, p. 385 (1969).

127. C. A. Streuli, Anal. Chem., 31, 1652 (1959).

128. K. Yates and J. B. Stevens, Can. J. Chem., 43, 529 (1965).

129. R. E. D. McClung, J. Chem. Phys., 55, 3459 (1971).

130. M. J. Jorgenson and D. R. Hartter, J. Am. Chem. Soc., 85, 878 (1963).